UNAMBIGUOUS FULL MULTINUCLEAR NMR ASSIGNMENT OF 4-AMINO-1,1,2,2,9,9,10,10-OCTAFLUORO[2.2]PARACYCLOPHANE & NMR DIFFERENTIATION OF ITS ENANTIOMERS, AND RELATED COMPOUNDS

by

SHERYL RABINOWITZ

A thesis submitted to the

Graduate School-Camden

Rutgers, The State University of New Jersey

in partial fulfillment of the requirements

for the degree of Master of Science

Graduate Program in

Chemistry

written under the direction of

Professor Alex J. Roche

and approved by

Alex J. Roche

George A. Kumi

Belgin Canturk

Camden, New Jersey January 2013

Abstract

UNAMBIGUOUS FULL MULTINUCLEAR NMR ASSIGNMENT OF 4-AMINO-1,1,2,2,9,9,10,10-OCTAFLUORO[2.2]PARACYCLOPHANE & NMR DIFFERENTIATION OF ITS ENANTIOMERS, AND RELATED COMPOUNDS

by

SHERYL RABINOWITZ

THESIS DIRECTOR:

PROFESSOR ALEX J. ROCHE

For the first time the full multinuclear ^{1}H, ^{13}C, and ^{19}F assignments were established for 4-amino-1,1,2,2,9,9,10,10-octafluoro[2.2]paracyclophane (OFP-NH_2). These were achieved by using a combination of 1D, COSY, and HETCOR NMR techniques. The assignments were later confirmed by nOe experiments. The interaction of OFP-NH_2 with different chiral shift reagents was explored, and it was shown that it is possible to clearly detect both enantiomers of the planar chiral OFP-NH_2 (in both the ^{1}H and ^{19}F NMR). This method of chiral discrimination was also shown to be applicable to other similar chiral OFP derivatives.

Dedication

THIS THESIS IS DEDICATED TO MY HUSBAND LARRY AND CHILDREN DAVID AND JASON. THE LOVE AND SUPPORT THEY GAVE ME THROUGHOUT THIS PROCESS GAVE ME THE POWER TO COMPLETE THIS THESIS.

Acknowledgements

With the utmost gratitude, I would like to express my thanks to Dr. Roche. I chiefly thank you for sharing your masterful experience of Organic Chemistry with me. From you, I learned how to be a teacher to others and I have now seen the interest in Chemistry ignite in my students' minds just as you had sparked my interest in Organic Chemistry. You truly are the BPE!

I am also thankful to the other members of my thesis committee, Dr. George Kumi and Dr. Belgin Canturk. I most appreciate Dr. Kumi using his valuable time to assist me with this endeavor. My former Roche Research Group fellow member and mentor, Belgin, in 2003, encouraged me to speak to Dr. Roche about becoming a member of his group and now she serves as a member of my Committee! Who would have ever thought? THANK YOU!!!

My research partner, Alex Marchione also has my sincere appreciation for collaboration on work discussed in our paper.

Mr. Steven "Buzz" Chew is acknowledged as a great lab assistant for the research presented here.

To Anne Loyle Langholz, I am seriously appreciative and thankful to you for choosing me to be your lab assistant and helping me to the very end just because you are my friend.

To Anna, My "Roomie", thank you for always helping me with my ChemDraw, being my friend through it all, and being the best cheerleader ever!

Table of Contents

List of Figures

List of Spectra

List of Schemes

Abbreviations

PCP	[2.2]-Paracyclophane
OFP	1,1,2,2,9,9,10,10-Octafluoro-[2.2-]Paracyclophane
OFP-NH_2	4-amino-1,1,2,2,9,9,10,10- Octafluoro-[2.2-]paracyclophane
OFP-di-NH_2	4,12-Diamino-1,1,2,2,9,9,10,10-Octafluoro-[2.2-]Paracyclophane
diamino-NH_2	4,12-Diamino-1,1,2,2,9,9,10,10-Octafluoro-[2.2-]Paracyclophane
o' di-NH_2	4,12-Diamino-1,1,2,2,9,9,10,10- Octafluoro-[2.2-]Paracyclophane
COSY	2D Correlation Spectroscopy
HETCOR	2D Heteronuclear Correlation Spectroscopy
nOe	Nuclear Overhauser Effect
HOESY	2D Heteronuclear Overhauser Effect Spectroscopy
$CDCl_3$	Deuterated Chloroform
CSR	Chiral Shift Reagent
CSA	Chiral Solvating Agent
CDA	Chiral Derivitizing Agent
CLSR	Chiral Lanthanide Shift Reagent
LSR	Lanthanide Shift Reagent
HFC	3-Heptafluorobutyrylcamphor
Yb(tmhd)$_3$	2,2,6,6-Tetramethyl-3,5-heptanedionato)ytterbium
YbFOD	Tris(6,6,7,7,8,8,8-heptafluoro-2,2-dimethyl-3,5-octanedionato)ytterbium
$^{x}J_{yz}$	J=scalar coupling x=number of bonds between coupled nuclei y/z= nuclei that are coupled together y=z homonuclear coupling (COSY) y≠z heteronuclear coupling (HETCOR)

Chapter 1: Introduction

Cyclophane chemistry is a well-established field because the first cyclophane, [2.2]metacyclophane (**1**) (Fig.1.1) was first prepared by Pelligrin over a century ago (1899).[1] The field of cyclophane chemistry continues to grow and the discovery of new derivatives and new synthetic strategies is principally due to the increasing field of supramolecular chemistry.

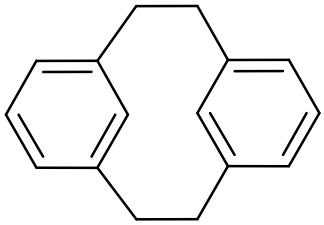

1

Figure 1.1: [2.2]Metacyclophane

The incorporation of atoms and/or functional groups into the cyclophane framework alters the chemical and physical properties making them desirable for a number of applications in material science, which include polymers with very stable surfaces for printed circuits, new materials for medical application and drug delivery, and use as ligands in stereoselective synthesis.[2-13] The research presented in this thesis will focus on the NMR spectroscopic analyses of specific fluorinated[2.2]paracyclophanes.

Cyclophanes

Cyclophanes, first described by Cram, [14] Shubert, [15] and Smith, [2] consist of aromatic rings that are joined together by an aliphatic chain that forms a bridge between the aromatic

systems. Cyclophanes have received widespread attention in organic chemistry as they are synthetically challenging and offer interesting physical and chemical properties.[16] Some of these properties include interesting transannular interactions, directing effects and spectroscopic properties. Because of their distinctive structure, cyclophanes are widely studied and offer versatility.[2]

Paracyclophane (PCP)

Paracyclophanes contain aromatic rings and aliphatic bridges connecting the rings. In these molecules, the bridges connect the aromatic rings at the *para* position. This can bring the rings into close proximity so that the π-orbitals are directly interacting to form an extended aromatic system.[14] The interaction between the aromatic rings creates an interesting phenomenon, the *transannular effect*.[7] It was observed that when a substituent was attached to one of the rings, the electronic properties of other rings are affected. This has been proven by both spectroscopic and reactivity studies.[13]

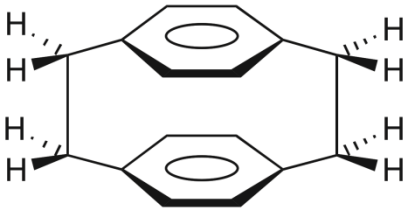

2

Figure 1.2: [2.2]Paracyclophane (PCP)

The smallest stable paracyclophane is referred to as [2.2] Paracyclophane (PCP) (**2**). PCP was originally known as 'di-*p*-xylene' and was first isolated by Brown and Farthing in 1949.[17] In order to study the electronic interactions between "face to face" arranged aromatic systems described earlier, Cram and Steinberg synthesized the same cyclophane

two years later by a designed new synthetic strategy.[14]

PCP was the foundation for many substituted moieties with substituents ranging from simple single unit species, such as a halogen, to complex ring structures, such as another cyclophane. These substituted analogs displayed prime examples of the "*transannular* effect" and have served as the backbone for bridge-substituted analogs, which are discussed later in the chapter.

Nomenclature of Cyclophanes

Cram introduced a nomenclature system for cyclophanes, which was complementary to the IUPAC rules.[14] Later on, Schubert[15], Smith[2], and Vogtle[4] systematized it. Cyclophane nomenclature requires the number of carbons in the bridge be placed in order of decreasing length in square brackets in front of the name. The position of the bridge is designated by bridge connectivity as *ortho*, *meta*, or *para*.

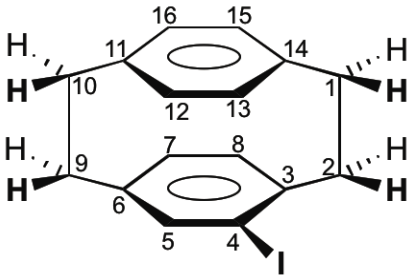

3

Figure 1.3: Numbering Scheme for Cyclophanes

The numbering of a [2.2]paracyclophane begins at the bridge carbon (C-1) and continues down the bridge to the lower deck, assuming that C-2 through C-9 are in the same plane, and proceeding in a clockwise progression. Numbering continues to the upper deck

through C-10 and around the upper ring in a counter clockwise progression ending with C-16. Once substituents are introduced to the rings, they must each be numbered such that the lowest possible value is given to each substituent according to their position on the ring. Therefore, the molecule in Fig. 1.3 would be correctly referred to as 4-Iodo[2.2]paracyclophane (**3**).

Octafluoro[2.2]Paracyclophane (OFP)

Fluorination of a cyclophane induces special aspects to the aromatic ring system. These include influencing the directing effects of electrophilic aromatic substitution and the transannular communication.[18] Exploration of these effects led to the first synthesis of the fully bridge fluorinated analog**,** 1,1,2,2,9,9,10,10-octafluoro[2.2]paracyclophane (OFP) (**4**) (Fig. 1.4) performed by Chow, *et al*. in 1970.[19] This method involved a pyrolitically-induced synthesis of OFP and had a relatively low yield of 9-28%.

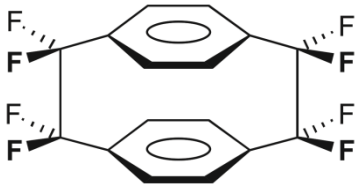

4

Figure 1.4: Octafluoro[2.2]paracyclophane (OFP)

In 2000, Dolbier, *et al*. performed a synthesis of OFP by the 1,6 reductive elimination of CF_2X groups where X=Cl.[20] This synthesis provided a much more practical lab procedure and also had an increased yield of 60% (Scheme 1.1).

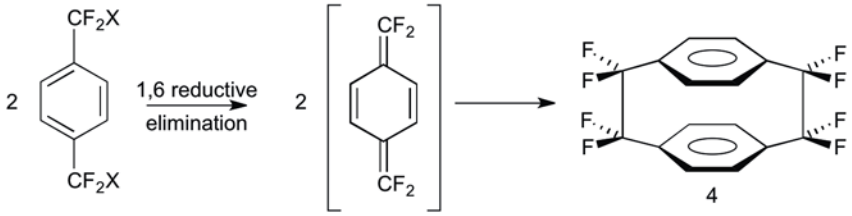

Scheme 1.1: Synthesis of OFP via a 1,6 Reductive Elimination

With the advancement of the synthetic methods of bridge fluorinated[2.2] paracyclophanes, [5-7,13,20-25] OFP has attracted increased attention both industrially and academically. The main motivational drive for new and improved syntheses of these compounds arises from the fact that OFP is an industrially significant compound. OFP and its derivatives are used commercially as monomers for Parylene-type-polymers. Parylene-HT and VIP™ theses polymers have unique physical and chemical properties including a low dielectric constant, high thermal stability and low moisture absorption.[25] These Parylene polymers are stable at temperatures as high as 450 ^{0}C and are of interest for coatings for electronic devices. Synthesis of the Parylene polymer is described in Scheme 1.2.

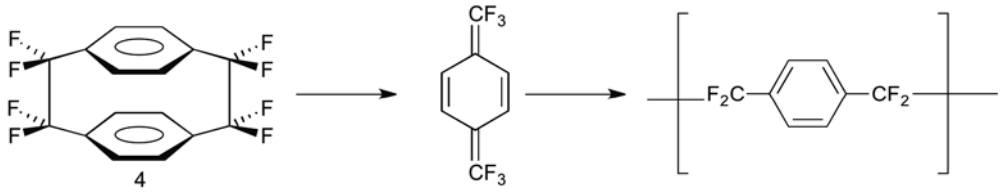

Scheme 1.2: Formation of the Parylene Polymer

OFP has served as the core structure to many substituted analogs. The substitution allows for detailed spectroscopic analyses. Monosubstituted moieties containing both electron withdrawing i.e., (-NO_2, -CF_3 ...) and electron donating i.e. (–NH_2, -OH…) groups were first synthesized and described by Roche and Dolbier in 1999.[21] Substitution syntheses,

including aromatic ring substitutions were subsequently reported by Roche and Canturk in 2005 (Fig. 1.5).[22]

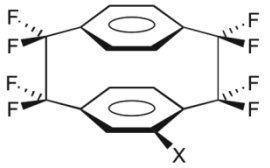

Figure 1.5: Monosubstituted OFP Derivatives

In addition to the many monosubstituted derivatives that have been synthesized to date, many disubstituted derivatives have been synthesized as well. With disubstituted analogs reported here, substitution always takes place on the previously unsubstituted ring. Three disubstituted isomers are shown in Figure 1.6.

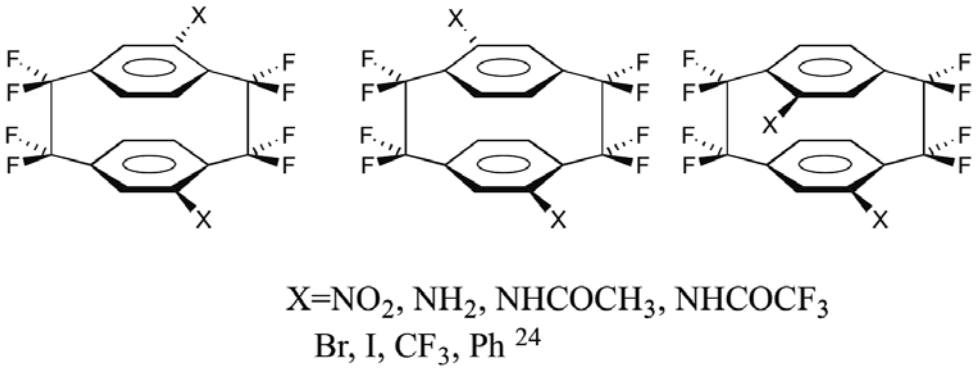

Figure 1.6: Disubstituted Analogs of OFP

Roche and Dolbier first synthesized all the analogs shown in Fig. 1.6 in 2000.[24] Candidates for the research presented in this thesis were selected from Figures 1.5 and 1.6. The ^{1}H, ^{13}C, and ^{19}F NMRs were taken for each of the mono- and di- substituted derivatives described. The NMR spectra of OFP-NH_2 gave the best spread of peaks and the most resolution of these peaks for all of these nuclei. It is for this reason that OFP-NH_2 was chosen to begin this research.

Chirality

Chirality is one of the most important concepts in nature and science and particularly significant in biological processes. Chirality describes why seemingly similar molecules can behave very differently. Many of the molecules that are biologically important are chiral, these include proteins (and their constituent amino acids), and the nucleic acids DNA and RNA, which hold the information necessary for proteins to be synthesized. [26,27] Chirality implies the need for handedness when it comes to identifying the stereochemistry of chiral molecules. Molecules display chirality if they have non-superimposable mirror images.

Common examples of chirality include hands and feet and the importance of this topic was evident in 1966 when Cahn, Ingold and Prelog famously stated “Chirality expresses the necessary and sufficient conditions for the existence of enantiomers”. [28]

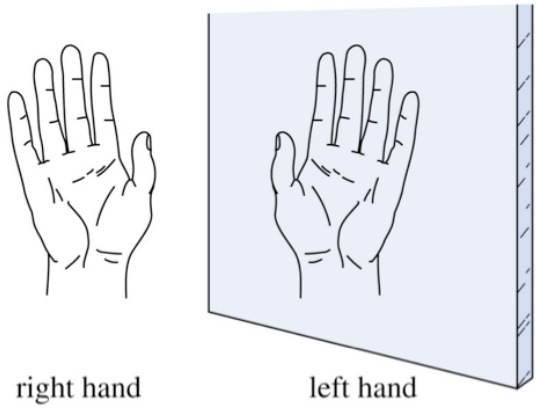

Figure 1.7: Chirality and Handedness

The hands shown in Fig. 1.7 are mirror images of each other. If they were stacked on top of each other, the thumbs would be pointing in different directions and are therefore deemed as chiral species. There are three types of chirality: central, axial, and planar. A molecule that exhibits central chirality usually includes a tetrahedral atom with four different substituents. A molecule that includes restricted rotation about an axis, such as DNA, can exhibit axial chirality, which is chirality about the axis. Planar chirality can be observed in a molecule when there is restricted rotation about a plane. Cyclophanes studied for this research all exhibit planar chirality.

Nomenclature of Enantiomers

The R/S system is used for denoting enantiomers. According to the Cahn–Ingold–Prelog (CIP), convention rules each chiral element (either tetrahedral center, axial, or planar) is identified as *R* or *S* according to a system by which its substituents are each assigned a priority that is based on atomic number. For a chiral tetrahedral center, the molecule is oriented so that the lowest-priority of the four is pointed away from a viewer, then two possibilities are seen. If the priority of the remaining three substituents decreases in clockwise direction, it is labeled *R* (for *Rectus*, Latin for right), if it decreases in counterclockwise direction, it is *S* (for *Sinister*, Latin for left).[29] The two enantiomers of the amino acid, alanine, are shown in Figure 1.8.

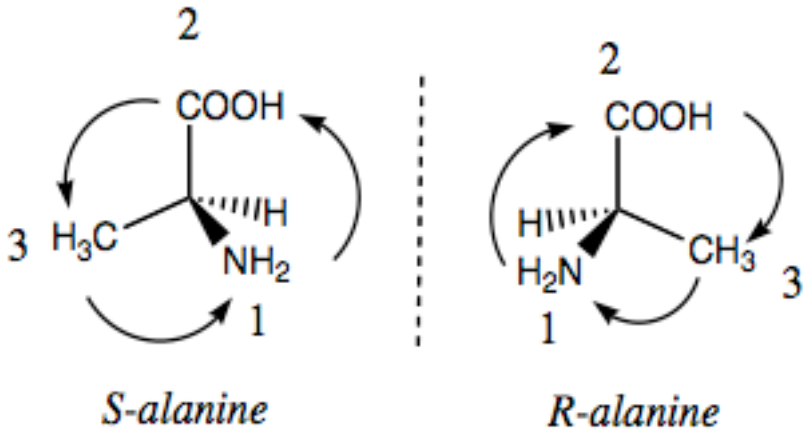

Figure 1.8: S and R Enantiomers of Alanine

Axial chirality is a special case of chirality where the molecule does not possess a chiral center. Instead, the element of chirality is presented as chirality about an axis. The axis of chirality is recognized as an axis about which a set of substituents is held in a spatial arrangement that is not superimposable on its mirror image. Enantiomers of axially chiral compounds are usually given the stereochemical labels R_a and S_a (where the subscript "a" denotes axial chirality). The enantiomers of axially chiral compounds are designated with the same CIP priority rules for tetrahedral centers.[30] The chiral axis is viewed end-on and the nearest and two furthest substituents on the axial unit are ranked by priority. A 3D structure is required to determine the R and S conformations of axial chiral molecules. BINAP (2,2'-bis(diphenylphosphino)-1,1'-binaphthyl) is a molecule that exhibits axial chirality (Fig. 1.9).

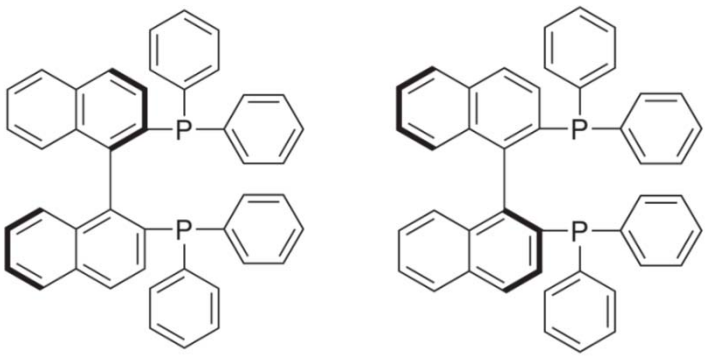

R S

Figure 1.9: BINAP, an Example of Axial Chirality

Planar chirality is observed in molecules that have two planar or *pseudo* planar rings that have restricted rotation about the connecting bond. Designations of enantiomers exhibiting planar chirality are assigned as follows: enantiomers, R_p and S_p (where the subscript "p" denotes planar chirality), are initiated by selecting a plane that contains as many atoms as possible. The descriptor is determined by viewing the chiral plane from the out-of-plane atom closest to the atom of highest priority, which is chosen according to the Cahn-Ingold-Prelog (CIP) system. This atom is denoted as the pilot atom and assigned as atom number one. If the three adjacent atoms, labeled a, b, c, have a clockwise array in the chiral plane when viewed from the pilot atom, the descriptor is R_p. If they have a counterclockwise array, then the descriptor is S_p.

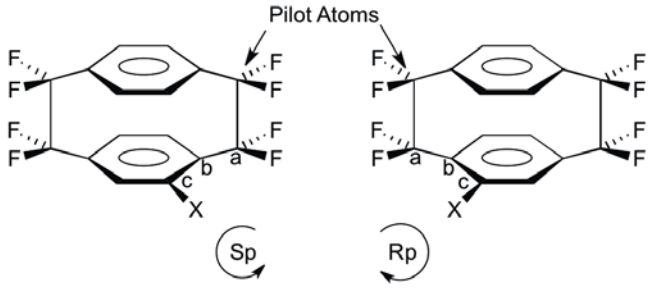

Figure 1.10: Planar Chirality Designation of Enantiomers

Appropriately substituted [2.2]Paracyclophane derivatives can exhibit planar chirality and are designated R and S as described in Fig. 1.10.

Nuclear Magnetic Resonance (NMR)

Nuclear Magnetic Resonance (NMR) is one of the most common techniques used for the analysis of chiral compounds.[31] NMR has unmatched versatility as an analytical technique as much information can be revealed about chemical compounds from a small sample. NMR can be used for many types of compounds and over half of the elements on the periodic table have an NMR active isotope. In order to be NMR active, isotopes must have an odd atomic number or an odd atomic mass. Fluorine-19, Carbon-13, and Hydrogen-1 are all NMR active nuclei and they represent the major amount of atoms in each of the samples analyzed in this thesis. Organic chemists prefer NMR to other types of spectroscopic analysis as NMR provides a convenient, informative, and non-destructive technique. For these reasons, the use of NMR to determine enantiomeric purity is desirable.

Some of the most common NMR machines are 300 MHz and have the capability to measure proton spectra at 300 MHz, carbon spectra at 75.5 MHz and fluorine spectra at 282 MHz.[23] Most of the spectra presented in this thesis were run on a Varian 300 MHz NMR machine.

Chapter 2: Experimental and Basic NMR Introduction

Experimental

Each of the compounds to be used for analyses (Fig.2.1) were synthesized and/or purified according to the literature procedures.[21,24] The synthesis scheme of one of these derivatives, OFP-NH_2, is demonstrated in Scheme 2.1. The primary method of purification was column chromatography using silica gel.

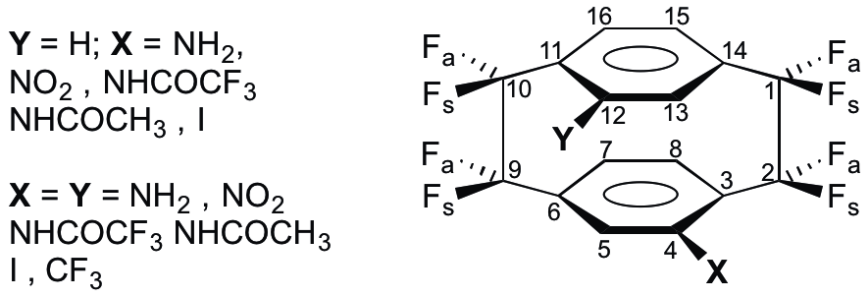

Figure 2.1: Synthesized Mono- and Di-substituted Compounds

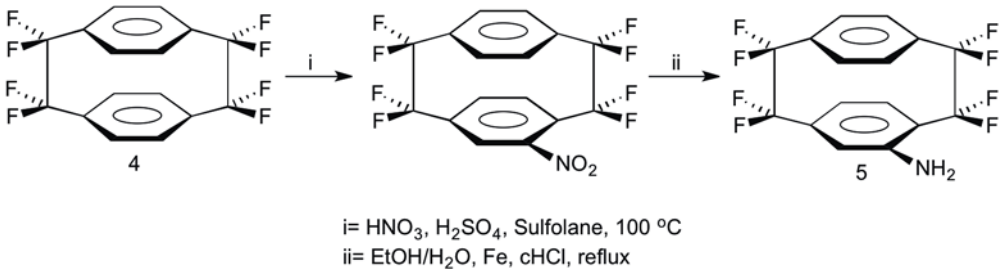

Scheme 2.1: Synthesis of OFP-NH_2 (5)

NMR Characterization of OFP and OFP-NH_2

Cyclophanes have very appealing spectroscopic properties, which increased the interest

in analyzing these compounds. ^{1}H and ^{19}F NMR spectra of all the above compounds **(**Fig.2.1) were obtained and studied but only the compounds providing the most resolved and separated spectra will be thoroughly investigated. ^{1}H and ^{19}F NMR is often used to explore the spectroscopic and structural properties of bridge fluorinated compounds such as those synthesized for this research.

^{1}H NMR Analysis of OFP-NH_2

OFP (Fig.2.2) with unsubstituted benzene rings has three planes of symmetry. These symmetrical aspects are designated as follows; the first plane of symmetry can be drawn through the center of the bridges, the second through the top half of each ring horizontally, and the third through the top half of each ring vertically.

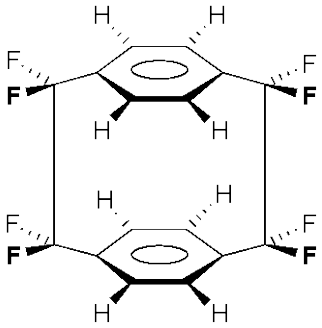

4

Figure 2.2: Eight Chemically Identical Protons of OFP

These symmetrical characteristics render all of the protons to be chemically equivalent. All eight aromatic protons are identical and are displayed as a single resonance and appear as a singlet at 7.3 ppm.[23] This assumes that the J_{F-H} coupling is too small to

observe on our 300 MHz NMR machine. One of the most appealing aspects of cyclophane NMR is the effect of ring substitution on the spectra. When a single hydrogen on the ring is replaced by a different substituent, the three planes of symmetry are destroyed. It is for this reason that monosubstituted derivatives, like OFP-NH_2, feature seven different aromatic hydrogen signals in the ^{1}H NMR (Spectrum 2.1). These signals are strongly influenced by the "*gem* effect" and the shielding and deshielding effects of the substituents. The "*gem* effect" shifts the pseudo-*geminal* substituent downfield as it becomes deshielded compared to the other peaks in the spectrum. This shift is primarily caused from the gem position's close proximity in space to the substituent. Electron donating substituents have a shielding effect that tends to shift peaks upfield while the electron withdrawing substituents demonstrate a deshielding effect and tend to shift peaks downfield.[32]

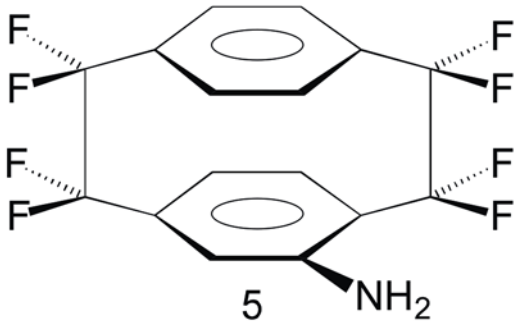

Figure 2.3: Monosubstituted OFP-NH_2

Electron withdrawing or donating ability of substituents impact the chemical shifts of all aromatic protons on the cyclophanes analyzed. The amino substituent, which is electron donating, shifts most peaks downfield. Seven aromatic hydrogen signals are observed in

the ^{1}H NMR spectrum of OFP-NH_2, like all mono substituted OFP derivatives, but there is also a signal that stems from the protons from the amino substituent (-NH_2).

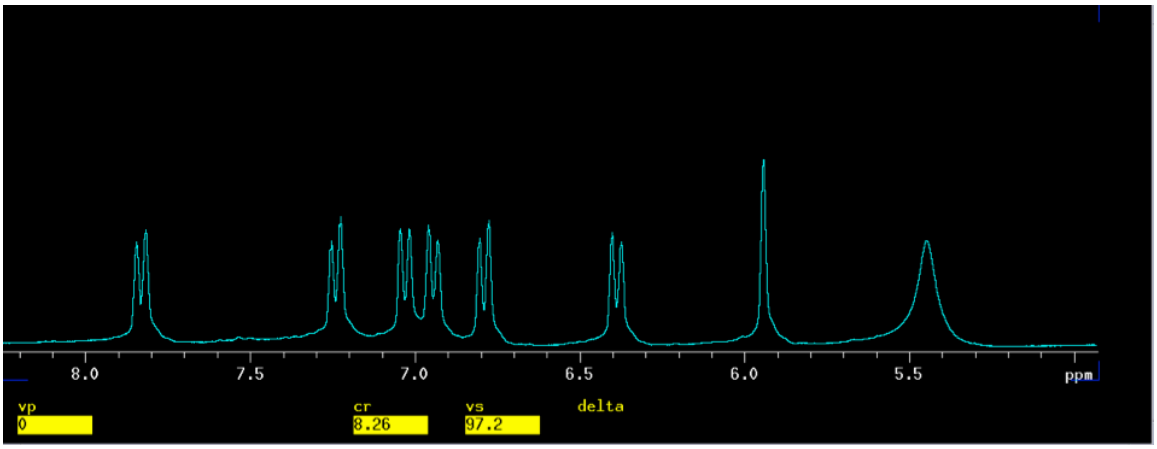

Spectrum 2.1: ^{1}H NMR Spectrum of OFP-NH_2

The aromatic hydrogen signal that appears at approx. 5.9 ppm (Spectrum 2.1) was predicted to be the singlet from the *ortho* proton. The *ortho* proton would be the only aryl proton to not have a $^{3}J_{H-H}$ coupling as the amino substituent is located three bonds away. A sharp singlet would be observed from this proton only. Like most ^{1}H NMR spectra of paracyclophane derivatives, the doublet that is shifted furthest downfield should stem from the *gem* proton, which is transannularly adjacent to the functional group. This effect stems from that particular substituent being affected through the close proximity in space to the amino group, or other, substituent.[4]

Splitting patterns for NMR are often seen as with varying peak multiplicity (doublets, triplets, etc.), however, when the chemical shift difference in Hertz is of the same order

as the J coupling, new patterns in the spectrum are revealed. These patterns are most often seen as a leaning of a pair of doublets towards one another. The resultant pairs of doublets are referred to as an AB system. The AB designation is used to indicate the closeness in chemical shift of the two nuclei as A and B are close to each other in the alphabet. (Other letters may be used to indicate an increased difference in chemical shift such as an AX system where X can be any letter of the alphabet. The further from X=B, the increased difference in chemical shift). Figure 2.4 demonstrates how a decrease in the J coupling constant can bring the AB quartets closer to one another.[34] AB quartets are seen in the ^{1}H and ^{19}F NMR spectra of OFP derivatives and will appear in spectra throughout this thesis.

Figure 2.4: AB Pattern Diagram [34]

^{1}H NMR of OFP-diNH_2

For the compounds studied here, if a second substitution takes place on the unsubstituted ring, the substitution reintroduces an element of symmetry. Shown in Fig. 2.5 are the three isomers that are formed from this additional substitution.

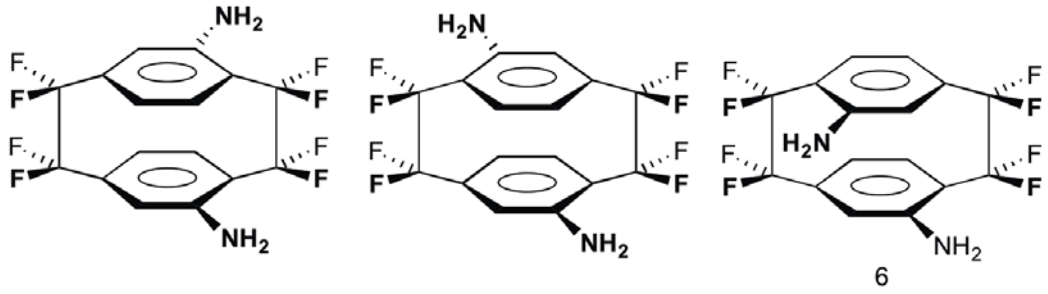

Figure 2.5: Di-NH_2 Derivatives: pseudo *meta*, pseudo *para*, pseudo *ortho*

^{1}H spectra of ortho' diNH_2 show one singlet at approximately 6.78 ppm and two doublets, one at approximately 6.40 ppm and one at 6.94 ppm (Spectrum 2.2). The three peaks that are shown stem from the aromatic ring protons. The amino peak that is not shown, would be further upfield at approximately 5.25 ppm. The ^{1}H NMR of the *pseudo ortho* derivative (Fig. 2.5c) is shown in Spectrum 2.2.

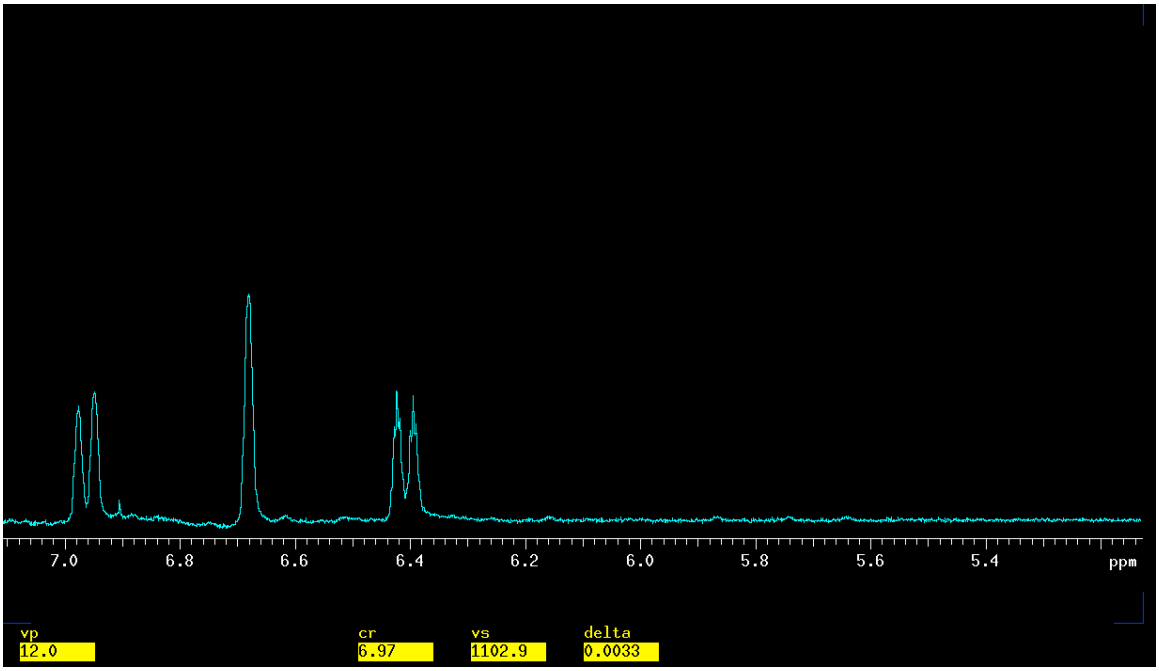

Spectrum 2.2: ^{1}H NMR of OFP-diNH$_2$

A prime example of an AB quartet is seen in Spectrum 2.2. The doublet that appears at 6.40 ppm and the doublet at approximately 6.94 ppm arise from adjacent protons on the aromatic ring of OFP-NH$_2$. Doublets slope towards one another, which is typically a characteristic of an AB pattern.

^{19}F NMR Analysis of OFP-NH$_2$

The unsubstituted OFP molecule has the three planes of symmetry discussed earlier in the ^{1}H NMR section. It is due to this symmetry that all eight bridge fluorines are chemically equivalent and therefore give a single signal which is a singlet (if the J_{FH} is too small) in the ^{19}F NMR at approximately $\delta = -117$ ppm.

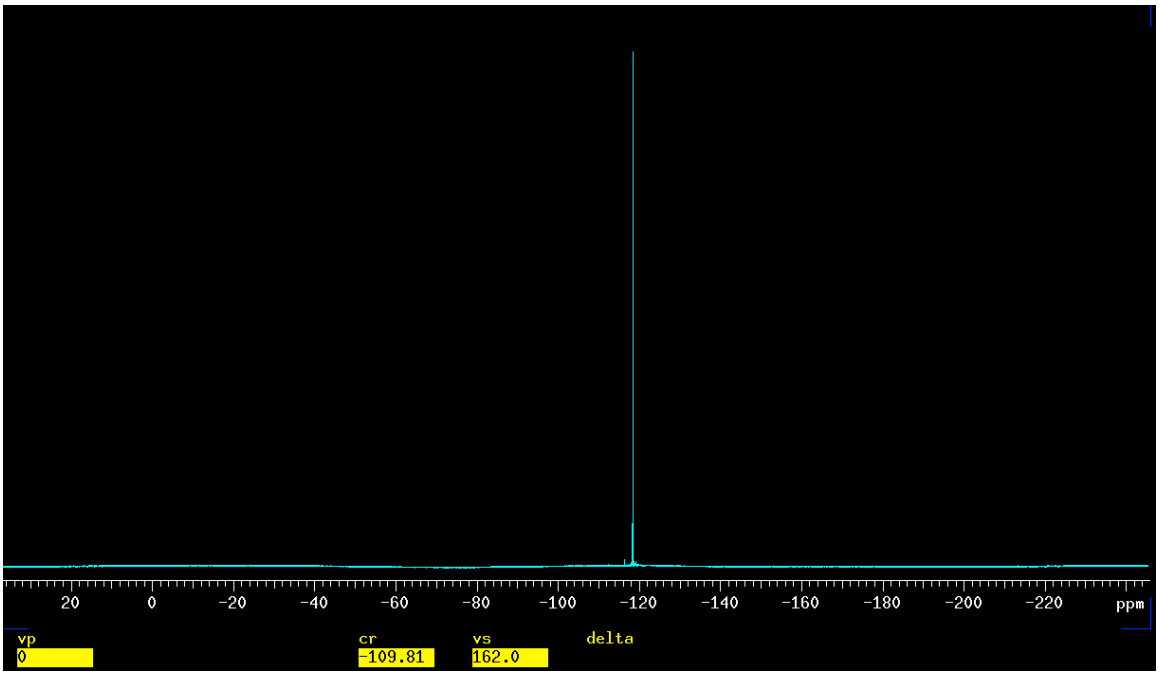

Spectrum 2.3: ^{19}F NMR of OFP

Once again, the substitution of an amino group for an aromatic ring hydrogen destroys all of the symmetry and renders all eight fluorines as both chemically and magnetically different (eight fluorine signals).

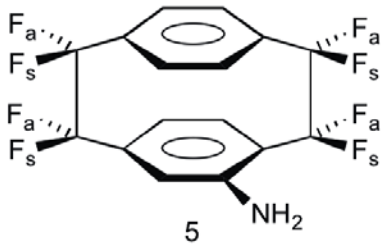

5

Figure 2.6: *anti* and *syn* Fluorines Indicated on OFP-NH_2

The ^{19}F NMR spectrum of OFP-NH_2 has many peaks spread out in a very small area spanning from approximately -105 to -120 ppm with $^{2}J_{F\text{-}F}$ values of about 240 Hz. This full spectrum is shown below (Spectrum 2.4).

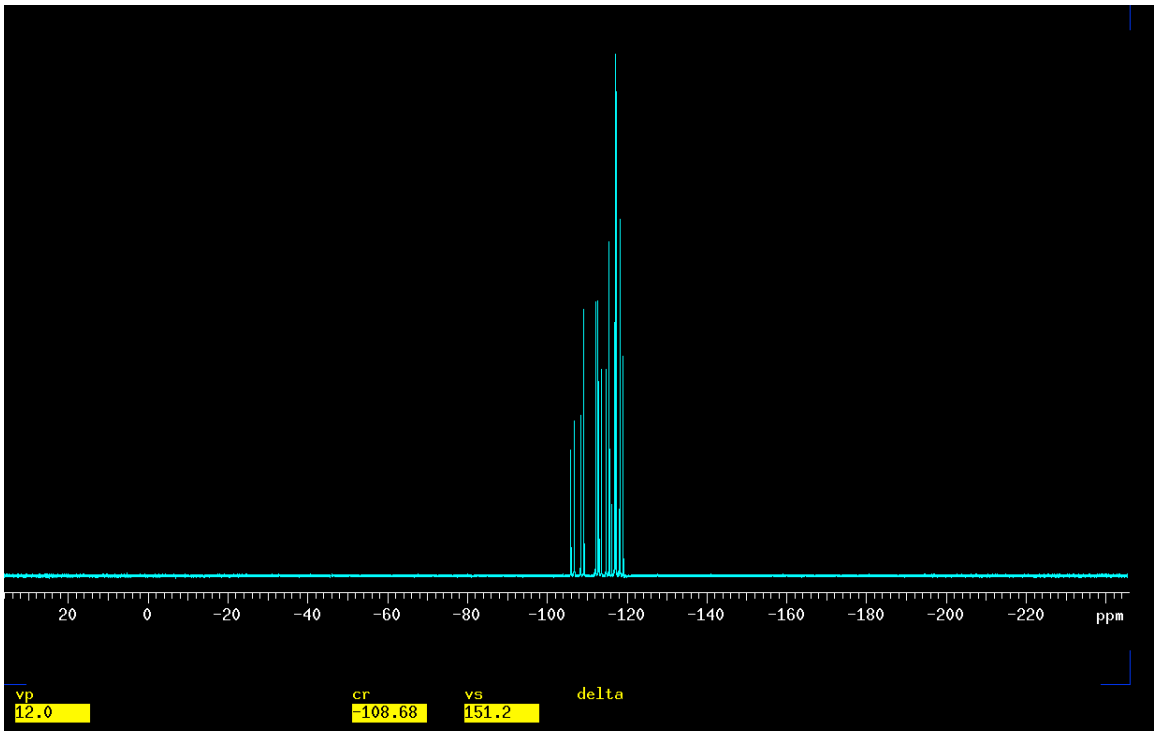

Spectrum 2.4: ^{19}F NMR Spectrum of OFP-NH$_2$

For analysis, the spectrum needs to be expanded to reveal the information contained in this concentrated spread of peaks (Spectrum 2.5). The integration of 1:1:2:1:3 is shown in this spectrum and verifies that all eight fluorines are represented. With eight fluorines giving sixteen peaks, it was evident that each of the bridge fluorines gave rise to a doublet.

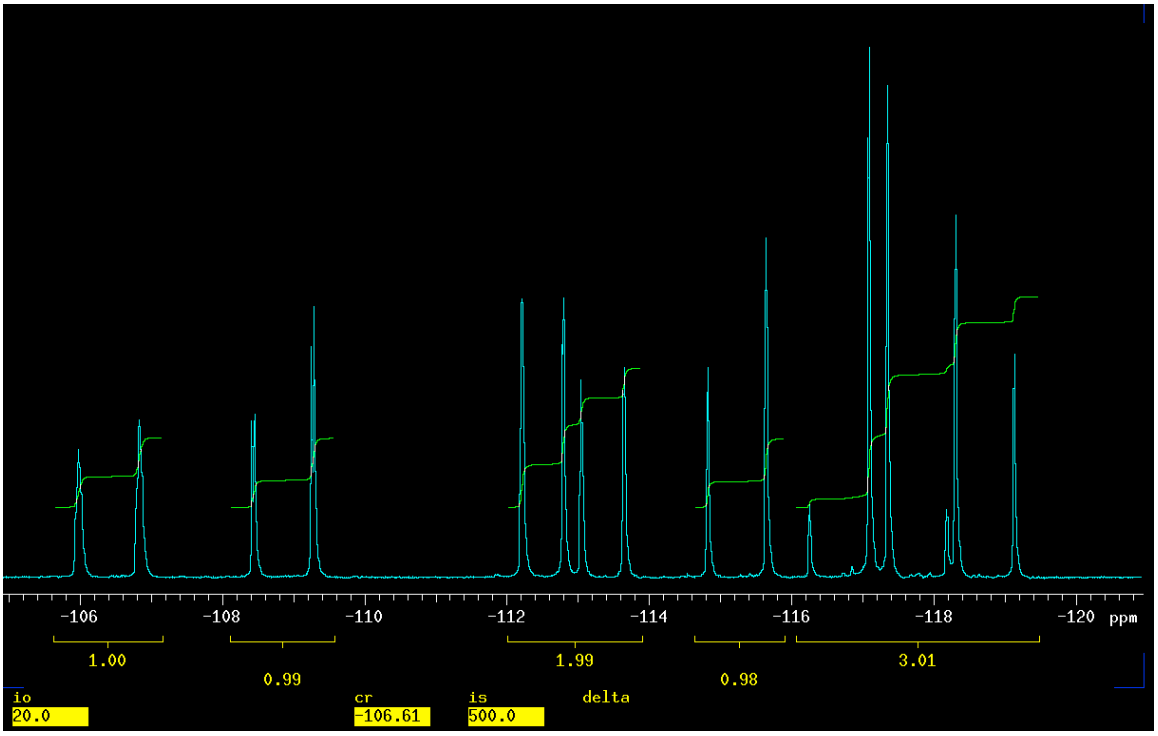

Spectrum 2.5: Expanded ^{19}F NMR of OFP-NH_2 w/Integration

These eight doublets are members of an AB system and, in actuality, four AB quartets. The four geminal pairs of fluorines, which give rise to this AB pattern, are shown in Fig. 2.7. Each of the bridge fluorines show a strong coupling to and are split by their geminal partner ($^2J_{FF}$). It is because of this splitting that each fluorine gives rise to a doublet in the spectrum. The splitting patterns and coupling constants are in place such that an AB pattern is present.

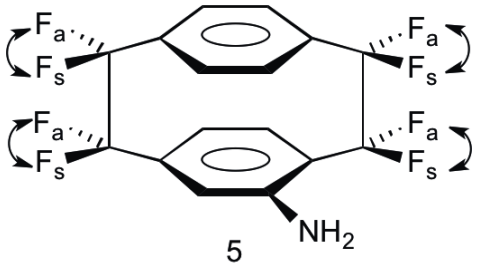

5

Figure 2.7: The Four AB quartets of OFP Derivatives

As depicted in Figure 2.7 the four AB quartets consist of each pair of bridge fluorines, F-1s and F-1a, F-2s and F-2a, etc. It is the strong coupling of each fluorine to its geminal fluorine partner that gives rise to these eight doublets (four AB quartets).

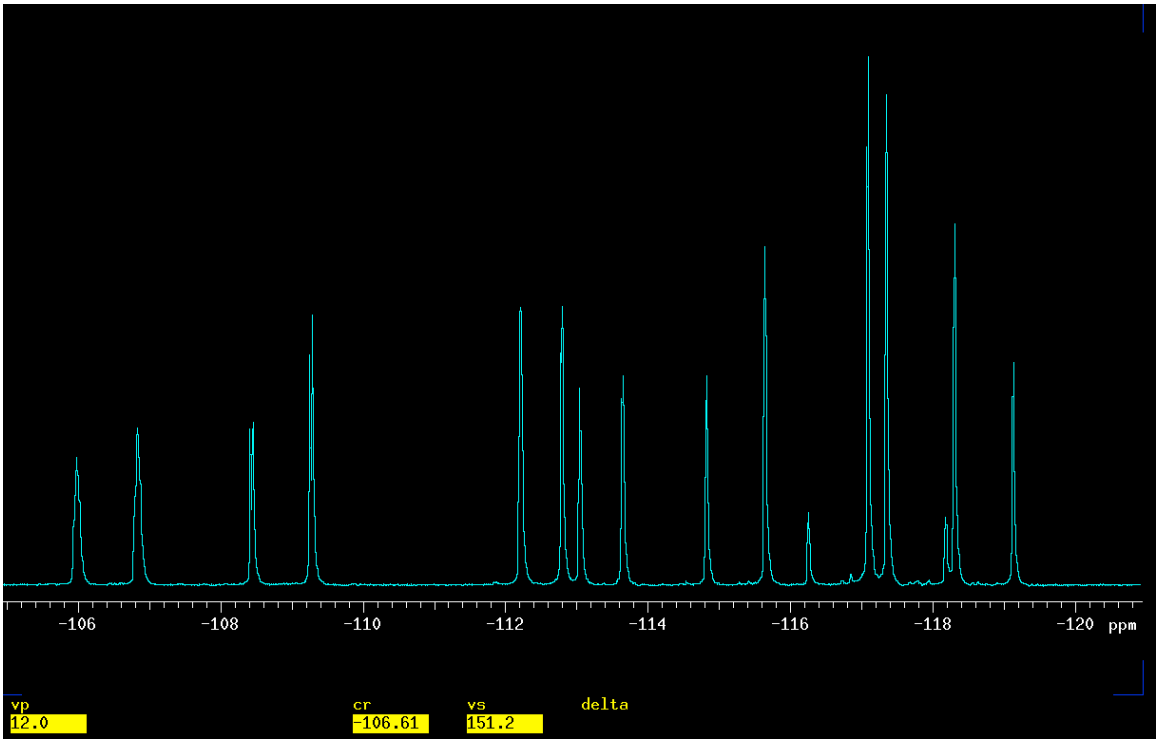

Spectrum 2.6: ^{19}F NMR of OFP-NH$_2$

Splitting Spectrum 2.6 into two parts by dividing it at -114 ppm, two AB quartets will be present in each of the two halves. The quartets that are furthest upfield from -115 to -119 ppm are almost perfectly symmetrical with the two doublets that are more shielded sloping away from each other and the two deshielded doublets doing the same but having

a greater difference in peak intensity. The half of the spectrum that is furthest downfield also has a pair of AB quartets that are slightly less obvious to identify the coupled doublets initially.

One doublet in Spectrum 2.6 appears as a doublet of doublets but none of the other doublets show this effect. Upon assignment of the doublets at -109 to -110 ppm, it was shown that particular fluorine atom showed a strong coupling to its geminal fluorine but it also had a weaker coupling to a vicinal fluorine on the bridge. The strong coupling results in the doublet and that doublet is split into a doublet of doublets by the weaker coupling to the vicinal fluorine.

The ^{19}F NMR of the disubstituted analog displays eight peaks. The increase in symmetry results in the F-1s and F-1a being equivalent to F-9s and F-9a. Also, F-2a and F-2s are equivalent to F-10a and F-10s. The four resultant doublets visible in this spectrum each arise from the two different geminal pairs of fluorines on the bridge.

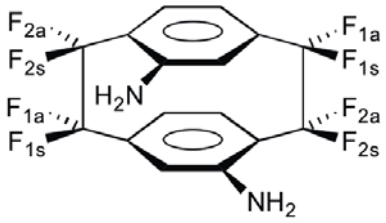

6

Figure 2.8: *anti* and *syn* Fluorines Indicated on *ortho'* OFP-diNH_2

The four doublets are more specifically, two AB quartets. From this spectrum it also appears that the doublet that is furthest downfield at -108 ppm is a doublet of doublets (Spectrum 2.7). F-1s shows the same splitting patterns as the mono substituted analog.

So the two fluorines at that particular position on the bridge will be strongly split by their geminal partner but will also show a weaker coupling and therefore smaller splitting to a vicinal fluorine.

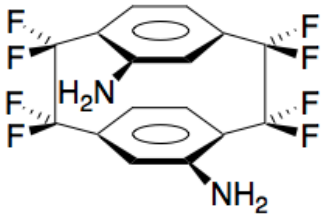

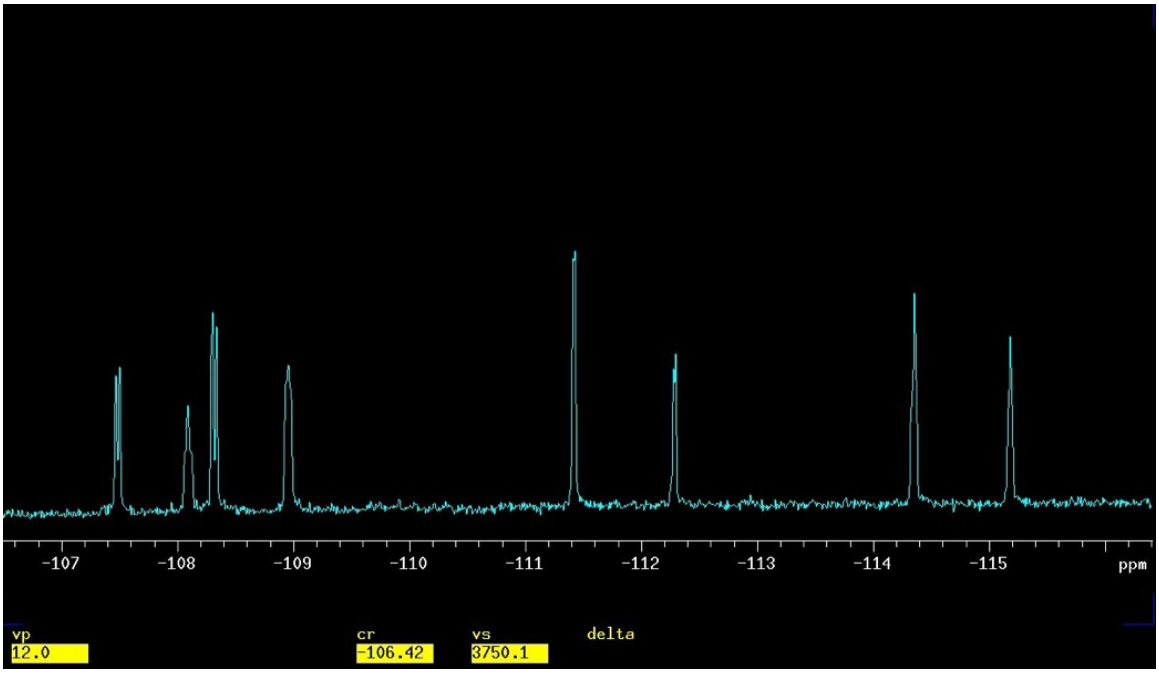

Spectrum 2.7: ^{19}F NMR of *ortho*' OFP-diNH$_2$

Chapter 3: Unambiguous Atomic Assignment of the ^{1}H,^{13}C, and ^{19}F NMR for OFP-NH_2

NMR characterization of cyclophanes has been of major analytical importance to organic chemists for many reasons including those discussed earlier in this thesis. Previously, the NMR of these cyclophanes had been used for structural confirmation but individual unambiguous atomic assignments were not yet assigned. The research presented here led to a change in that reality. Designation of these unambiguous assignments was accomplished with several NMR experiments, 1D and 2D, COSY and HETCOR performed on a Varian 300 MHz NMR machine. These findings were further verified with additional NMR experiments, Nuclear Overhauser Effect (nOe) performed on a higher field NMR machine, which also had multiple high field channels. The work discussed here was published in the journal of Magnetic Resonance in Chemistry in 2005. Much of the research contained in this chapter is taken from that paper.[35]

^{1}H and ^{13}C NMR assignments

OFP is a symmetrical molecule as discussed in chapter two and the addition of any ring substituent gives rise to chemically non-equivalent nuclei and therefore more complicated spectra. Similar effects are seen for all the nuclei studied i.e., ^{1}H, ^{19}F, and ^{13}C, and each will be analyzed in this thesis.

4-Amino-1,1,2,2,9,9,10,10-octofluoro[2.2]paracyclophane, (OFP-NH_2), is the resulting compound when an amino substituent is added to one of the rings. This amino substitution affects the NMR spectra for all of the nuclei on the compound. The once

chemically equivalent nuclei are now all distinctly unique. The rest of this chapter will give insight into the experimentation and analysis that allowed for the unambiguous proof of which atom gives rise to which peak for each of the atomic nuclei in OFP-NH_2.

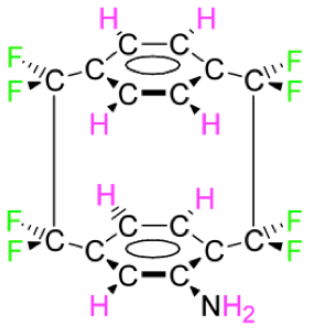

Figure 3.1: Chemically Different Atoms of OFP-NH_2

There are eight chemically different hydrogen and fluorine atoms and sixteen different carbon atoms in one molecule of OFP-NH_2. Analysis begins with the hydrogen assignments. As well as the usual numbering of the hydrogen atoms (Fig. 3.2) the eight chemically different hydrogens are given specific name designations.

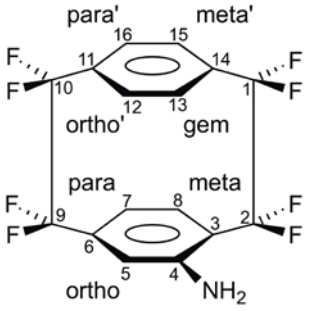

Figure 3.2: Numbering Scheme and Aryl Positions for OFP-NH_2

Hydrogen-5 (H-5) is deemed the *ortho* position, H-7 the *para* position, and H-8 the *meta* position. As the identification moves to the upper deck, the protons are labeled with the

same name but now with a prefix of pseudo. H-12 is the pseudo *ortho* (ortho'), H- 15 pseudo *meta* (meta'), and H-16 pseudo *para* (para'). The last proton that is located directly above the amino substituent, H-13, is given the position name of pseudo *gem* ,the geminal or "twin" position. The pseudo *gem* proton may also be simply referred to as the *gem* proton as there is no *gem* position on the lower ring for comparison. The latter naming will be used throughout this thesis.

The eight chemically different hydrogens give rise to the ^{1}H NMR spectrum of OFP-NH_2 (Spectrum 3.1).

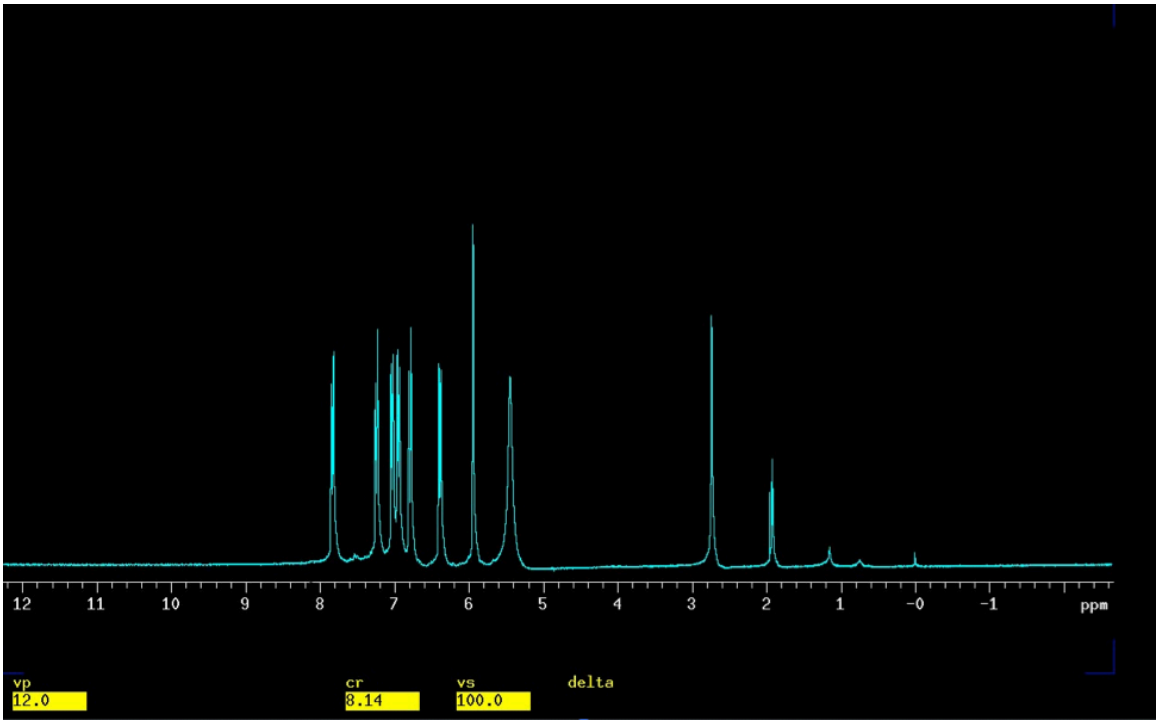

Spectrum 3.1: ^{1}H NMR of OFP-NH_2 d_6-Acetone

The ten peaks in Spectrum 3.1 could be presumed and explained as one peak from each of the chemically different hydrogens and one from the solvent (along with the expected

deuterated acetone solvent peak, 1.99 ppm, and dissolved water, 2.79 ppm) but which peak arises from which Hydrogen?

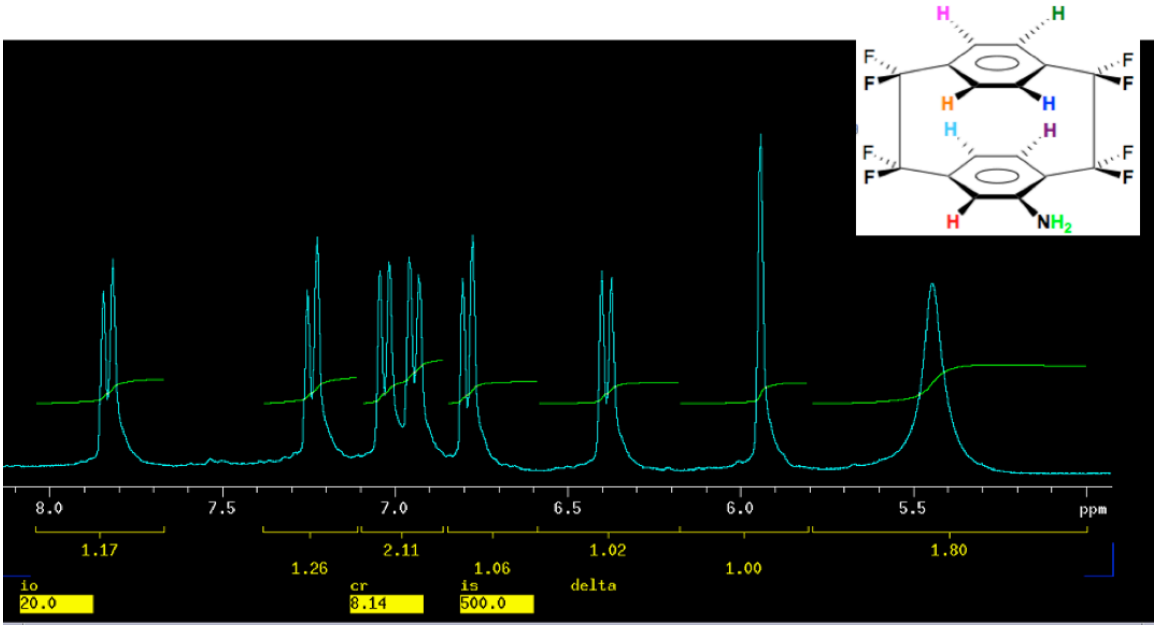

Spectrum 3.2: Expanded ^{1}H NMR of OFP-NH$_2$

An expanded view of ^{1}H NMR of OFP-NH$_2$ (Spectrum 3.2) shows an integration of 1:1:2:1:1:1:2 for a total of nine hydrogens. The integration at approximately 6.80-7.15 ppm is resultant of the two doublets under that integration curve but the only other peak with integration of two is seen at approximately 5.4 ppm. This peak, which is a broad singlet, could only be derived from one possible signal, the nitrogen's protons. The two hydrogens that are a part of the amino substituent are the only two hydrogens that are chemically equivalent and therefore would be interpreted by NMR to give a single signal with integration of two. Therefore, this broad singlet must be derived from the amino hydrogens, green dot above it. The other singlet at approximately 5.9 ppm has an integration of one. The only hydrogen on the molecule anticipated to be a singlet with an integration of one would be the *ortho* hydrogen (H-5). The *ortho* hydrogen does not have

any adjacent neighbors to couple to or be split by and so a single signal, a singlet, would arise only from the *ortho* hydrogen, light blue dot above it.

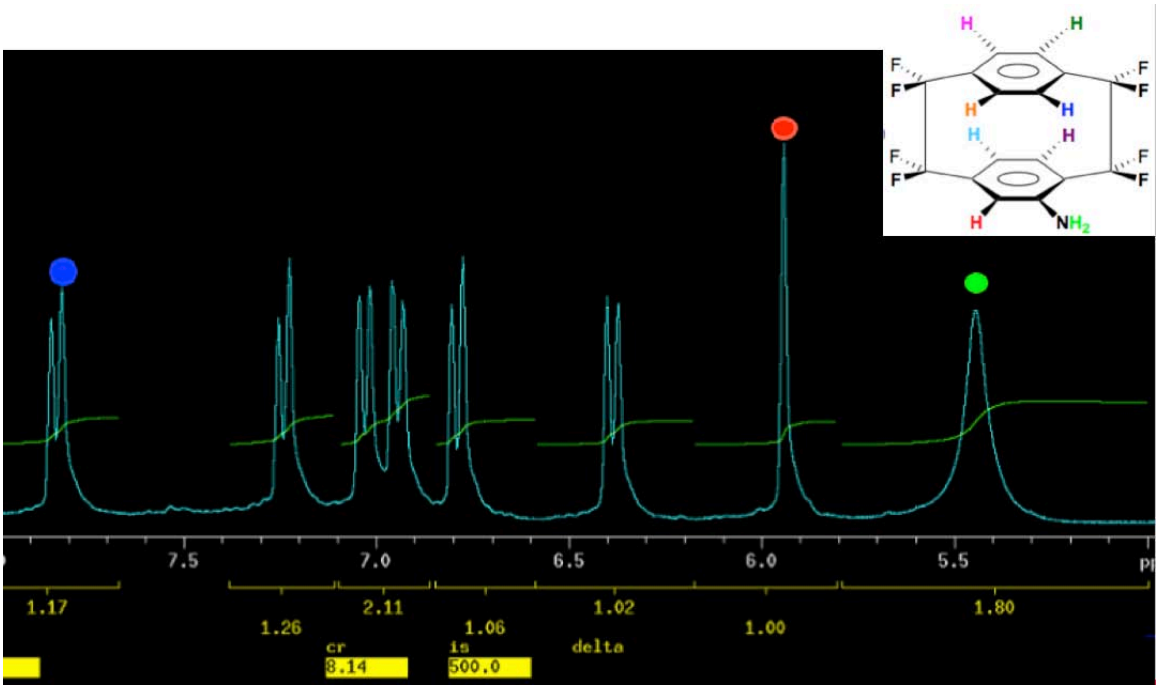

Spectrum 3.3: Expanded ^{1}H NMR of OFP-NH$_2$ With Some Proton Designations

One other signal can be assigned just upon inspection; the doublet that appears at approximately 7.8 ppm with an integration of one would arise from the *gem* position hydrogen. The *gem* shift would shift this positioned proton downfield, because of the deshielding of this nucleus, and away from the other aromatic proton signals and would have to be this doublet. The doublet arises from the splitting of the *gem* position proton, red dot above it, with the pseudo *ortho* proton.

^{13}C NMR spectrum of OFP-NH_2

There are sixteen chemically different carbons and four different types of carbons on OFP-NH_2. The four red carbons are positioned on the bridge and described as bridge carbons. The four blue carbons are designated as bridgehead carbons. The green carbons are on the aromatic ring and form C-H bonds and the light blue carbon is also on the ring, shown, but forms a C-N bond.

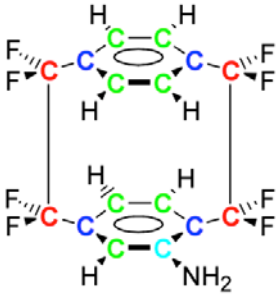

Figure 3.3: Carbons of OFP-NH_2

These sixteen carbons give rise to the ^{13}C NMR spectrum below (Spectrum 3.4). The ^{13}C NMR spectrum of OFP-NH_2 shows that most of the peaks are located between 110 - 140 ppm.

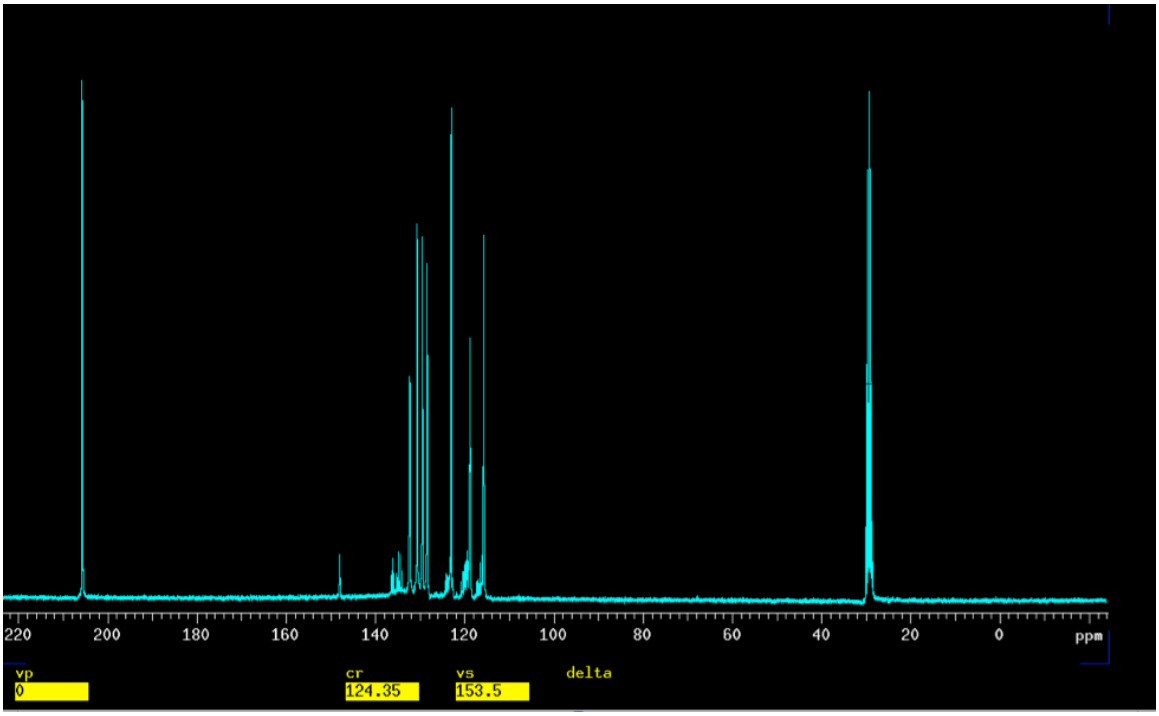

Spectrum 3.4: ^{13}C NMR of OFP-NH_2

Expanding the spectrum in this area can allow for clear investigation.

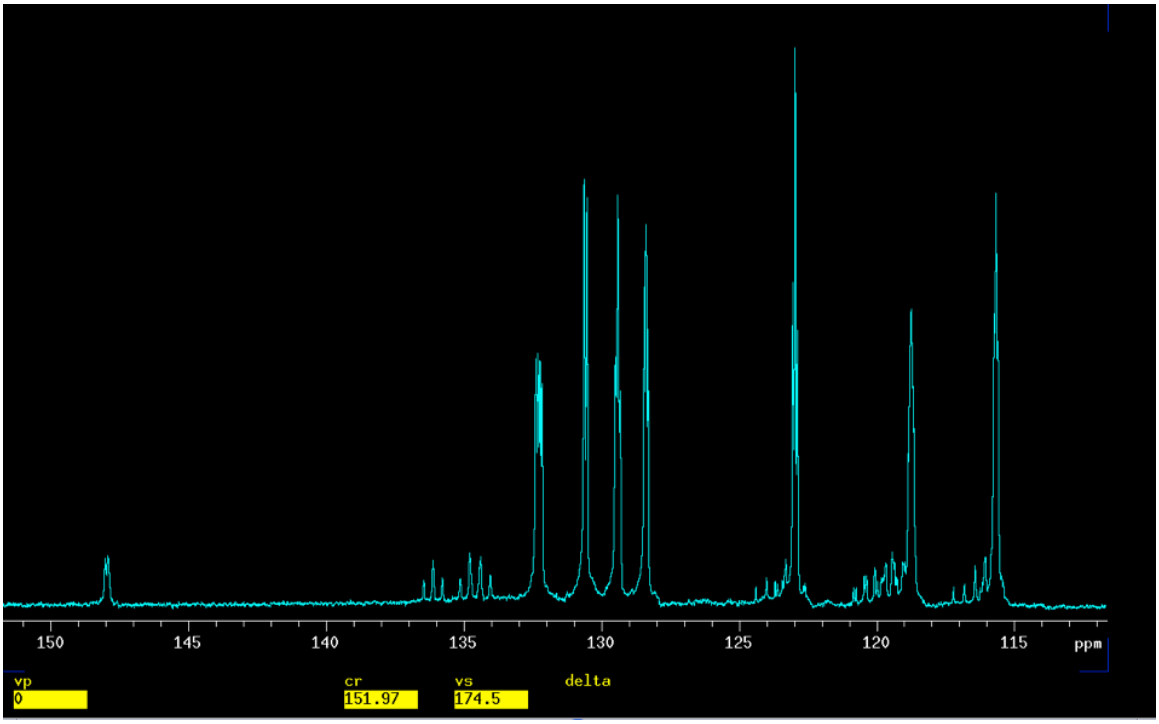

Spectrum 3.5: Expanded ^{13}C {^{1}H} NMR of OFP-NH_2

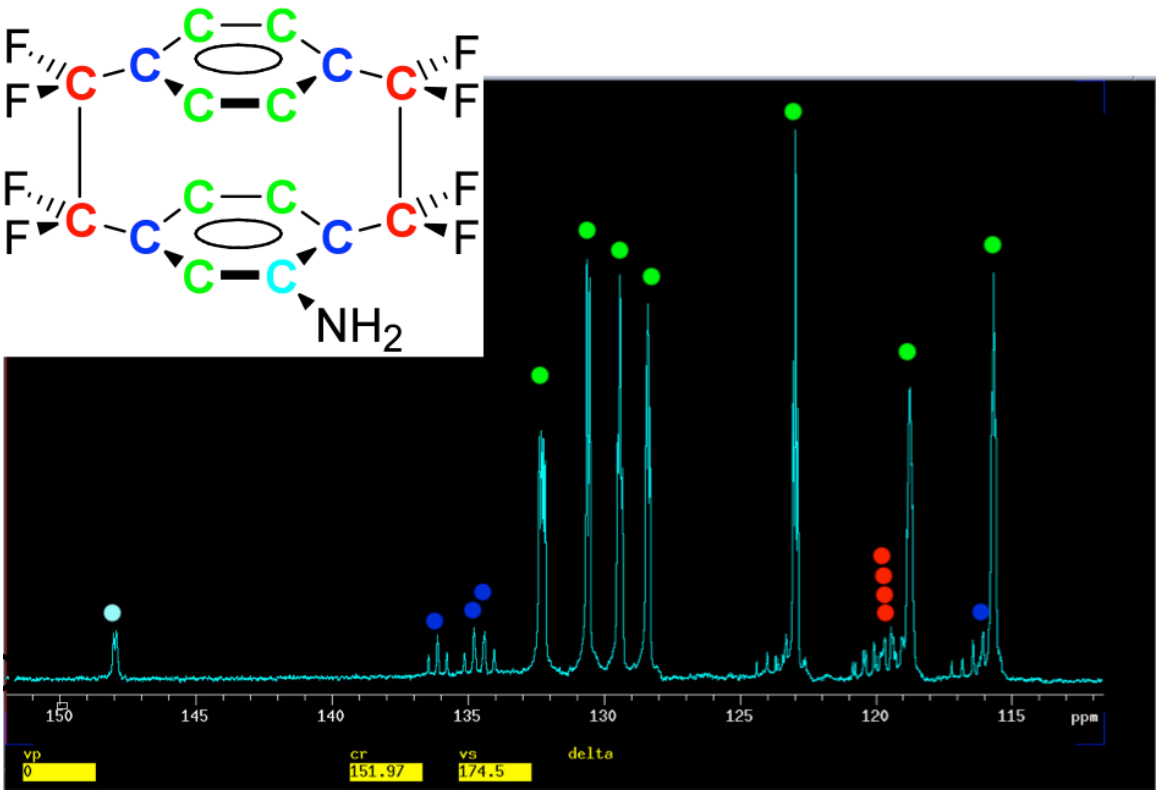

Spectrum 3.6: Expanded ^{13}C {^{1}H} NMR of OFP-NH_2 (color coded)

Chemical shifts, intensity, and apparent coupling allowed for initial peak approximations that correlate to the distinct positions on this structure. The carbon attached directly to the nitrogen (C-4) is located furthest downfield at approximately 147.8 ppm as this carbon is deshielded and has a light blue dot above it. The four bridge carbons are located between 119.0-120.2 ppm and have red dots above them. The blue dots indicated the bridge head carbons and are found in the region of 134-137 ppm and one further upfield at approximately 116 ppm. The aromatic carbons give rise to the most prominent peaks on the spectrum and are designated with a green dot above them. In order to analyze these peaks, isolated expansions will need to be shown. Both Spectra 3.6 and 3.7 are proton decoupled, {^{1}H}, and this allows for the proton coupling to be eliminated so

that the carbon-fluorine coupling can be explored. Decoupling is the result of continually exciting the coupling nuclei, which eliminates the coupling interactions to the detected nuclei.

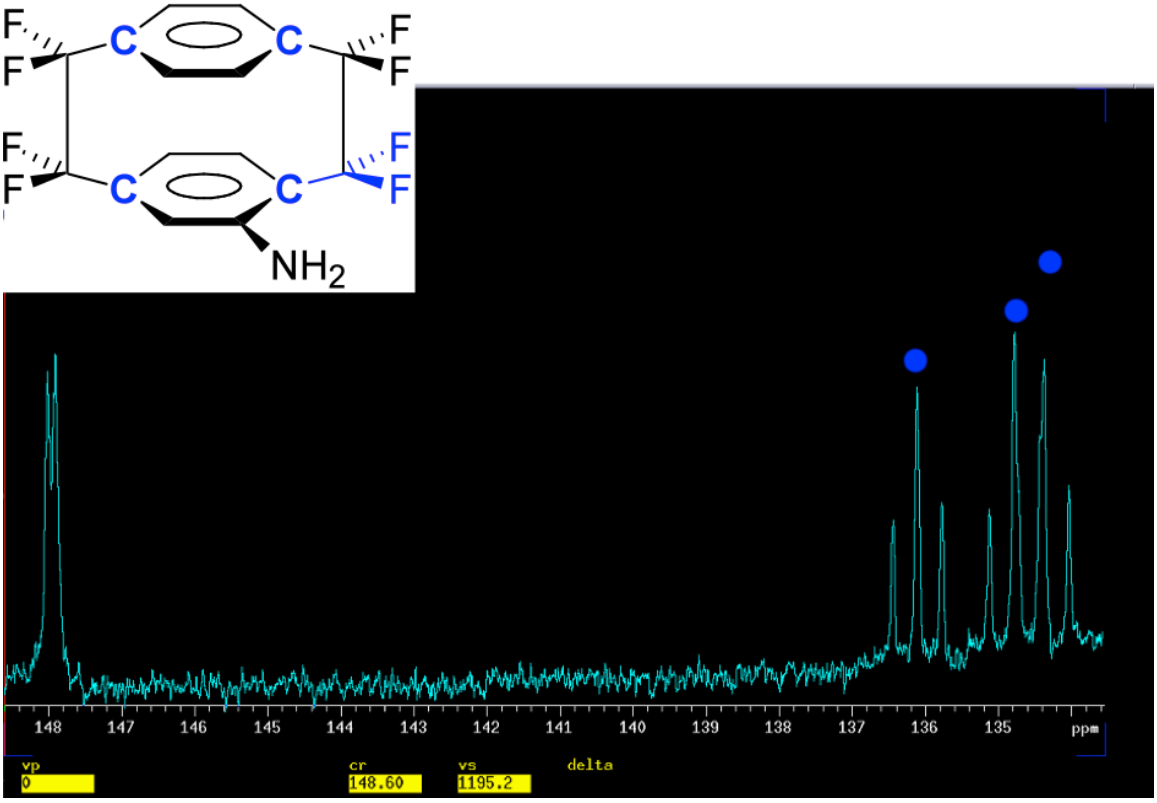

Spectrum 3.7: Expanded ^{13}C {^{1}H} NMR of OFP-NH_2-Bridgehead Carbons

Bridgehead carbons give rise to triplets spread out through 136.3-133.9 ppm three triplets are present, each stemming from one of the bridgehead carbons. Each of these carbons is two bonds away from two fluorines and thus is presented as a triplet. Carbon-3 is in blue above and two bonds away from the two blue fluorines. This carbon would also be two bonds away from the *meta* hydrogen and the splitting would be more complex so this is the reason for the decoupled experiment. The triplet at approximately 135.8 ppm appears

as a true triplet but the other two triplets are actually overlapping and appear to be a quartet but are in fact two triplets.

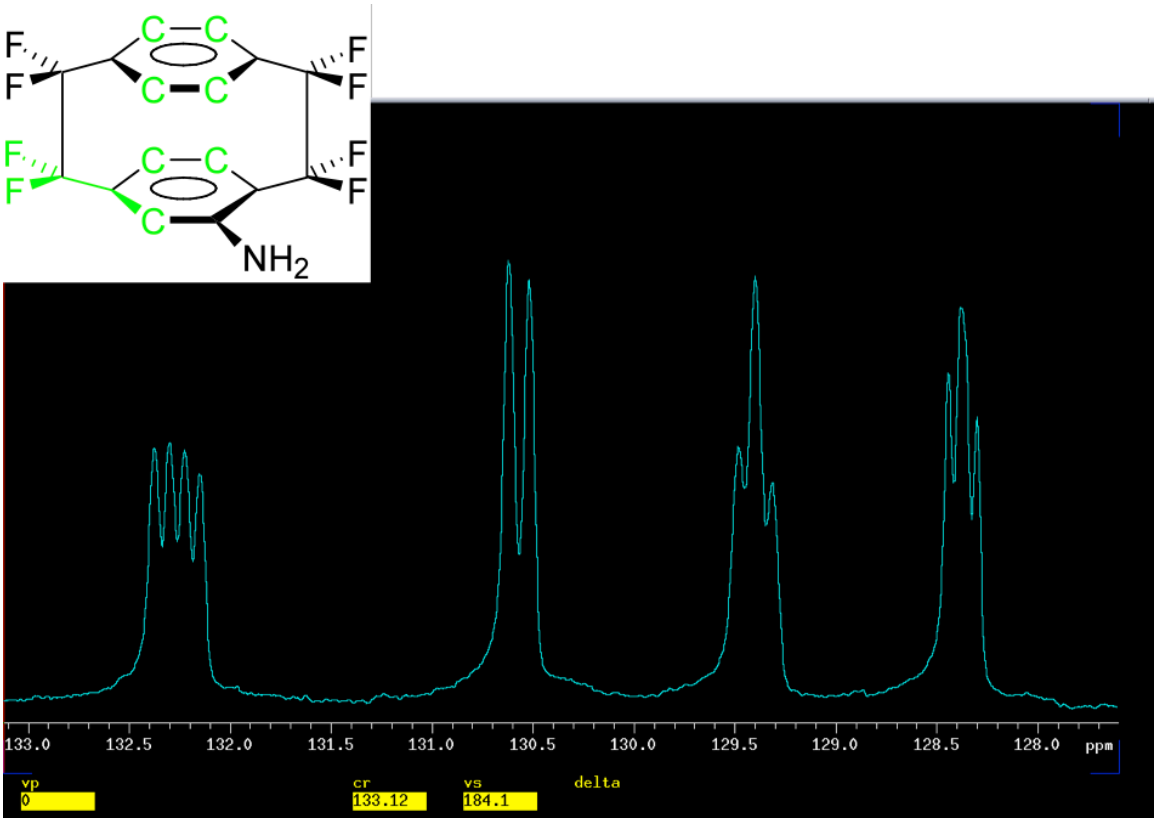

Spectrum 3.8: Expanded ^{13}C {^{1}H} NMR of OFP-NH_2 coupling

Various forms of $^{3}J_{F\text{-}C}$ coupling are seen in this most interesting spectrum. The apparent quartet at approximately 132.1 ppm is in actuality a doublet of doublets. Each of the fluorines on a bridge carbon will both couple to a carbon that is three bonds away resulting in a doublet. Because the coupling of the two fluorines with the same carbon atom are similar but not exactly equal, the peaks overlap slightly to give what would at first glance be a quartet. If the coupling of these two doublets had been equal, then a triplet would have been observed.

The doublet at approximately 130.5 ppm stems from Carbon-15 (established later). Due to the slight rotation of the upper deck ring upon bottom deck substitution, the upper deck rotates slightly away from the substituent and affects the coupling of Carbon-15 to each of the fluorines on Carbon-1. This allows for the Karplus equation to be applied to this specific carbon. The geometry of the slightly rotated carbon forms a dihedral angle of approximately 180^0 to one fluorine and approximately 90^0 to the other. The carbon-fluorine coupling for the 180^0 angle will be approximately 7 Hz and will result in a doublet. The carbon-fluorine coupling for the dihedral angle close to 90^0 will have close to a 0 Hz coupling and so no splitting will be observed from this coupling. C-15 is presented as one signal, which is the only apparent doublet in Spectrum 3.8**.** Two triplets, one at approximately 128.2 and one at 129.2 ppm, are the result of aromatic ring carbons coupling to two geminal fluorines. Each fluorine couples to one carbon slightly differently and a triplet is observed from each carbon.

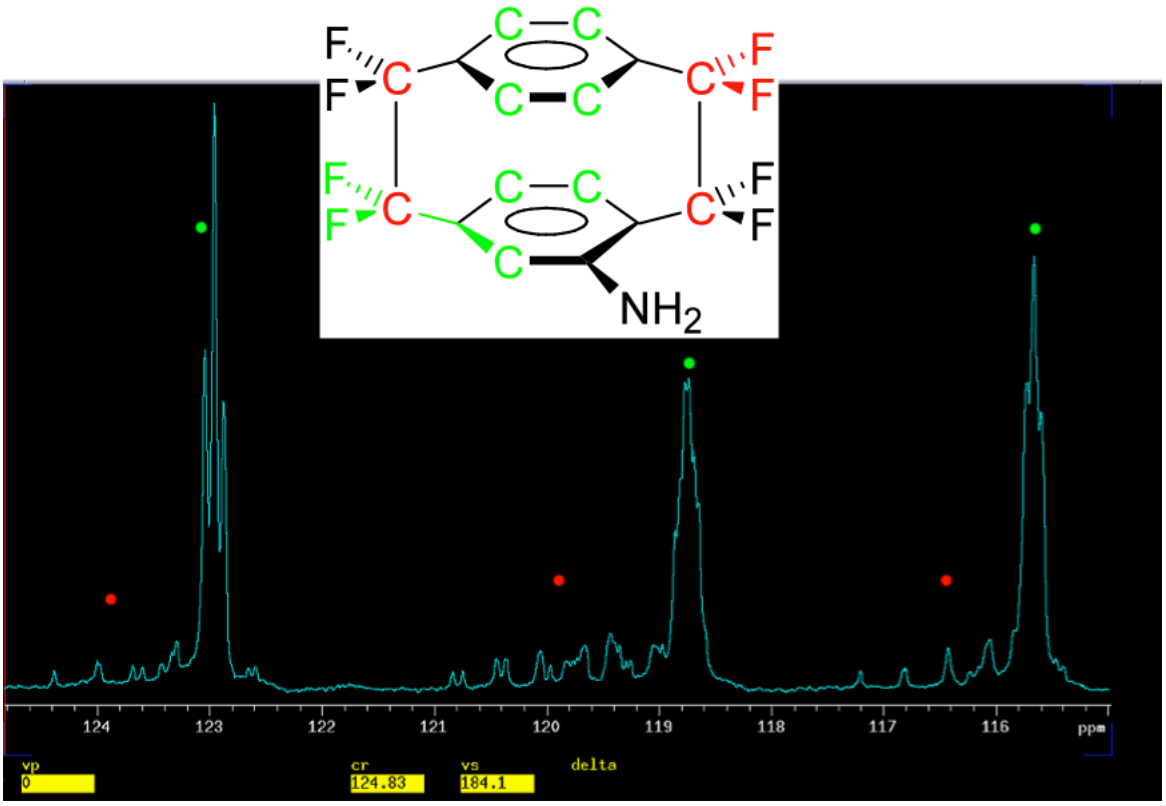

Spectrum 3.9: Expanded ^{13}C {^{1}H} NMR of OFP-NH_2

Tripletesque peaks indicated with a red dot in Spectrum 3.9 are formed from $^{1}J_{F\text{-}C}$ coupling of bridge carbons to their attached fluorines, each one bond away. They are imperfect triplets because there is also a $^{2}J_{F\text{-}C}$ coupling being detected and shown in the signals. Various $^{3}J_{F\text{-}C}$ coupling from ring carbons and *geminal* fluorine pairs are indicated with a green dot above. All of these spectra presented so far help with conformational analysis but few of them can give unambiguous atom to peak assignments.

The $^{13}C\{^{1}H\}$ spectra were examined so far, but further investigation by decoupling the fluorine signals allowed new information to be revealed.

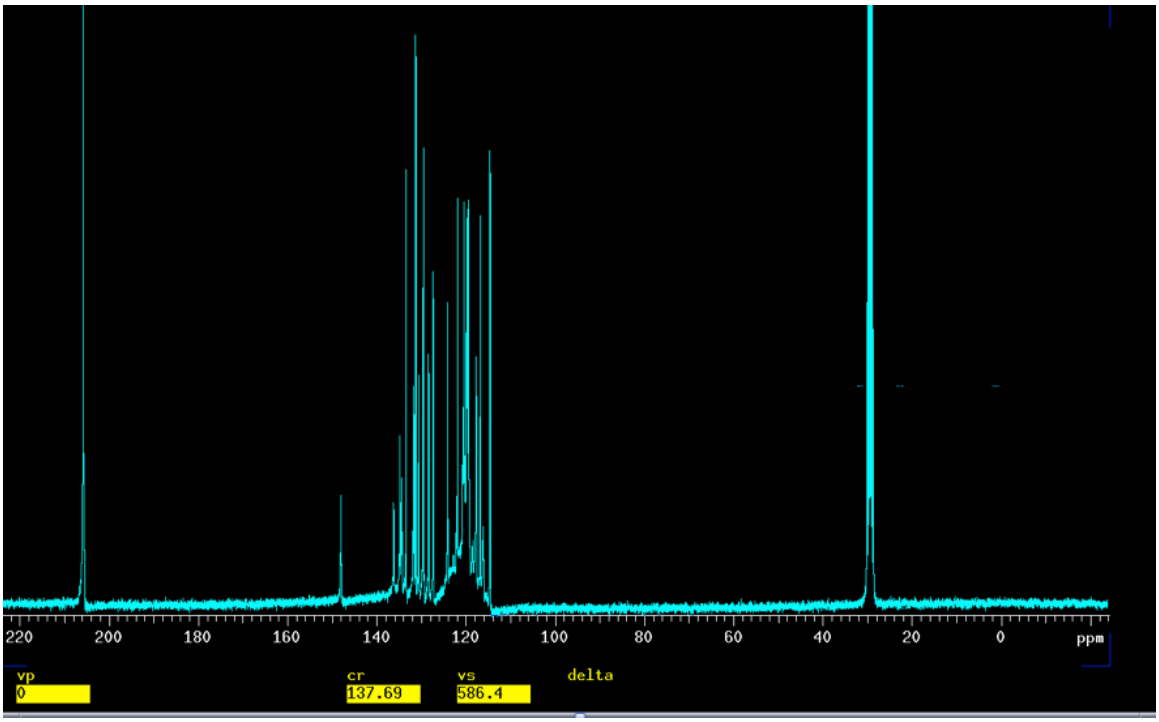

Spectrum 3.10: ^{13}C {^{19}F} NMR of OFP-NH_2

Fluorine decoupling now allows for carbon-hydrogen coupling to be explored. A concentrated area of peaks is seen between 118-136 ppm and this region will need to be expanded for analysis.

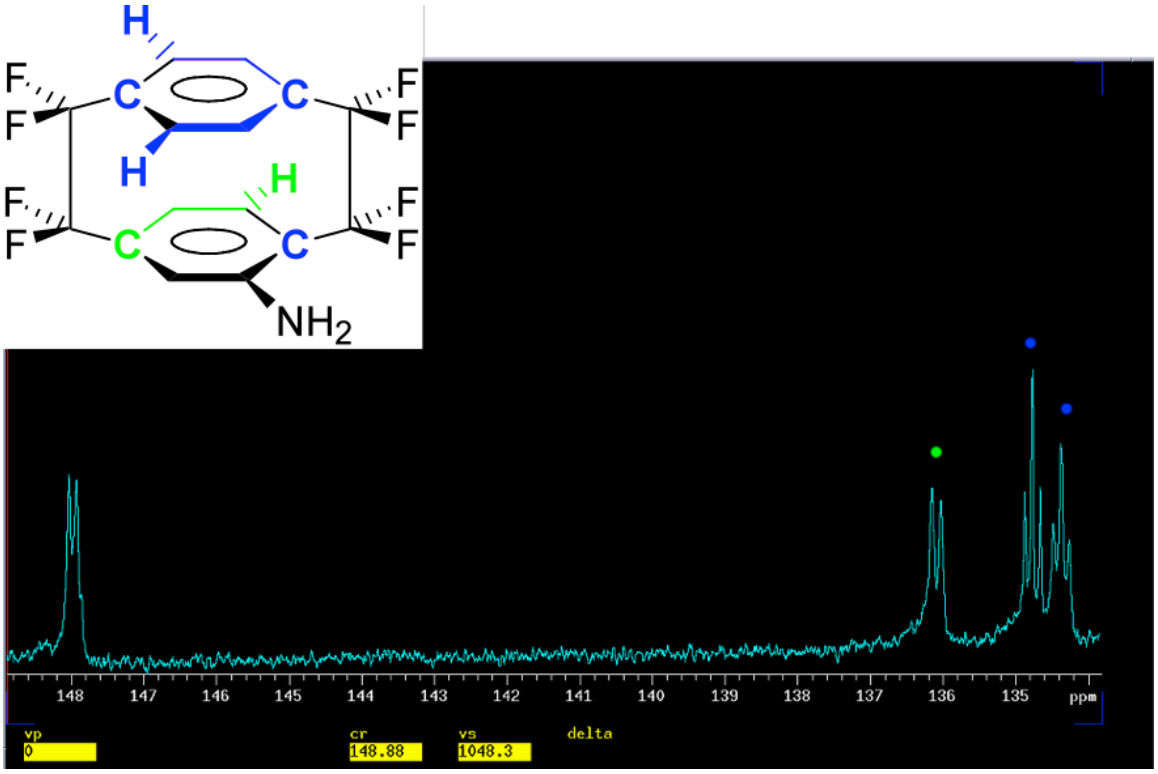

Spectrum 3.11: Expanded ^{13}C {^{19}F} NMR of OFP-NH_2

$^{3}J_{C\text{-}H}$ allows for all of the bridgehead carbons to be split by two hydrogens that are each three bonds away and result in a triplet, indicated with blue dots in Spectrum 3.11. The only exception is C-6, which is three bonds away from one hydrogen and three bonds away from the amino group's nitrogen. C-6 will result in a doublet and is indicated with a green dot at approximately 136.0 ppm.

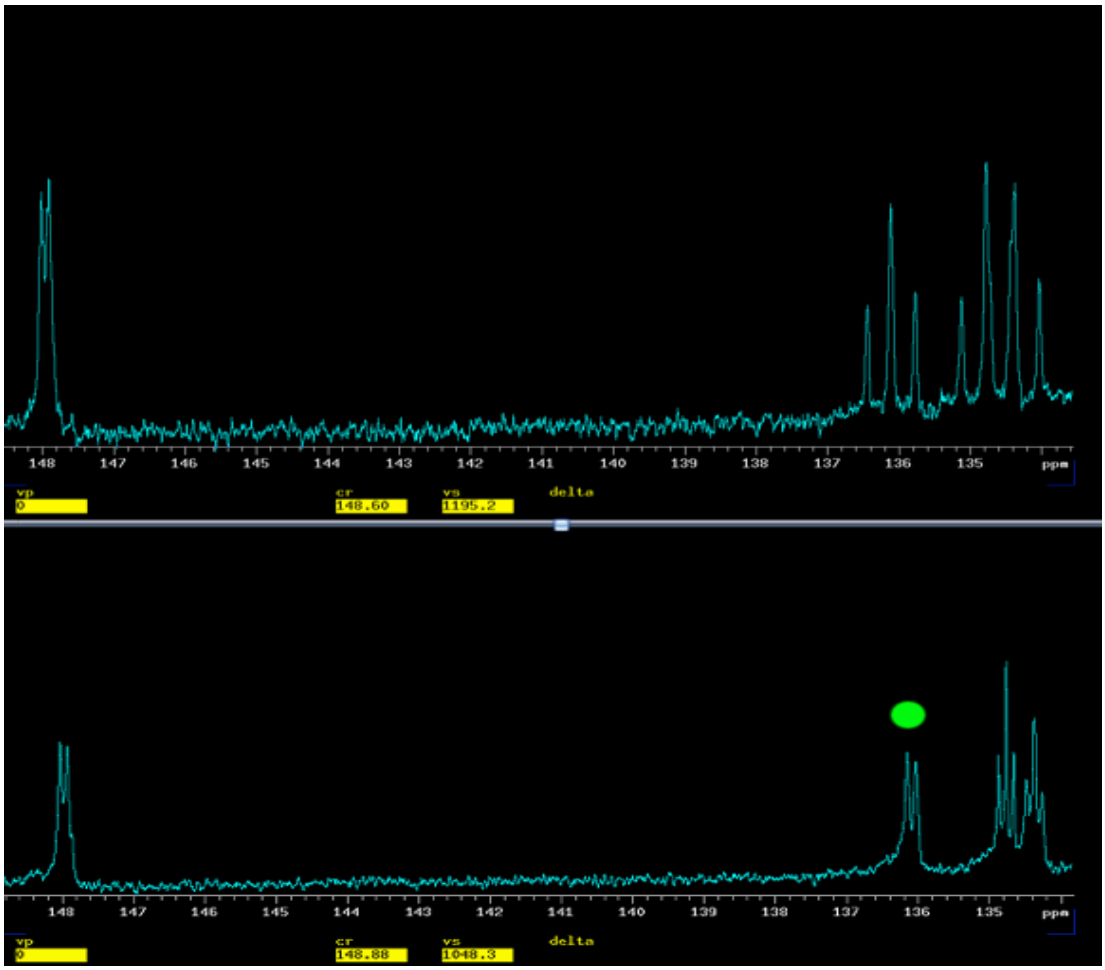

Spectra 3.7 & 3.11 Overlapped

Overlapping Spectra 3.7 and 3.11 allows for comparison of the peaks at approximately 136 ppm. In Spectrum 3.7, on top , the signal in this region resulted in a triplet, this NMR experiment was {^{1}H} so only F-C coupling is observed. That same region in the bottom spectrum shows a doublet. The bottom spectrum was {^{19}F} and only C-H coupling was observed which resulted in a doublet. The multiplicity seen with the decoupled experiments could only arise from the C-6 carbon and therefore the C-6 carbon can be unambiguously assigned.

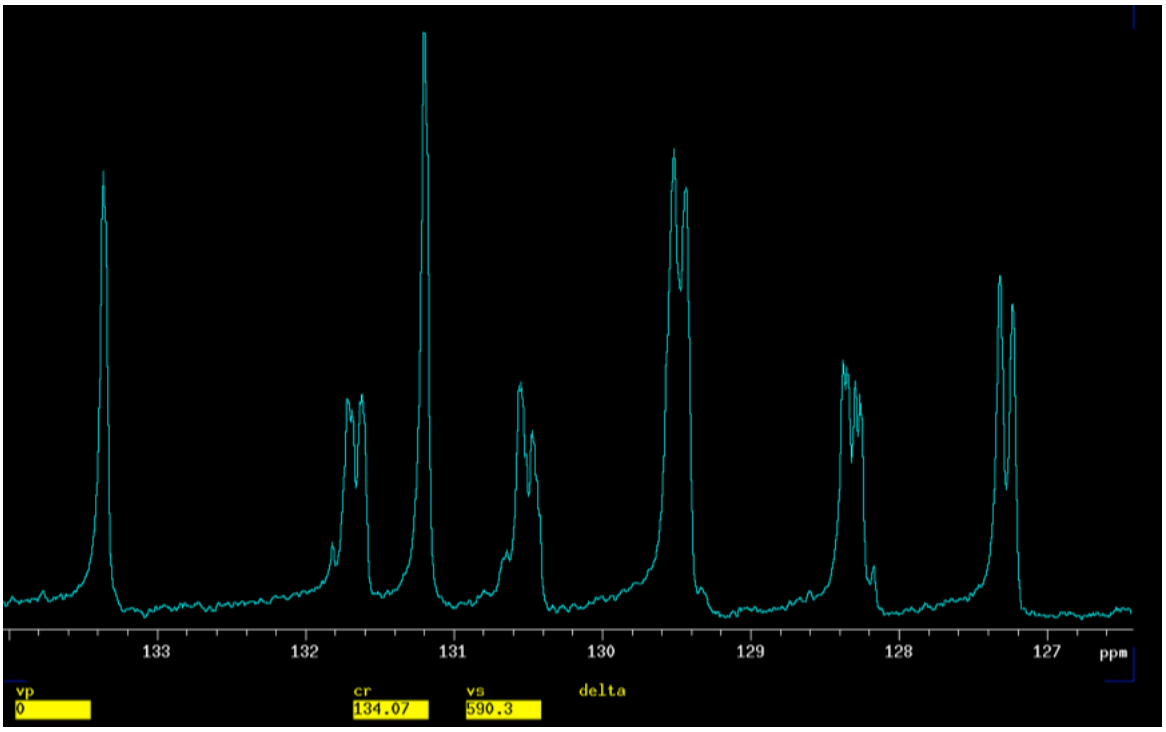

Spectrum 3.12: Expanded ^{13}C {^{19}F} NMR of OFP-NH_2

There are seven signals spread out between 127.0-133.5 ppm in Spectrum 3.12. Those signals appear to be five doublets and two singlets. Taking the relative coupling constants into consideration the doublets and singlets can be matched to form pairs of doublets.

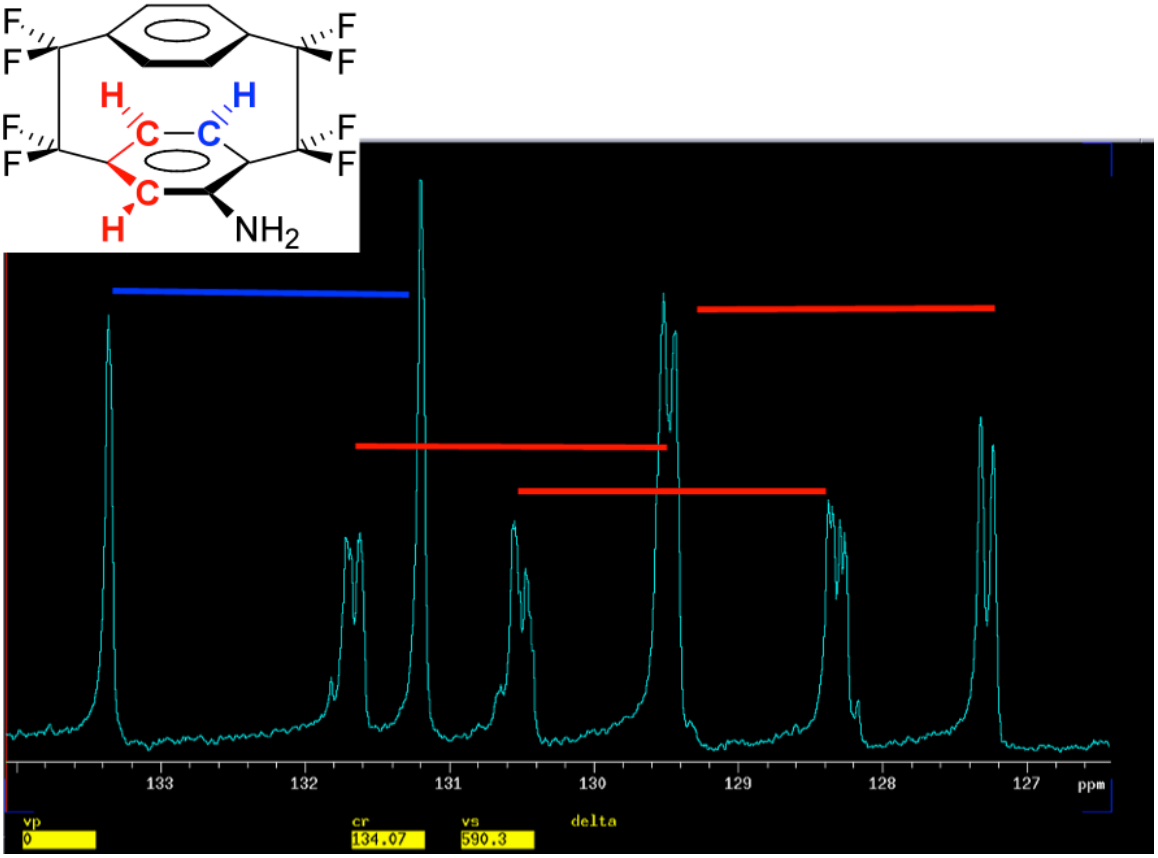

Spectrum 3.13: Expanded ^{13}C {^{19}F} NMR of OFP-NH_2 (Doublets)

Two singlets appear in Spectrum 3.13 and they can be identified by the relative coupling constant to find that they are a doublet. This doublet arises from the $^{1}J_{C\text{-}H}$ coupling of Carbon-8 to the attached hydrogen, H-8, and is marked in blue in Spectrum 3.13. The red marked peaks are not just doublets but doublet of doublets, which arise from both the $^{1}J_{C\text{-}H}$ and the $^{3}J_{C\text{-}H}$ coupling of the C-5 and C-7 to their adjacent hydrogen and the hydrogen that is three bonds away.

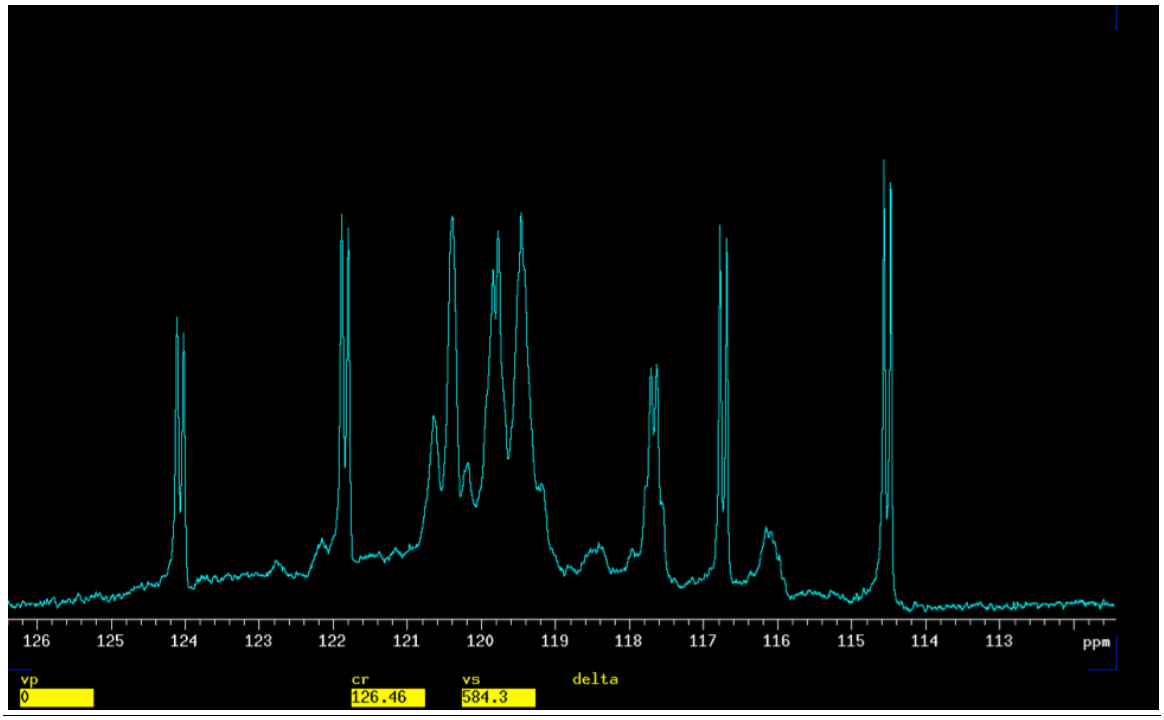

Spectrum 3.14a: Expanded ^{13}C {^{19}F} NMR of OFP-NH_2

Aryl carbons appear in the spectrum from 115.4-124.2 ppm (Spectrum 3.13). Complex peaks revealed in Spectrum 3.13 can be assigned using the previous technique.

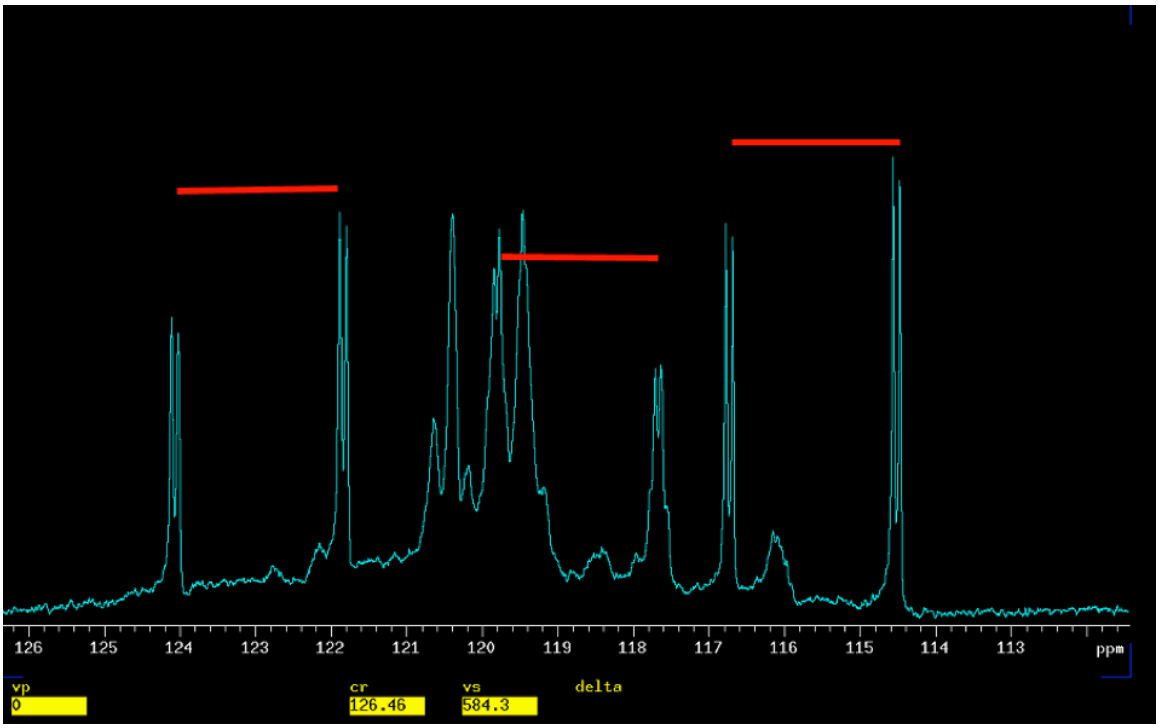

Spectrum 3.14b: Expanded ^{13}C {^{19}F} NMR of OFP-NH_2 (Doublets)

The doublets above arise from the aryl carbons $^{1}J_{C\text{-}H}$ and $^{3}J_{C\text{-}H}$ coupling and are paired based on coupling constants. There are actually three doublets of doublets shown in Spectrum 3.14.

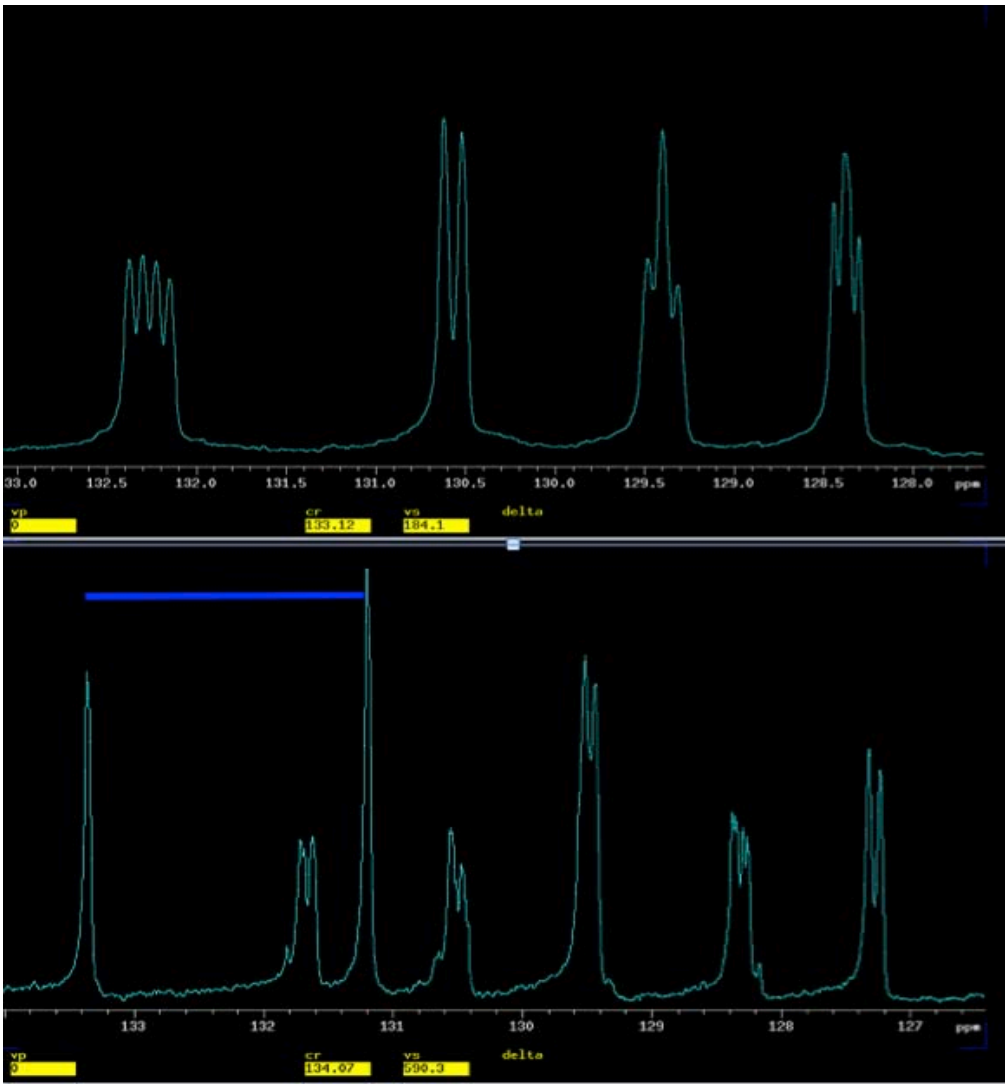

Spectra 3.8 & 3.13 Overlapped

Overlapping Spectra 3.8 and 3.13 allows for comparison of the peaks, doublets, which are furthest downfield in each of these spectra. In Spectrum 3.8**,** only C-F coupling is observed as it has been proton decoupled. This gives a doublet of doublets as two geminal fluorines each with slightly different coupling split this carbon. In Spectrum 3.13, on the bottom, the fluorines have been decoupled and now a doublet is seen. This doublet stems from the carbon being coupled to and split by a singlet adjacent hydrogen.

The only carbon that could display this type of splitting pattern is C-8 and therefore it is unambiguously assigned.

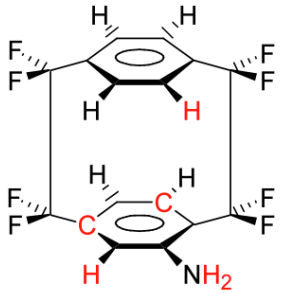

Figure 3.4: Unambiguously Assigned Atoms of OFP-NH_2 (at this point)

Correlation Spectroscopy (COSY)

Using these known atoms there is a method that can be applied to correlate one known signal to another unknown. Correlation Spectroscopy (COSY) relates peaks from like atomic nuclei that exhibit coupling to each other. The NMR machine can be set to identify specific coupling such as correlating hydrogens that are three bonds away from each other by utilizing a $^{1}H/^{1}H$ COSY using $^{3}J_{H\text{-}H} = 8$ Hz, for example. The *gem* position hydrogen, H-13, is known as of this point and COSY can give the *ortho'* peak as well (Fig. 3.5).

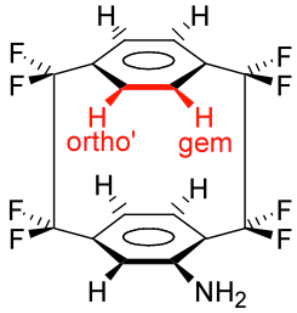

Figure 3.5: $^{1}H/^{1}H$ Correlation Spectroscopy gives *ortho'* from *gem*

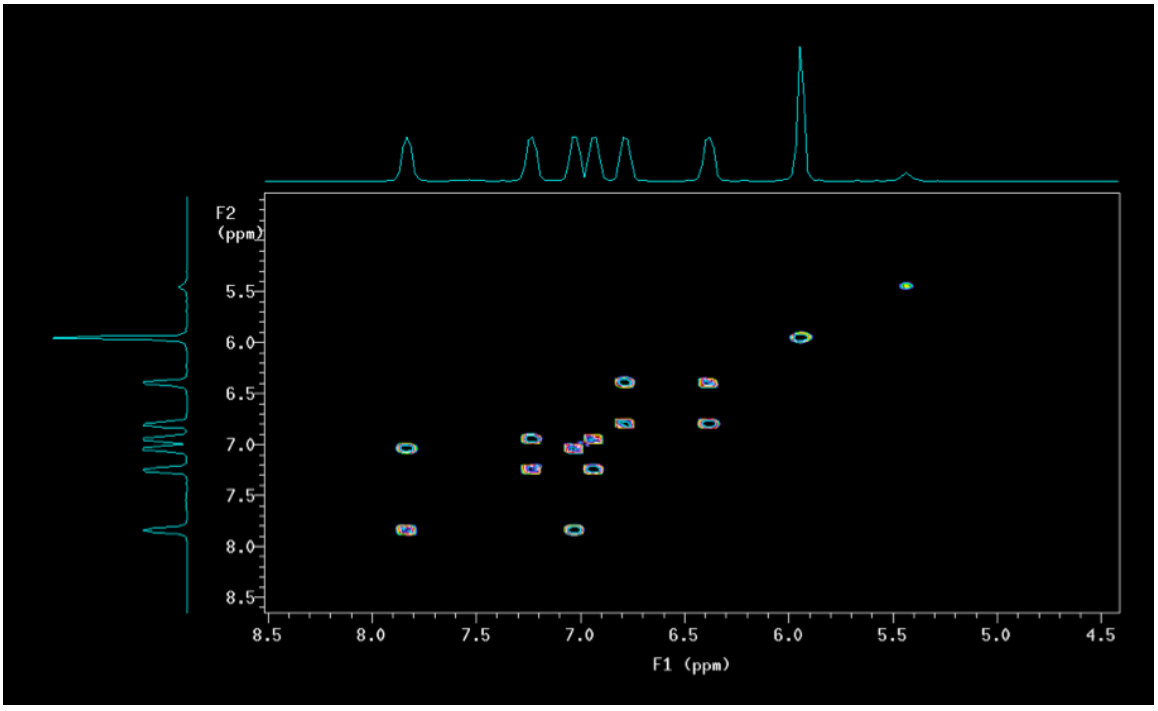

Spectrum 3.15a: $^{1}H/^{1}H$ COSY NMR of OFP-NH_2

While looking at the cross peaks for a COSY experiment, the diagonal peaks are ignored as they show each atom coupling to itself. While concentrating on the other cross peaks, the correlation of the *ortho'* to the *gem* can be seen.

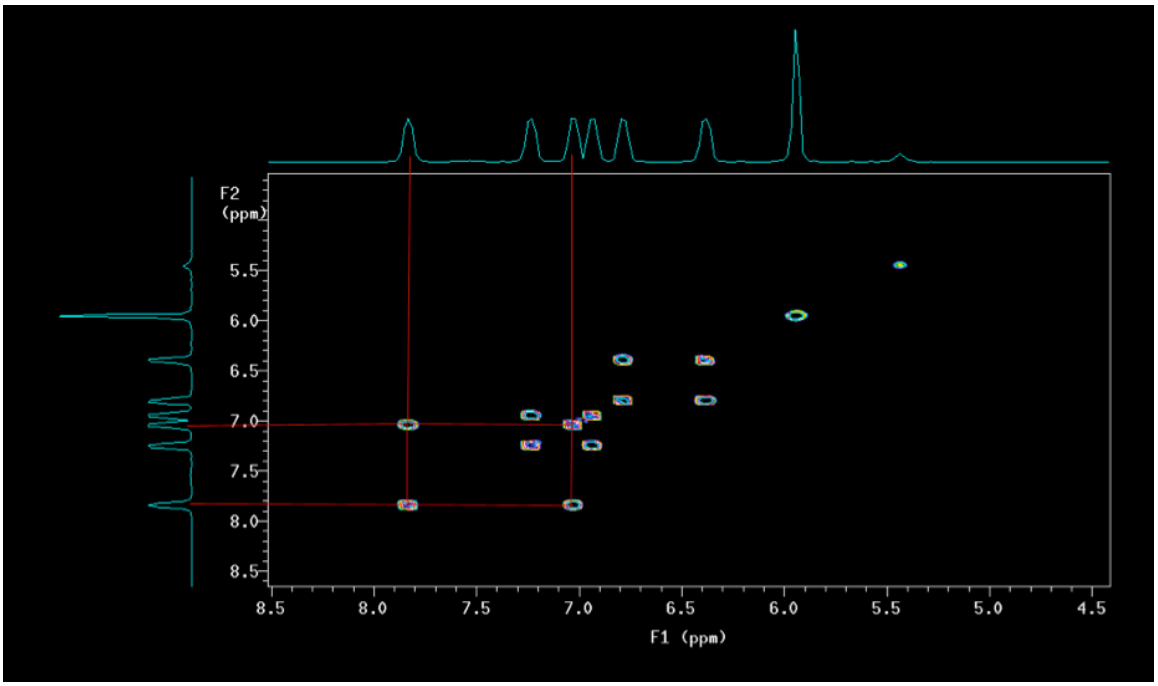

Spectrum 3.15b: $^{1}H/^{1}H$ COSY NMR of OFP-NH_2 Coupling of *gem* to *ortho'*

The peak at approximately 6.9 ppm shows a coupling to the peak at approximately 7.8 ppm. The known peak at 7.8 ppm has been designated as the *gem* peak and as a result the peak at 6.9 ppm has to be the *ortho*' as it is the only proton that would be three bonds away from the *gem* proton. Therefore H-12 is the peak at approximately 6.9 ppm and is unambiguously assigned.

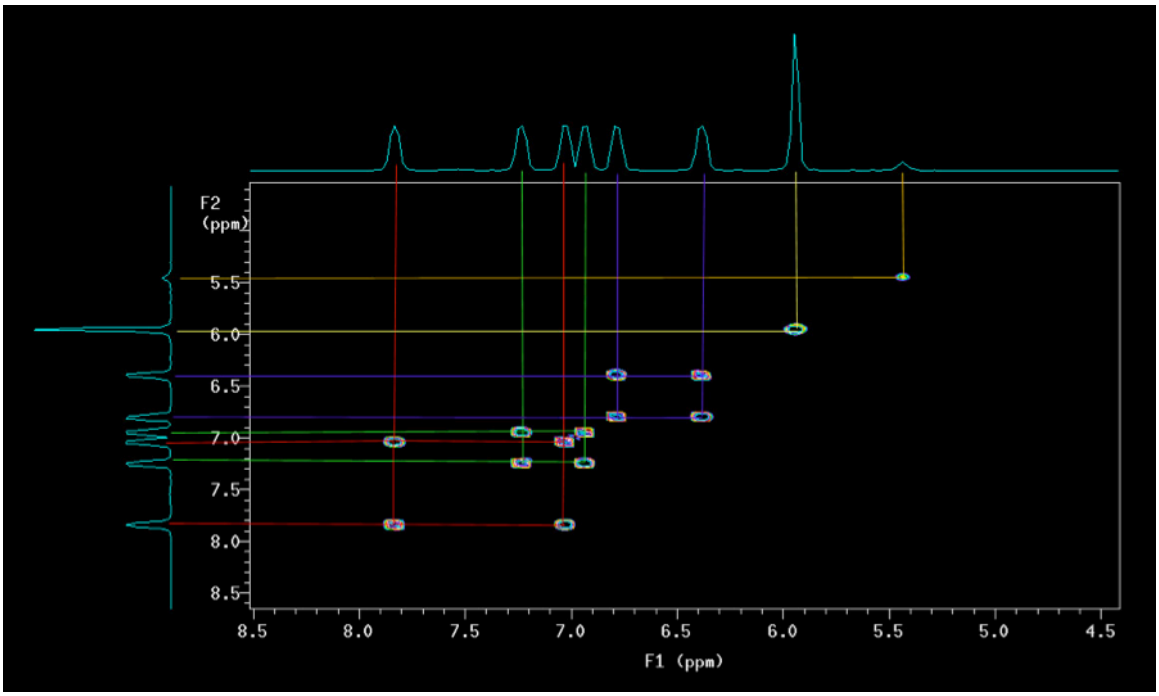

Spectrum 3.15c: $^{1}H/^{1}H$ COSY NMR of OFP-NH_2: Atoms and $^{3}J_{H\text{-}H}$ Coupled atoms.

Couplings of the *meta* to the *para* hydrogen and also the *meta'* to the *para'* hydrogen are evident from the COSY in Spectrum 3.15. Although the pairings are identified, the assignments of these aromatic protons required further investigation. At this point, the following pairs are known (Spectrum 3.16).

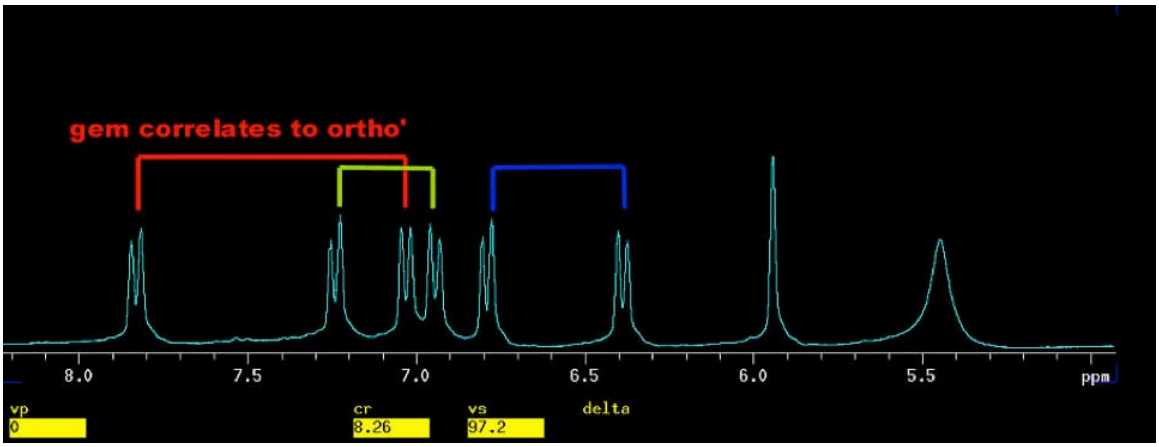

Spectrum 3.16: Paired Protons of OFP-NH_2

A similar experiment can be used to help to clarify the assignments of different nuclei. Heteronuclear Correlation (HETCOR) allows for such an experiment to be completed by correlating two different nuclei through their coupling interactions. Known hydrogens can now reveal attached carbons and known carbons attached hydrogens. Using a HETCOR optimized for $^{1}J_{C\text{-}H}$ = 140 Hz these correlations can be determined.

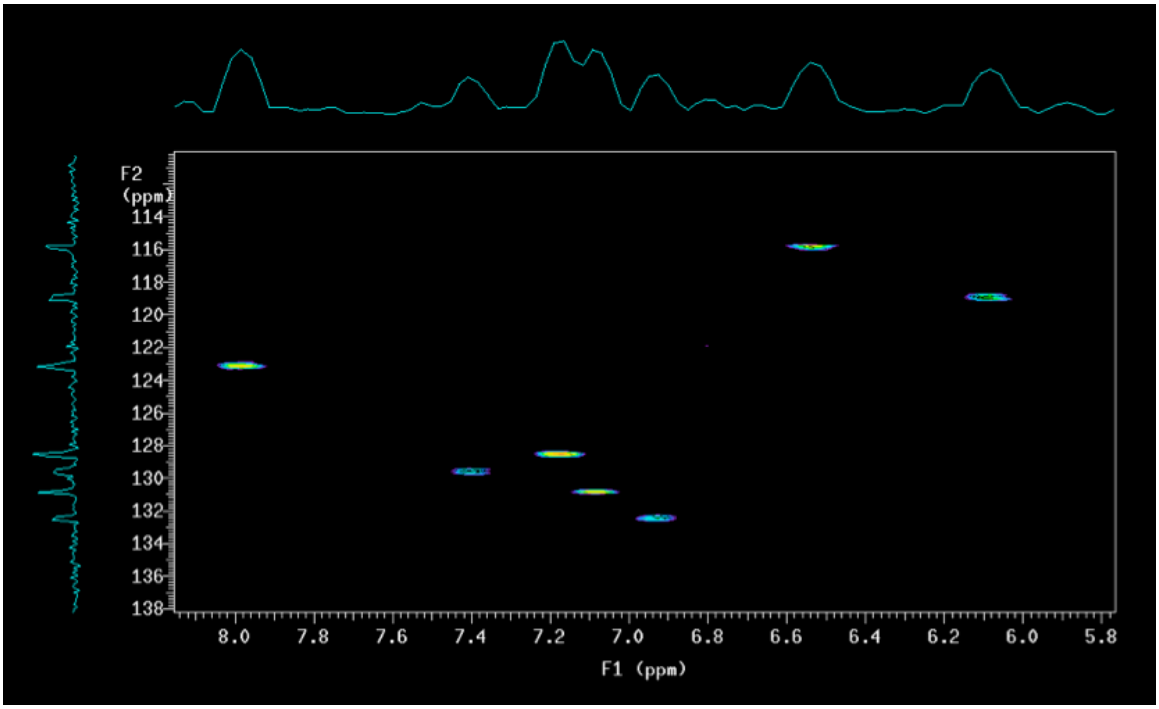

Spectrum 3.17a: C-H HETCOR ($^{1}J_{C\text{-}H}$= 140 Hz)

There are no diagonal peaks in a HETCOR experiment as spectra of different nuclei line each of the axes here Spectrum 3.17a. Upon inspection of Spectrum 3.17b there is a clear correlation of the ^{1}H NMR peak at approximately 7.18 ppm to the ^{13}C NMR peak at about 128.4 ppm just as there is a correlation of the ^{1}H peak at approximately 7.96 ppm to the ^{13}C peak at about 123.1 ppm.

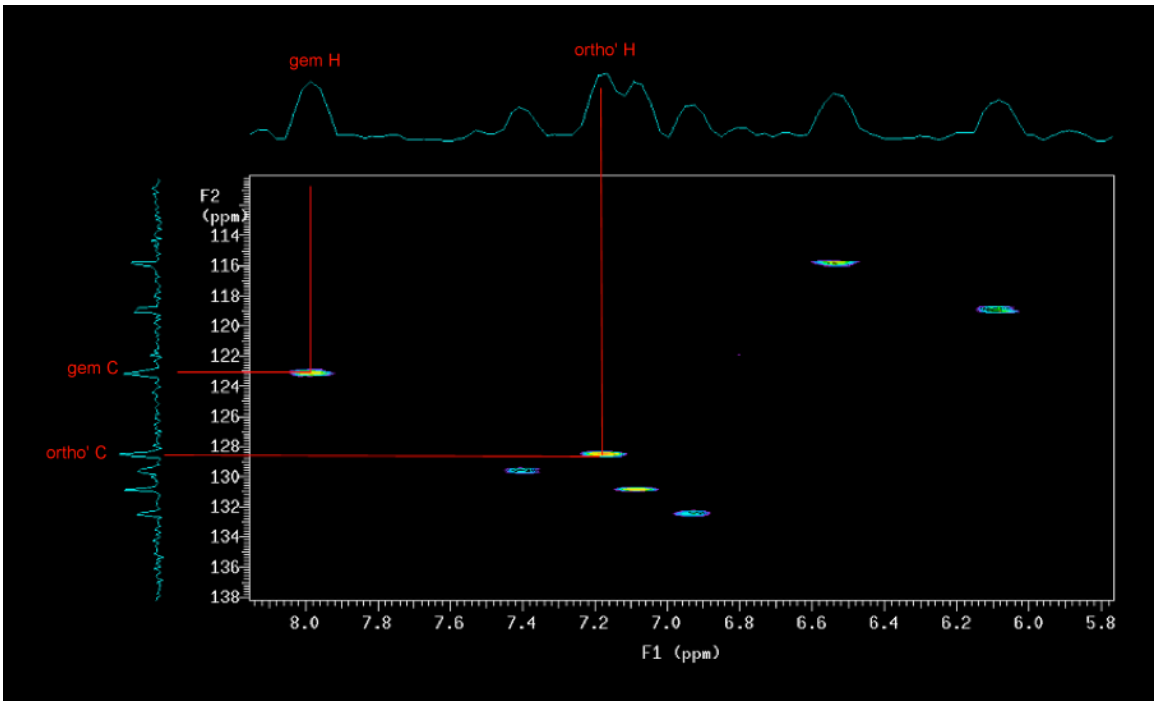

Spectrum 3.17b: C-H HETCOR Known H's Give Unknown C's

The known *gem* hydrogen at approximately 7.96 ppm is correlated to the *gem* position Carbon, C-13, at approximately 123.1 ppm. The known *ortho*' hydrogen peak at approximately 7.18 ppm is coupled to the carbon at approximately 128.4 ppm which must be the *ortho'* Carbon, C-12. At this time, known carbons can give previously unassigned hydrogens.

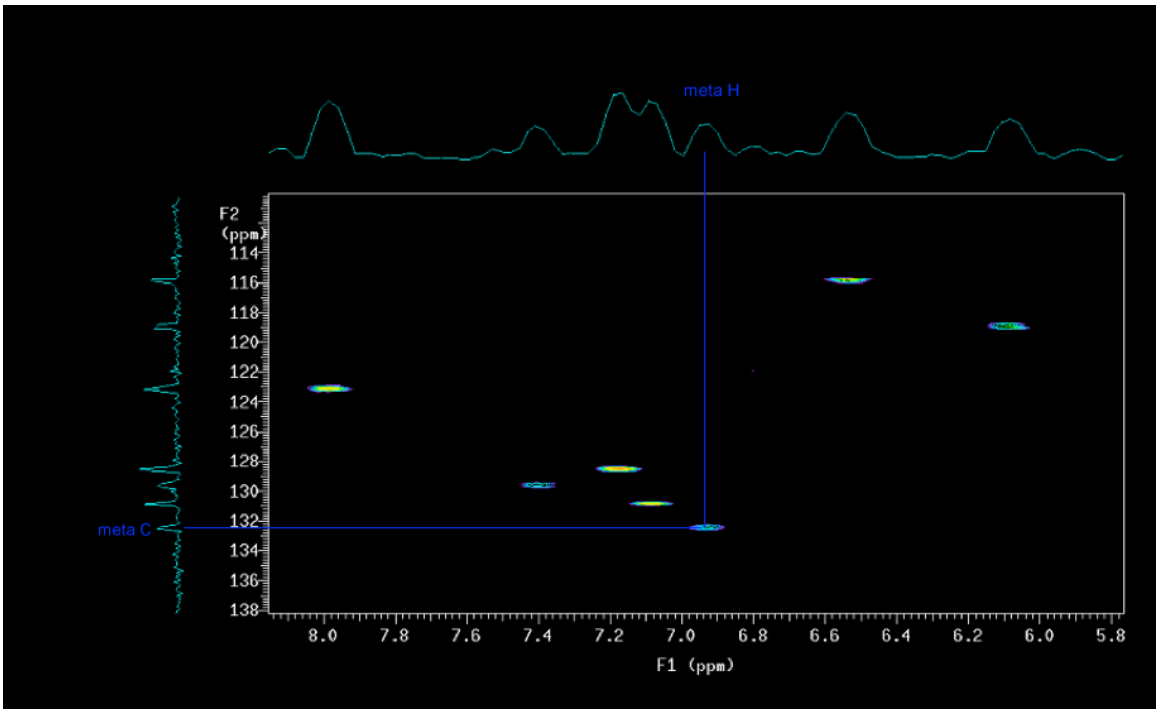

Spectrum 3.17c: C-H HETCOR Known Carbons Give Unknown Hydrogens

The known *meta* carbon at approximately 132.4 ppm shows a coupling to the hydrogen at approximately 6.86 ppm so that hydrogen must be the *meta* hydrogen, H-8. The unambiguously assigned atoms that are known at this point are shown in Fig. 3.6.

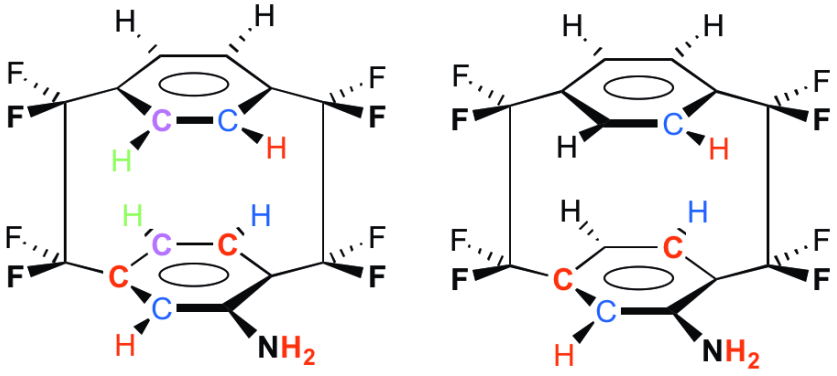

Figure 3.6: Known Atomic Assignments At This Point

The atoms in red on the left side diagram were known and using C-H HETCOR $^{1}J_{C-H}$, the blue atoms were assigned. The atoms in green on the right side were all determined using $^{1}H/^{1}H$ COSY. The pink atom was determined using $^{1}J_{C-H}$ HETCOR.

Three addition carbon assignments can be determined from the *gem* proton. Optimizing a $^{3}J_{C-H}$ HETCOR for 8 Hz can give each of the carbons that are three bonds away from the *gem* proton (Fig. 3.7). Implementing this experiment gives Spectrum 3.18.

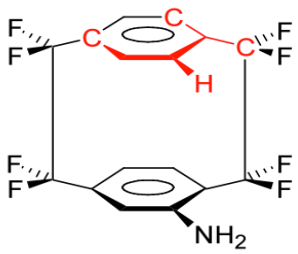

Figure 3.7: *gem* Hydrogen Gives Three Carbons Through $^{3}J_{C-H}$ =8Hz

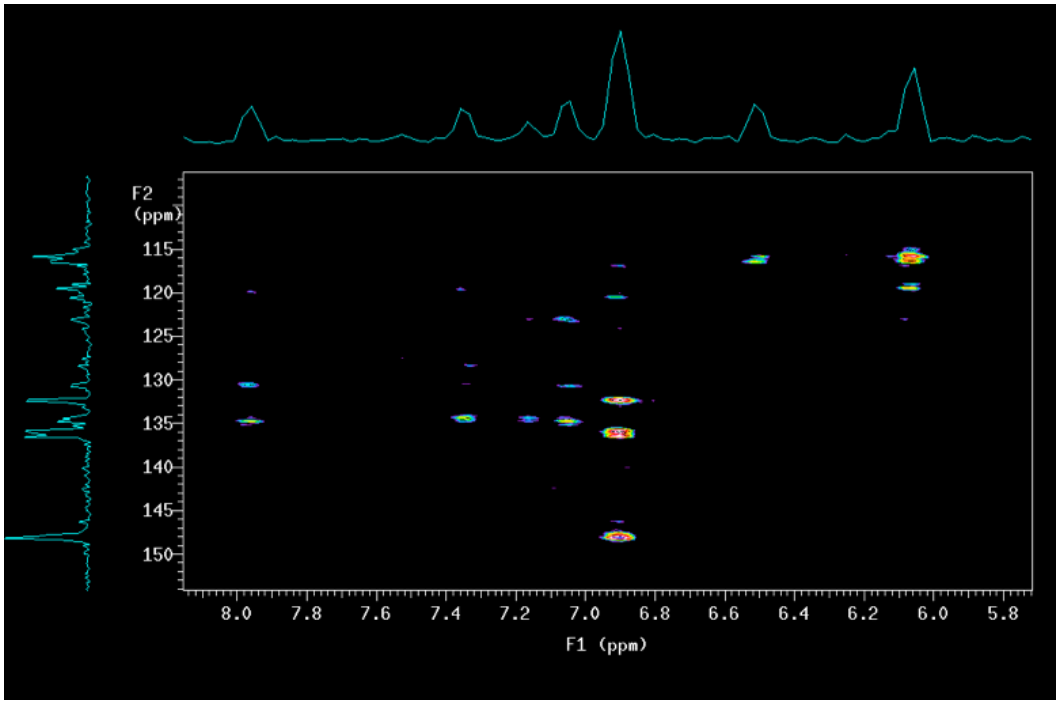

Spectrum 3.18a: $^{3}J_{C\text{-}H}$ HETCOR

The known *gem* hydrogen is, once again, seen at approximately 7.96 ppm couples to three carbons that are each three bonds away.

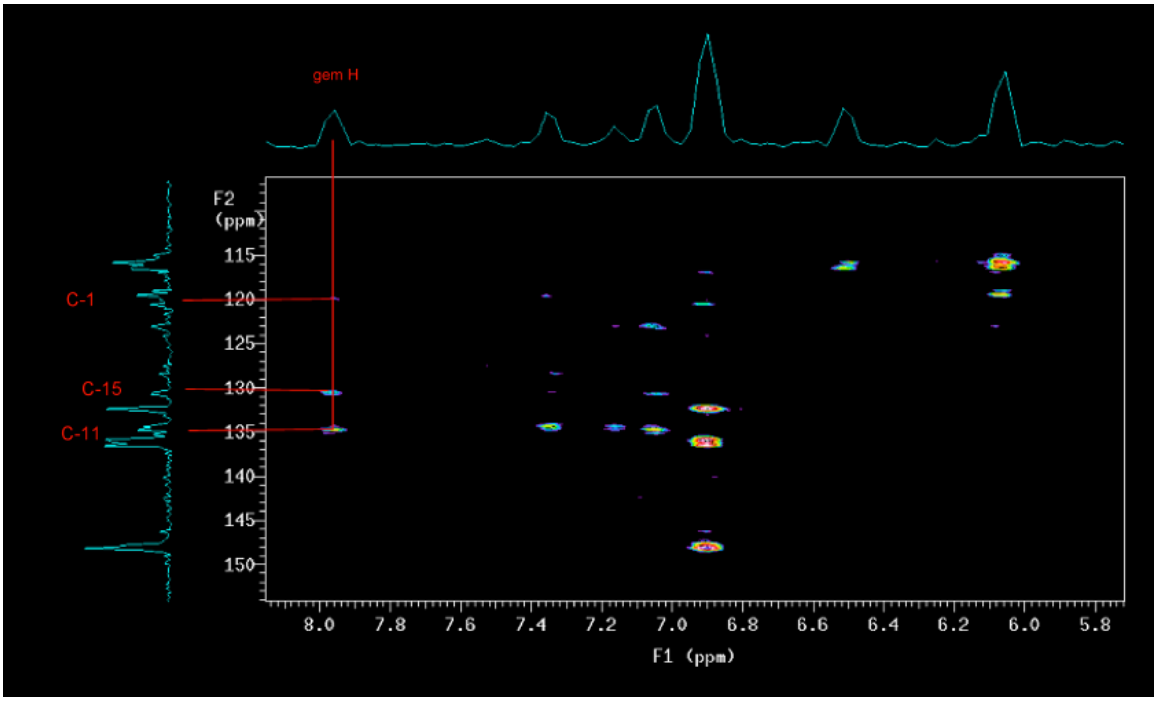

Spectrum 3.18b: $^{3}J_{C\text{-}H}$ HETCOR *gem* Hydrogen to Corresponding Carbons

As seen in Spectrum 3.18b the *gem* hydrogen couples to the C-1, C-11, and C-15 carbons. From the indicated regions of carbons in Spectrum 3.6, the carbons can be assigned according to their chemical shift region. Therefore C-1, C-11 and C-15 can be unambiguously assigned. This same technique was utilized to complete the assignment of the other atoms.

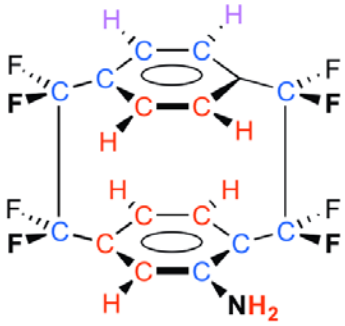

Figure 3.8: Completed Assignment of Hydrogen and Carbons of OFP-NH_2

The red atoms were all already known and the blue atoms were assigned using C-H HETCOR $^{3}J_{C\text{-}H}$. The pink hydrogens were assigned from C-H HETCOR but now with $^{1}J_{C\text{-}H.}$ The ^{1}H assignments in Spectrum 3.19 are in full agreement with all 1D, COSY and HETCOR experiments!

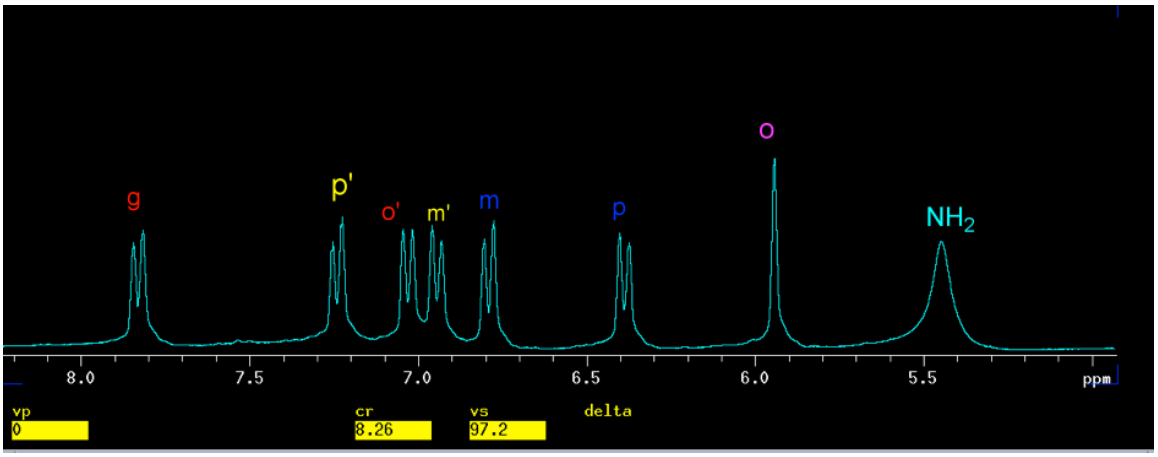

Spectrum 3.19: Fully Assigned ^{1}H NMR for OFP-NH_2

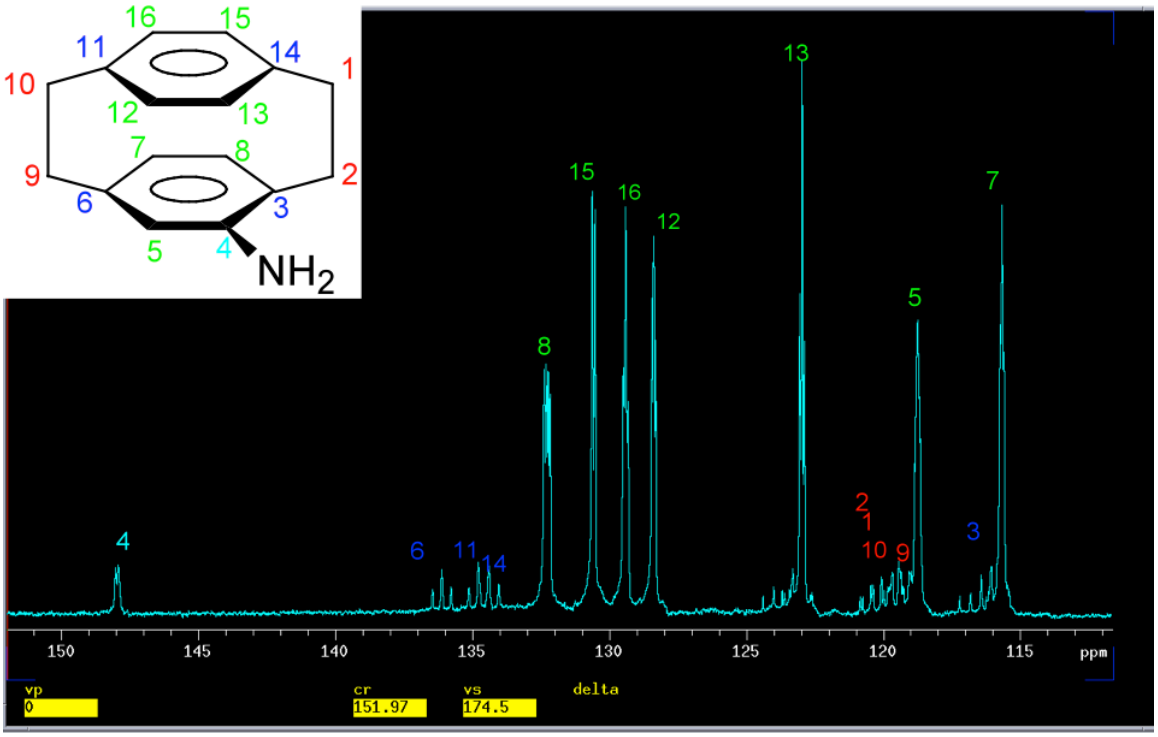

Spectrum 3.20: Complete ^{13}C {^{1}H} NMR Assignments of OFP-NH_2

The complete ^{13}C {^{1}H} NMR assignments of OFP-NH_2 in Spectrum 3.20 are all in agreement with 1D, COSY and HETCOR experiments so the unambiguous assignments of all carbons and hydrogens are complete. These unambiguous assignments assist in the assignment of the fluorine atoms.

^{19}F Assignments of OFP-NH_2

As described earlier introduction of the amino, or any, substituent to the OFP molecule makes each of the eight formerly chemically identical fluorines now each chemically unique. This monosubstitution affects the ^{19}F NMR spectrum and now instead of one single peak there are sixteen peaks generated from the eight fluorines.

The sixteen peaks are in fact eight doublets and are indicated with blue slashes in Spectrum 3.21.

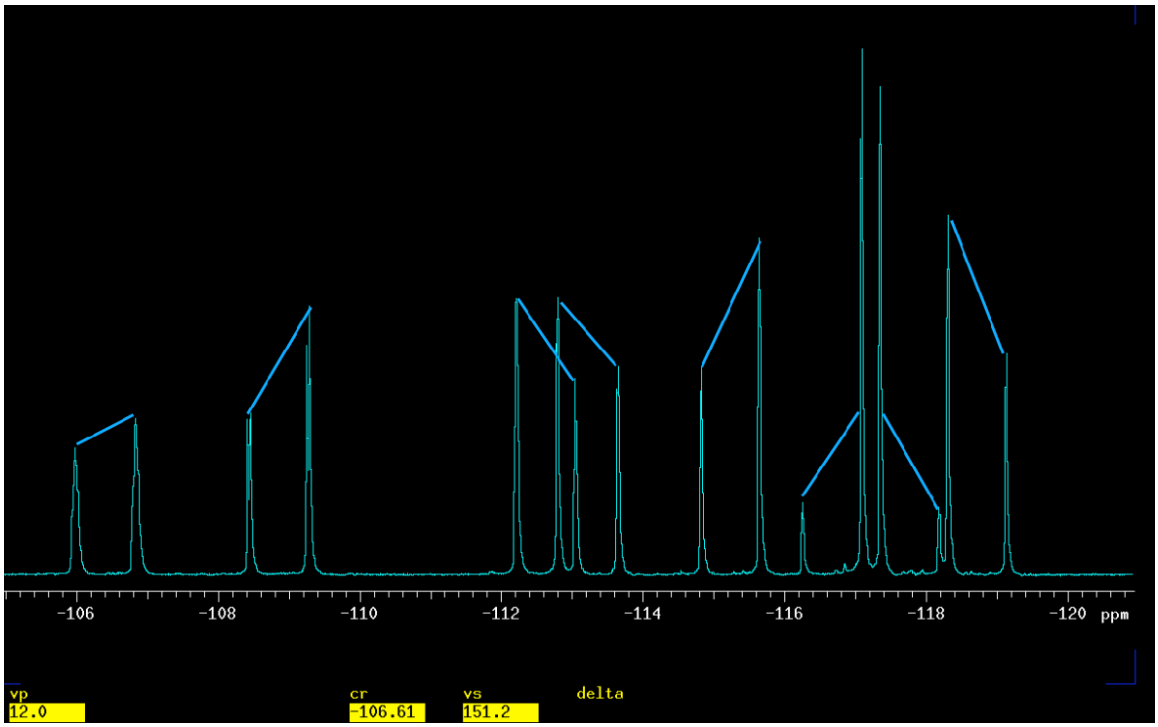

Spectrum 3.21: 8 Doublets of ^{19}F NMR of OFP-NH_2

Each doublet arises from a single fluorine coupling to another fluorine attached to the same carbon atom. In order to identify which fluorine corresponds to which doublet ^{19}F COSY was implemented.

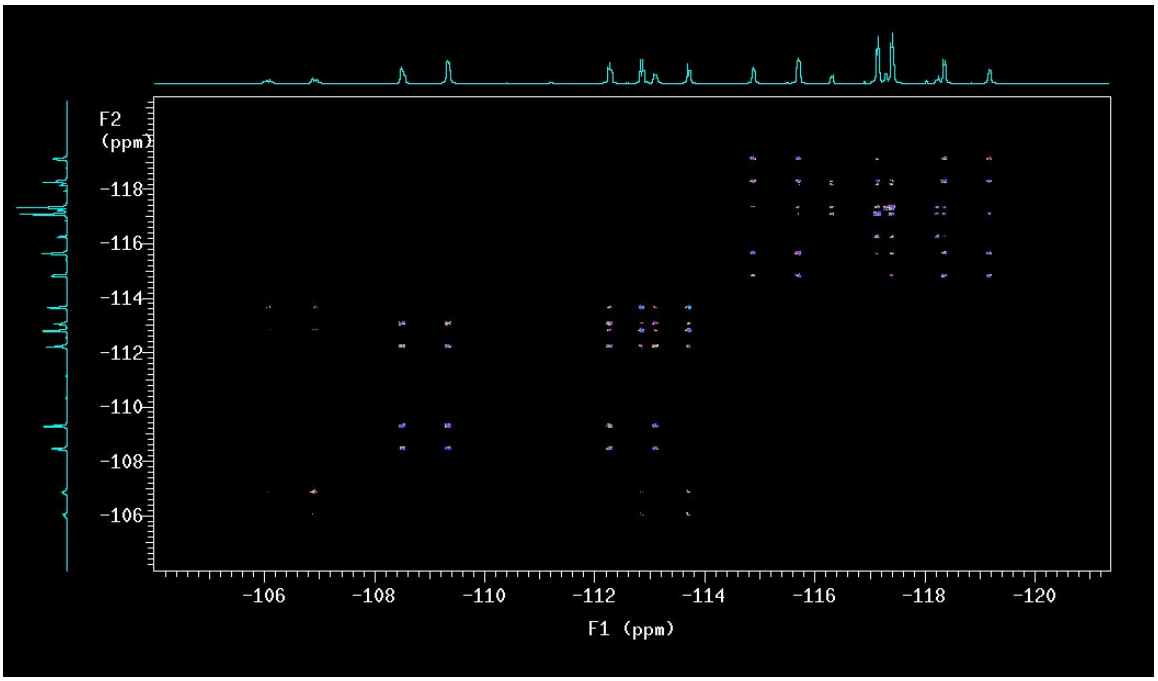

Spectrum 3.22: $^{19}F/^{19}F$ COSY of OFP-NH_2

The full $^{19}F/^{19}F$ COSY of OFP-NH_2 is shown in Spectrum 3.22 but in order to investigate this spectrum's information, expansion of each half of the spectrum will need to be explored.

Spectrum 3.23 shows a coupling of the doublet with peaks at approximately -114.8 and -115.8 ppm with the peaks at approximately -118.4 and -119.2 ppm. Also the peaks at approximately -116.3 and -117.2 show a coupling to the peaks at -118.0 and -117.6 ppm pairing another set of doublets.

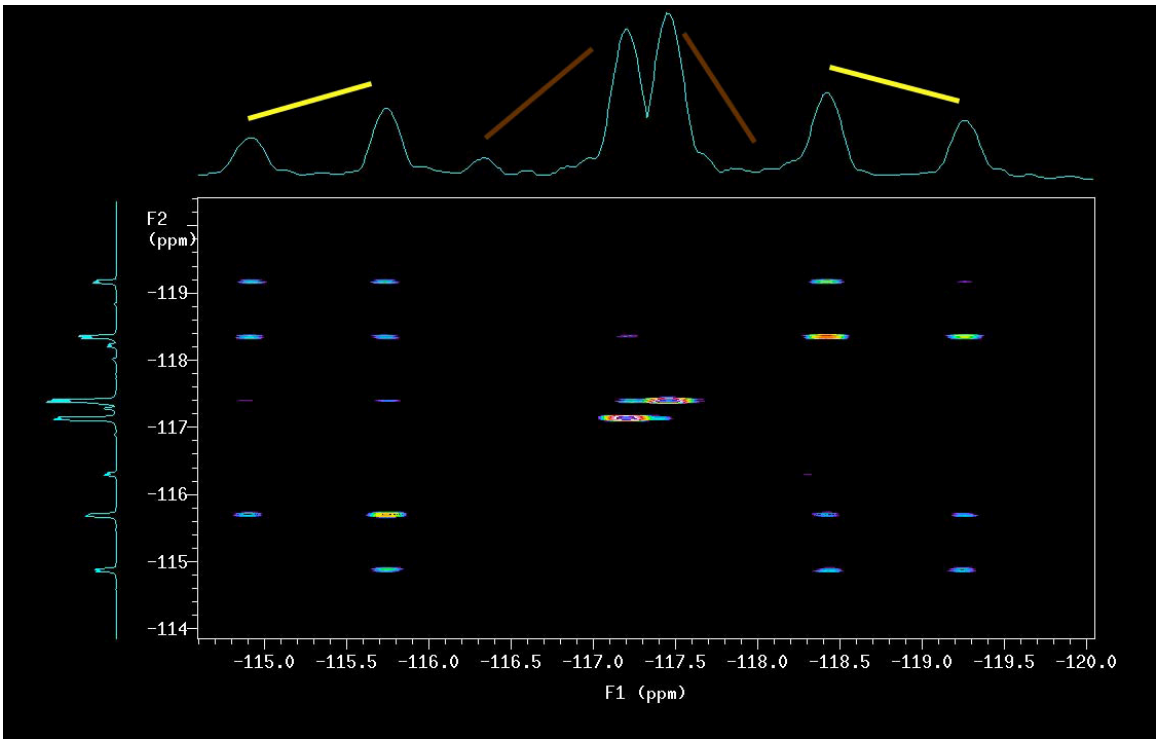

Spectrum 3.23: Right Side Expansion of $^{19}F/^{19}F$ COSY of OFP-NH_2

These couplings show that the outside two doublets are coupled to each other and indicated with yellow slashes while the inner two doublets are coupled to each other and indicated with burnt sienna dashes. Pairing of the doublets was evident upon initial inspection of the spectrum but the COSY experiment legitimized this presumption.

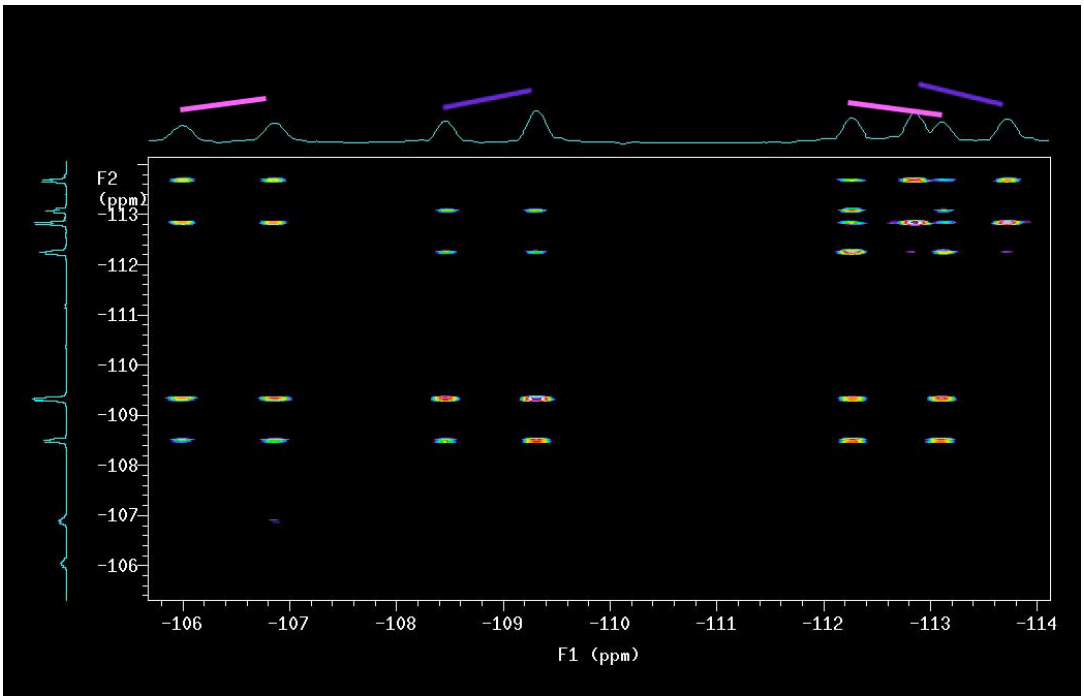

Spectrum 3.24: Left Side Expansion of $^{19}F/^{19}F$ COSY of OFP-NH_2

The initial inspection of these peaks did not lead to a quick analysis as it did with the right hand side of the spectrum. The off diagonal peaks shows coupling from the peaks at -106.0 and -107 ppm with the peaks at -112.2 and -113.0 ppm. These paired doublets are indicated with pink slashes. Peaks of -108.4 and -109.3 ppm couple to peaks at -112.9 and -113.8 ppm and are indicated with purple slashes.

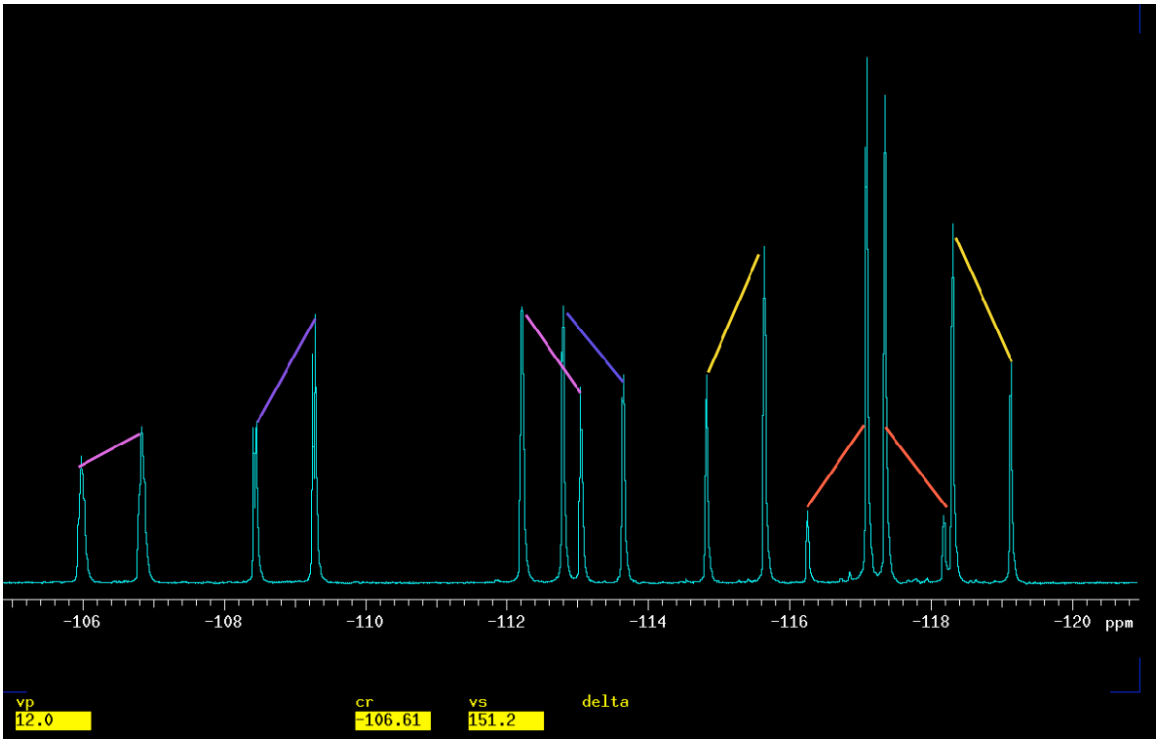

Spectrum 3.25: Designated Geminal Fluorines in the ^{19}F of OFP–NH_2

Two AB quartets coming from each bridge are color coded in Spectrum 3.25. Determining which fluorines are attached to which carbon can be achieved with F-C HETCOR experiments. Heteronuclear correlation set for $^{2}J_{F\text{-}C}$ =27 Hz will give fluorines that are two bonds away from each carbon.

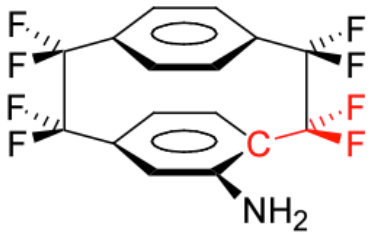

Figure 3.9: $^{2}J_{F\text{-}C}$ =27Hz HETCOR: Known Carbons Give Two Unknown Fluorines

The known ^{13}C spectrum running along the Y-axis of spectrum will show a correlation to the fluorine pairs on the X-axis.

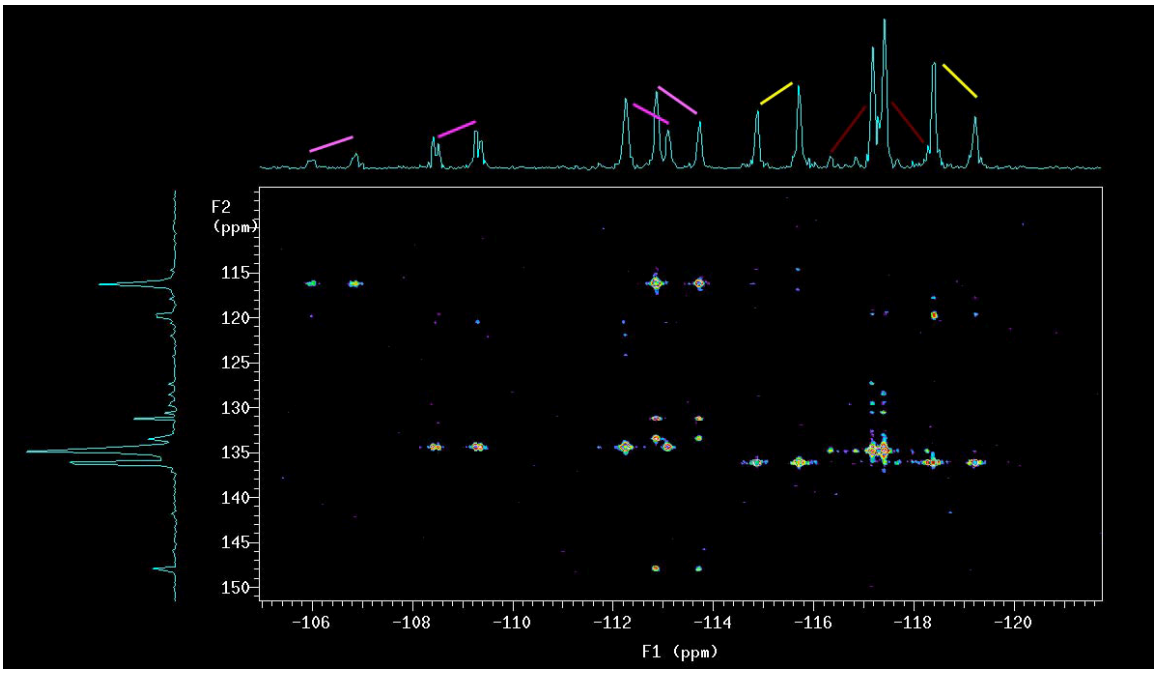

Spectrum 3.26: $^{2}J_{F\text{-}C}$ =27Hz HETCOR of OFP-NH_2

The known bridgehead carbons will give two fluorines each. The correlation of these carbons to the fluorine doublets is revealed in Spectrum 3.27.

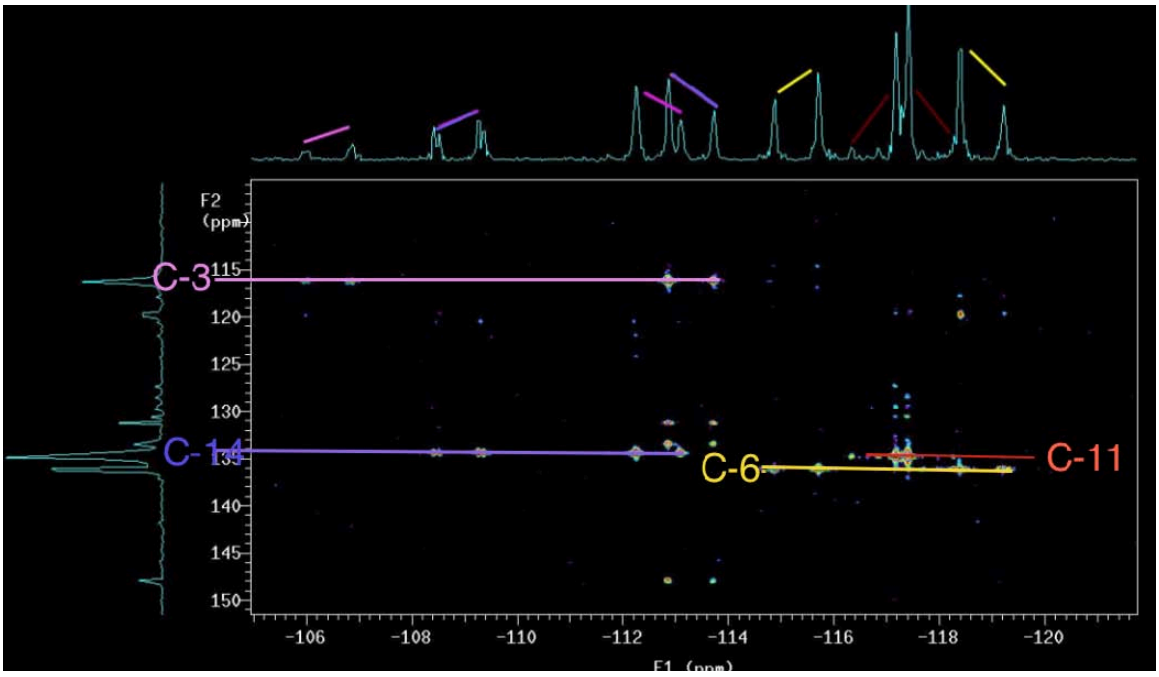

Spectrum 3.27: $^{2}J_{F\text{-}C}$ HETCOR Known Carbons to Fluorine Doublets

As C-3, C-6, C-11 and C-14 are already known, the above spectrum indicates correlation of these peaks to the pairs of fluorines. It can be seen above that C-3, at approximately 116.2 ppm can be correlated to the fluorines at -106.2 and -107.2 ppm and -112.4 and -113.2ppm. C-14, at approximately 134.2 ppm, shows a coupling to the fluorines at approximately -108.4 and -109.4 ppm and -112.8 and -113.8 ppm. C-6, at approximately -136 ppm, shows a coupling to the fluorines at -114.8 and -115.8 ppm and -118.4 and -119.4 ppm.

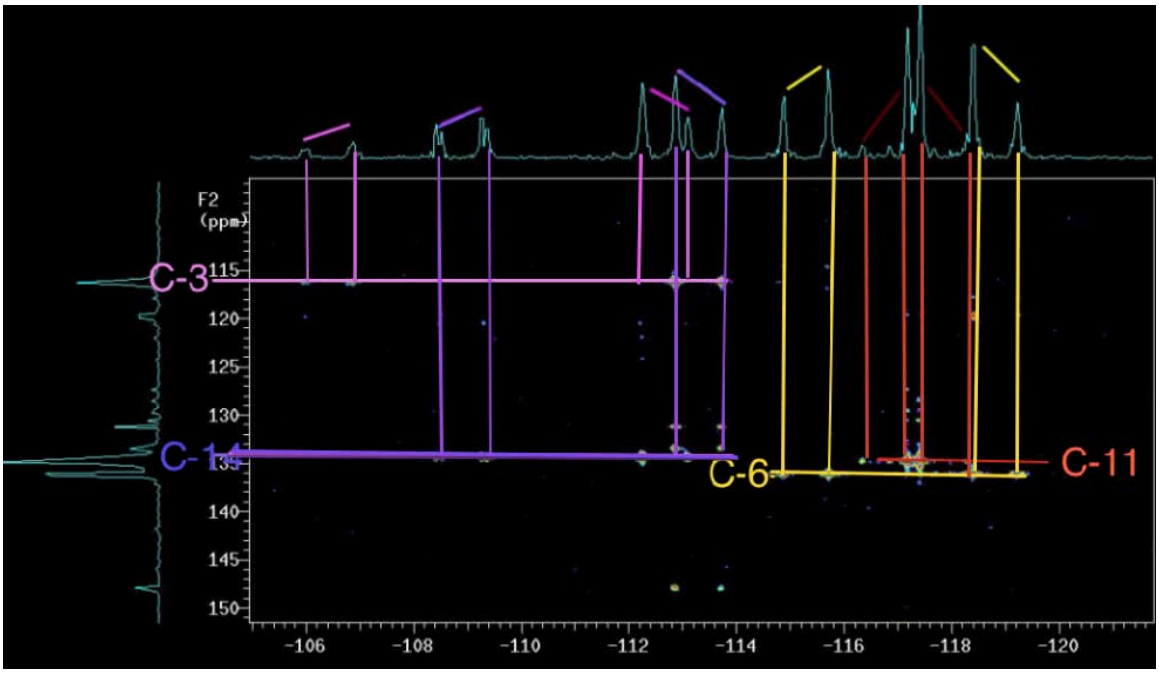

Spectrum 3.28: $^{2}J_{F\text{-}C}$ HETCOR Known Carbons to Fluorine AB quartets

Finally, C-11, at approximately 135.0 ppm, shows coupling to the fluorines at -117.2 and -118.2 ppm and 117.4 and -118.4 ppm. Spectrum 3.28. Each fluorine pair has been coupled to its geminal neighbor and each pair has been paired with a vicinal neighbor, but which fluorine is *anti* and which is *syn*?

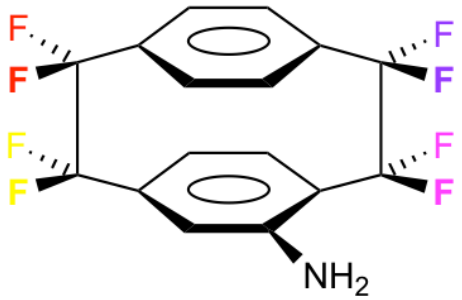

Figure 3.10: Pairs of Fluorines on Each Carbon

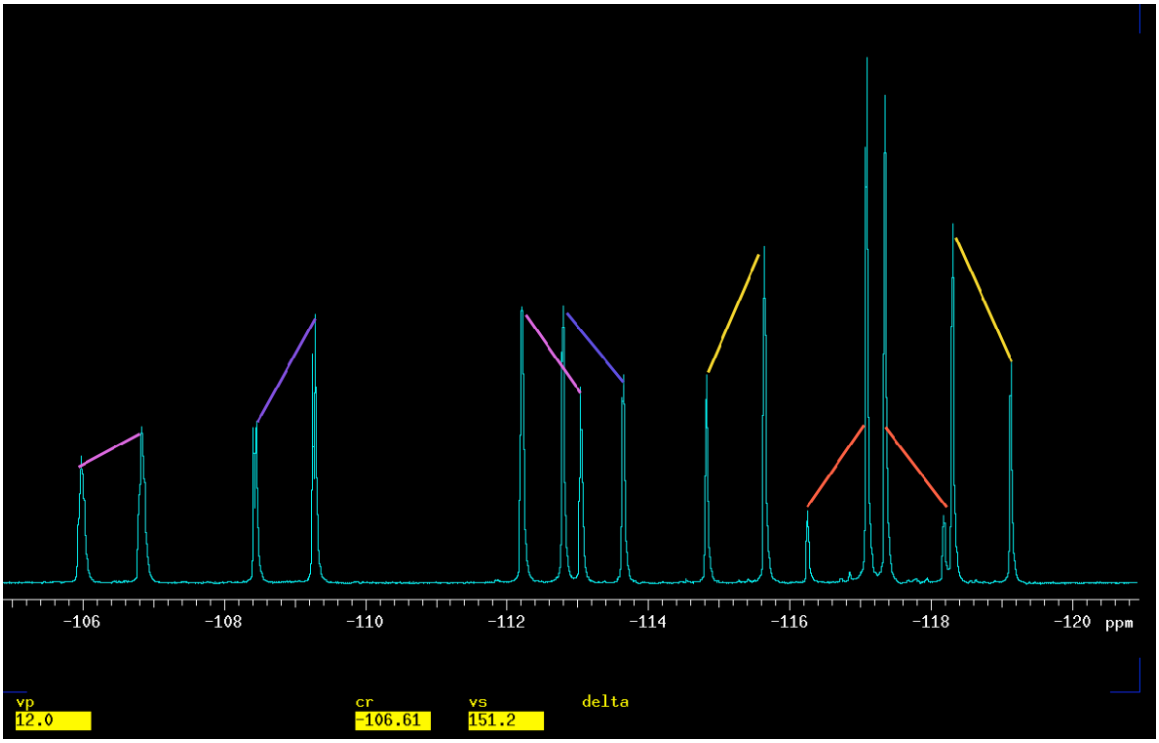

Spectrum 3.29: Known Fluorine AB Quartets

Karplus Equation

Distinguishing between anti and syn fluorines was accomplished with the implementation of the Karplus equation. Due to the fixed geometry of the rigid OFP skeleton, the Karplus equation could be employed to the $^{3}J_{F\text{-}C}$ coupling.[38] The Karplus equation allows for large and small $^{3}J_{F\text{-}C}$ coupling as governed by the dihedral angle, ϕ. When ϕ is close to a 180° angle there is a large coupling seen at about 7 Hz. When ϕ is close to a 90° angle there is a small coupling constant that is very close to 0 Hz(Fig. 3.11.).

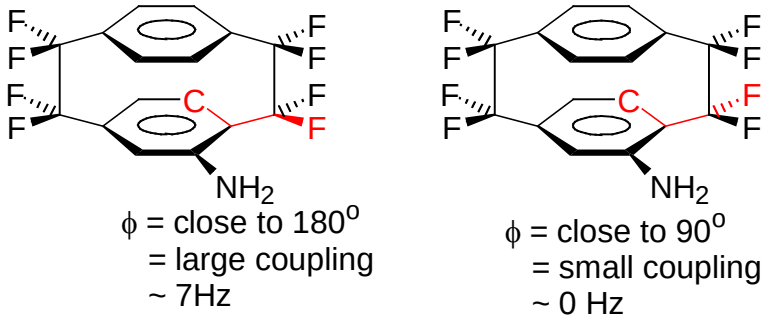

Figure 3.11: Karplus Equation Coupling Constant

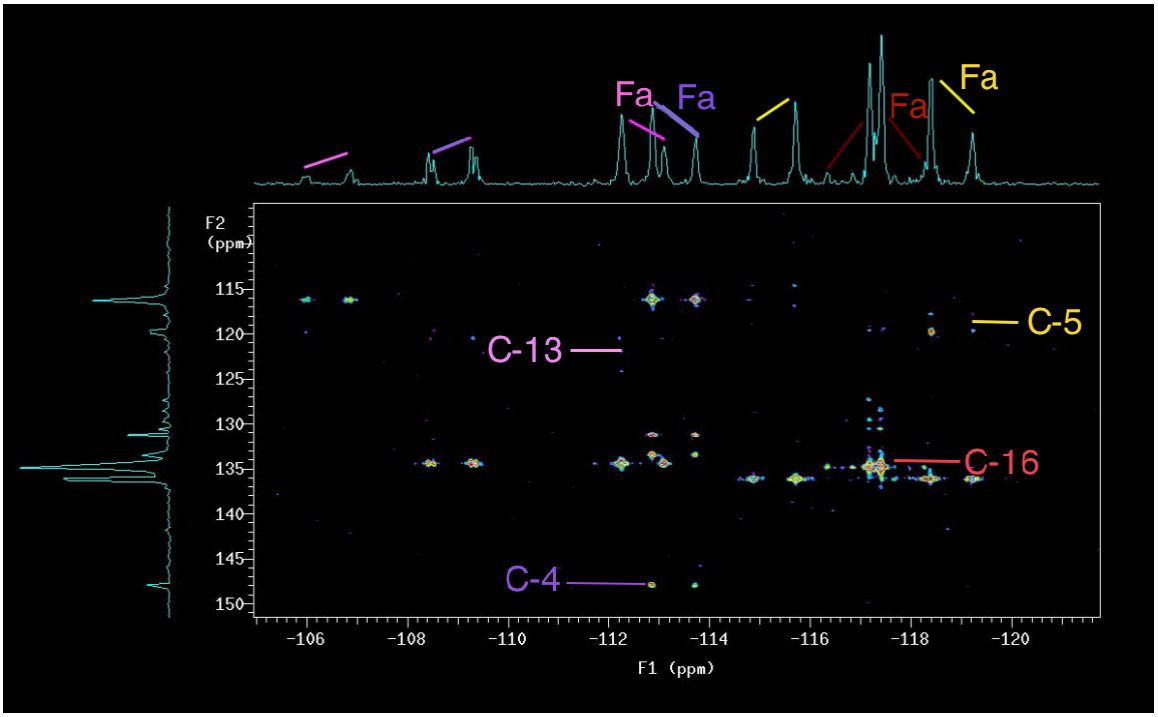

Spectrum 3.30: Pairs of Fluorine with $^{3}J_{F\text{-}C}$ = 7 Hz

Utilizing $^{3}J_{F\text{-}C}$ with a coupling constant optimized at 7 Hz could finally differentiate between the pairs of fluorine by providing the *anti*, with respect to the substituent, fluorines on the molecule. C-13 gave the *anti* fluorine at -112 ppm. C-4 gave the *anti*

fluorine at approximately -113 ppm. C-16 gave the *anti* fluorine at approximately -116 ppm and C-5 gave the *anti* fluorine at -188.6 ppm.

The *anti* designations then allowed for the unambiguous assignment of the *syn* partners. At last, all of the fluorines have been unambiguously assigned.

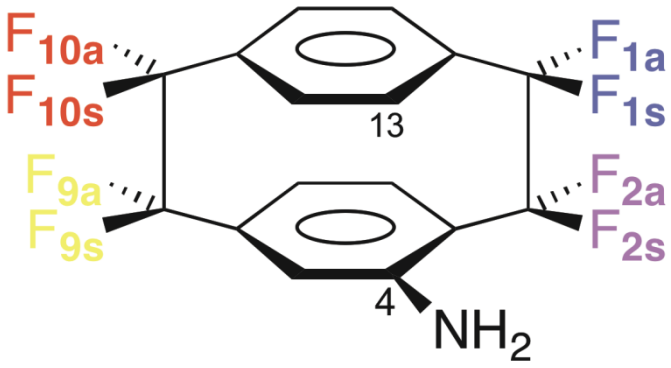

Figure 3.12: Assigned Fluorines for OFP-NH_2

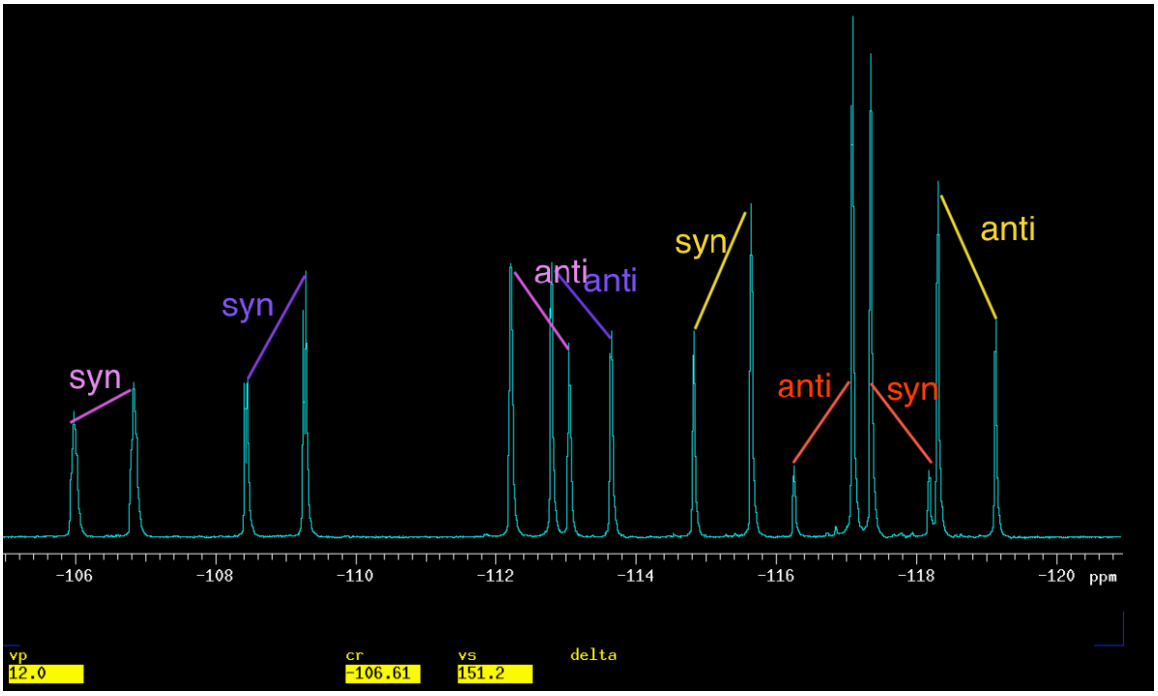

Spectrum 3.31: Assigned Fluorines for OFP-NH_2

Assignments Confirmed by nOe Experiments

The findings in this thesis were all conducted on a 300 MHz machine with traditional 1D, COSY, and HetCor experiments. All of these were verified by nOe experiments using a 400 MHz machine at DuPont by Alexander A. Marchione. The figure above indicates the assignments with the 400 MHz machine. A brief explanation of Marchione's analysis is given here.

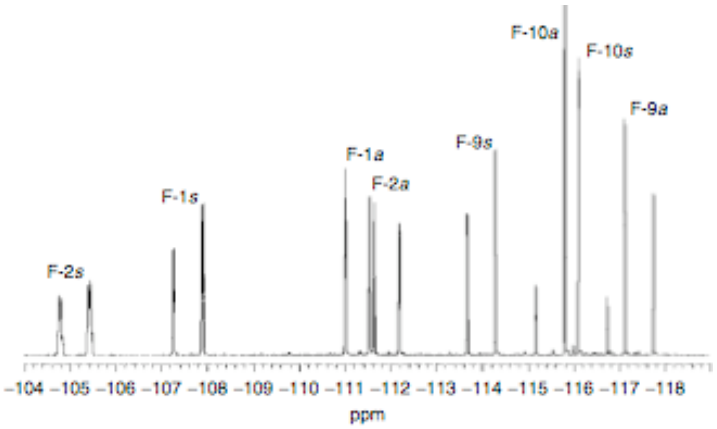

Spectrum 3.32: Expansion of the 400 MHz ^{19}F NMR spectrum of OFP-NH_2 with assigned Fluorines (Spectrum 3.32 reproduced from reference 35 with permission from the authors)

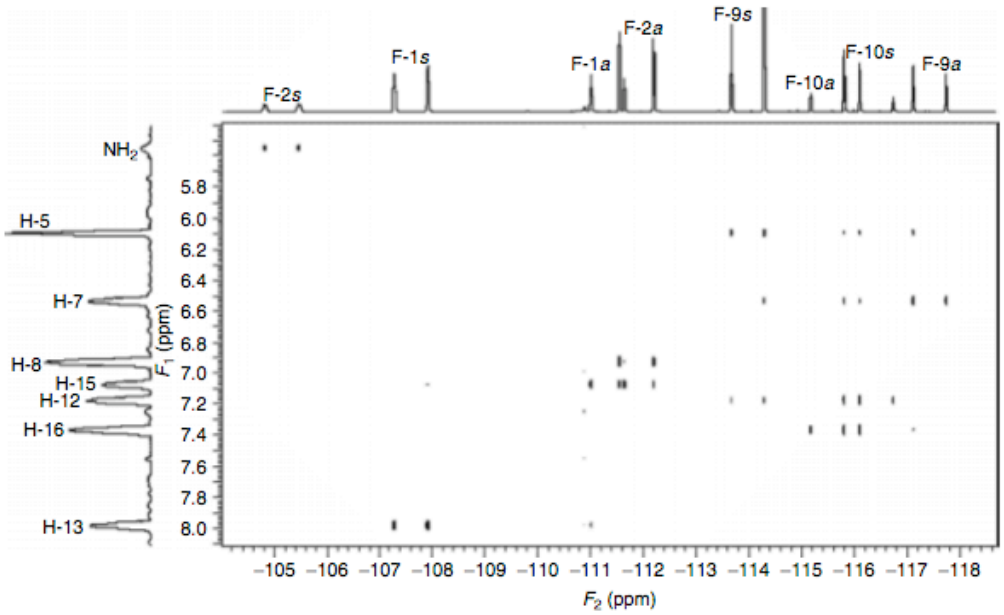

Spectrum 3.33: Expansion of F-H HOESY of OFP-NH_2 (Spectrum 3.33 reproduced from reference 35 with permission from the authors)

Beginning with H-5 the only hydrogen with initial clear assignment, it was shown to have a nOe with F-9*s*. ^{19}F COSY indicated F-9*a* and in turn F-9*a* exhibited a nOe to H-7. A ^{1}H COSY showed an H-7 interaction with H-8. With the lower deck hydrogens designated, it was found that using the weaker nOe interactions between fluorine and hydrogen atoms on the same side but on different decks could be used.

Beginning with F-9s, a strong nOe was shown with H-5 and a weaker nOe with H-12, the hydrogen that was located directly above H-5. Once H-12 was assigned, a ^{1}H COSY was used to reveal the neighbor, H-13, the *geminal* position. F-1*a* displayed a nOe to H-15 and then ^{1}H COSY was used to give H-16. This gave all of the ^{1}H atoms their permanent assignments. This further proved the assignments of all of the atoms on a molecule of OFP-NH_2.

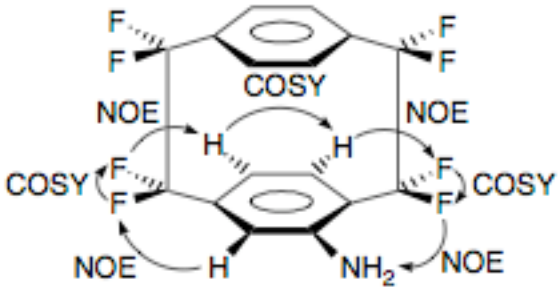

Scheme 3.1: The Protocol for Assigning the Lower Deck Atoms. (Scheme 3.1 reproduced from reference 35 with permission from the authors)

Conclusion

Two different methods were used to assign all of the atoms on OFP-NH_2. With both of these experimental methods confirming the same assignments, the first full multinuclear unambiguous atomic assignments of OFP-NH_2 was complete. These results were published in the Journal of Magnetic Resonance in Chemistry in 2005.[35]

Chapter 4: Chirality and OFP-NH_2

For all experiments conducted to determine the enantiomeric discrimination of compounds, OFP-NH_2 and OFP-diNH_2, an "in tube" method was utilized. Samples of each substrate were added to a 5mm NMR tube and solvated in *d*-chloroform, $CDCl_3$. To this same tube, varying but increasing equivalents of each chiral shift reagent was added and coordination occurred *in situ*. Analysis of the ^{1}H and ^{19}F NMR of the coordinated species were realized by implementing the 300 MHz Varian NMR machine.

Enantiomeric Differentiation

Determination of the enantiomeric excess (e.e.) of organic molecules by NMR can be carried out by various methods as described by Wenzel and Wilcox.[39] These techniques are based on the formation of diastereomeric entities which give different physical features and then different spectral characteristics to both enantiomers of a compound.[38] Objectives of enantiomeric differentiation include monitoring of the enantiomeric excess and determination of absolute configuration of a given enantiomer that is isolated from a mixture. A fundamental theorem in stereochemistry states that chirality can be recognized only in the presence of a chiral reference.[38-40] As NMR spectroscopy is an achiral method, a chiral environment must be created such that each enantiomer can be differentiated.

The strategy that has been most exploited, as first recognized from Raban and Mislow in 1965,[41] is to use optically pure chiral reagents to distinguish a pair of enantiomers through the formation of non-equivalent diastereomeric complexes. Diastereomers have different

chemical and physical properties from one another and their differentiation is a critical part of this research.

When a racemic mixture of R and S enantiomers is subjected to a chiral enantiopure environment, X, as long as they interacted in some fashion whether by coordination, hydrogen bonding, or covalent bonding, a new species is formed. Species of R---X and S---X that are the results of this interaction are called diastereomers. When this interaction occurs, it changes the relationship from enantiomeric, which is indistinguishable by NMR, to diastereomeric, which *is* distinguishable by NMR. OFP-NH_2 is a prime example of a molecule that displays planar chirality. The R and S enantiomers are displayed in Fig. 4.1.

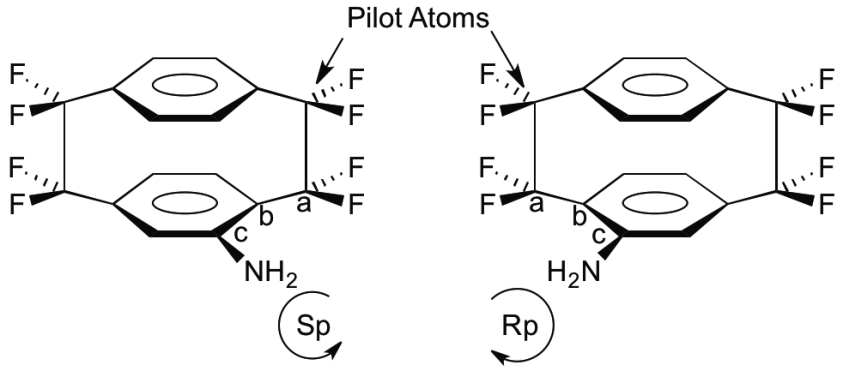

Figure 4.1: R and S Designation of Enantiomers of OFP-NH_2

The seemingly trivial difference in these molecules is vitally important to the pharmaceutical industry as enantiomers of medications can have different pharmacological effects on the body. As chemical synthesis advances and new medicines are being developed, the importance of enantiomers and their pharmacology are being explored. The mechanisms by which they interact with the body's chemistry

have been uncovered/displayed through studies, drug trials and experimentation on both single enantiomers and racemic mixtures. One of the most devastating effects of the result of a racemic mixture in prescription medication was the effect of the well-known drug, Thalidomide.

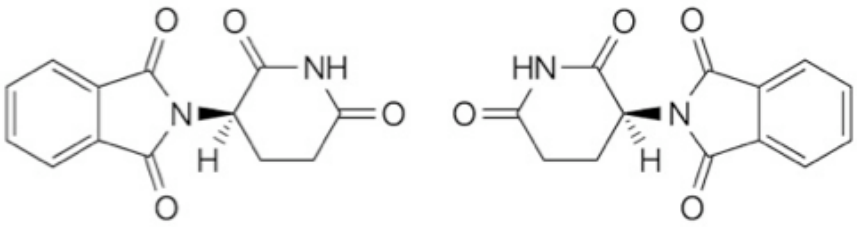

R S

Figure 4.2: R and S Enantiomers of Thalidomide

Thalidomide, a sedative originally used to treat morning sickness in the 1960's and currently in use to treat leprosy and multiple myeloma, is also a teratogen that induces birth defects in humans such as limb truncations and microphthalmia.[42]

The R enantiomer quelled morning sickness of pregnant women and served as a sedative, while the S enantiomer was teratogenic. With the knowledge of these adverse side effects being directly related to the different enantiomers, the need for enantiopure medications was imminent. The rapid surge in enantioselective synthesis has since produced a demand for accurate, reliable and convenient methods for measuring enantiomeric purity. This is so important that it has been deemed as one of the most critical facets of chiral chemistry and McCreary *et al*. reports that, "the direct

determination of enantiomeric purity is the central problem in the chemistry of chiral substances". [43]

One problem exists in the NMR analysis of these enantiomers and this is because enantiomers are not distinguishable by NMR. Enantiomers can only be distinguished in a chiral environment. The easiest way to induce this environment is the use of an enantiopure NMR solvent. However, deuterated enantiopure solvents are an extremely expensive option and therefore not practical in the research lab. There are more feasible options which can prove to be not only less expensive but more convenient to use, and they can give better results. Three options are available that fit this description which include Chiral Shift Reagents (CSR), Chiral Solvating Agents (CSA), and Chiral Derivatizing Agents (CDA). Each of these can be used to create a chiral environment and enable each enantiomer to be detected by NMR as diastereomers.

Diastereomers

Induction of a chiral environment within the NMR tube was effectively completed with the use of several CSRs and one CSA. Both types of chiral reagents form a coordination bond to the ligand and work in a similar manner.

An example of how useful a chiral reagent can be is demonstrated in Fig. 4.3. The spectra here show the separation of the D and L enantiomers of the amino acid alanine.

D and L are terms which are commonly used for enantiomers of amino acids as they relate chiral amino acids, like alanine to its parent molecule, glyceraldehyde.

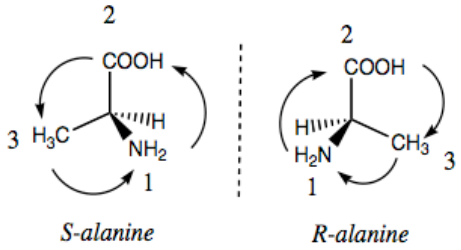

Figure 4.3: Alanine Methyl Group ^{1}H NMR 300 MHz with Acetonitrile-*d* (a) No CLSR, (b)0.02M Ytterbium(III)Nitrate, (c) 0.05M Ytterbium (III) Nitrate[39]

The D and L labels have no direct correlation to R and S. However, the D and L molecules respond similarly to the R and S enantiomers of our compounds and this separation is a useful example of the effectiveness of a chiral shift reagent.

The methyl hydrogens would give a doublet, Fig. 4.3a**,** as they are next to a CH group and the three equivalent hydrogens from the CH_3 group are split by the single neighbor from the CH group. With the addition of 0.02M of $Yb(NO_3)_3$, the peaks becomes broader and appears to start to become a quartet. With the addition of 0.05M $Yb(NO_3)_3$, the peaks have actually resolved into two doublets with each one coming from each of the isomers of alanine. The increase in peak height of the right side doublet is caused from the sample having an excess of the L moiety. Samples with less e.e. would show a separation of the peaks, but they would be of similar NMR integration.

Chiral Lanthanide Shift Reagents

One possible way to induce this effect is by the use of Chiral Lanthanide Shift Reagents (CLSRs). The discovery of the effect that paramagnetic lanthanide ions had on NMR spectra was one of the most significant developments in the entire field of NMR shift reagents.[44]

The first established use of CLSRs to determine enantiomeric purity was reported by Whitesides and Lewis in 1970.[45] Certain lanthanide^{+3} ions are paramagnetic which cause NMR perturbations that result in chemical shift effects of coordinated atoms. With achiral ligands, these are known as Lanthanide Shift Reagents (LSR), but when an enantiopure chiral ligand is bound to a lanthanide ion, the result is a CLSR. Ln^{3+} metals Europium (Eu) and Ytterbium (Yb) are downfield shift reagents while Praseodymium (Pr), is an upfield shift reagent. With CLSRs the substrate can be thought of as binding to the coordinately unsaturated metal.[44]

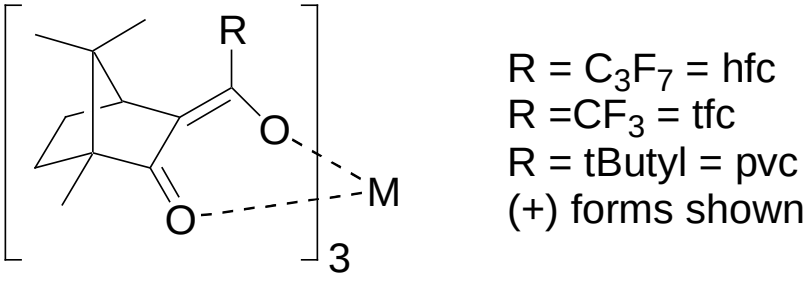

Figure 4.4: Most Common CLSR's (Shown in their 1R, 2S form)

Ligands are often tris β-diketonate camphor derivatives. 3-Heptafluorobutyrylcamphor (1R, 2S) (HFC) derivatives were designated as a useful reagent for these studies as HFCs

have shown to be a feasible auxiliary with substrates containing amino substituents. The heptafluoro groups of this ligand enhances the Lewis acidity of the lanthanide ion and results in stronger coordination to the substrate. [44] Literature has proven that the CLSR would display different NMR perturbations for the different enantiomers of the substrate, and thus allow observation of both enantiomers. OFP-NH_2 served as a feasible specimen for this research.

The basic structure of an OFP-NH_2 molecule exhibits planar chirality and therefore exists as enantiomers (Fig. 4.1). NMR analysis takes place when a single enantiomer of the CLSR, which has been designated as CLSR[R], was assumed to react with the R and S substrates of the analyzed species, OFP-NH_2. This coordination would result in the formation of two diastereomers, R-CLSR[R] and S-CLSR[R]. Because diastereomers are indeed distinguishable by NMR, the newly formed moiety should prove to be able to be identified as different species from the other. The interaction would take place between the metal^{+3} ion of the CLSR and would coordinate with the lone pair of electrons on the nitrogen of the amino substituent. Coordination of the lanthanide metal and the lone pair on the nitrogen of the amino group of OFP-NH_2 are shown in Figure 4.5.

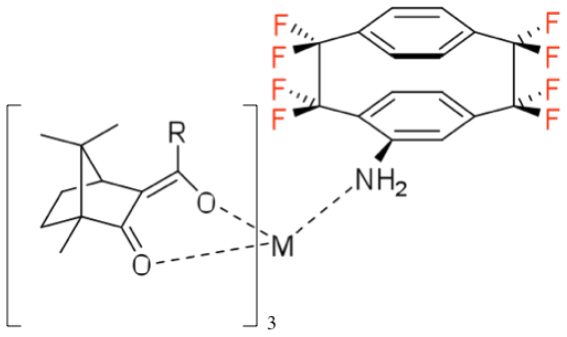

Figure 4.5: Coordination of CLSR with OFP-NH_2

Three Ln^{3+} HFCs were used to analyze their effectiveness. Eu^{3+}, Pr^{3+}, and Yb^{3+} CLSRs. These CLSRs were implemented in increasing equivalent concentrations for each sample. These three were chosen to analyze the effects of both upfield and downfield shift reagents and to further determine if the direction of field shift affects the resolution of the NMR spectra.

^{1}H NMR Analysis of OFP-NH_2

These experiments were performed for each chiral reagent and both ^{1}H and ^{19}F spectra were predicted to give good resolution of peaks. Analysis discussed in Chapter 3 allows for the following peak assignments, which was a crucial stepping-stone for the next portion of the analysis. The proton assignments are listed in Spectrum 4.1.

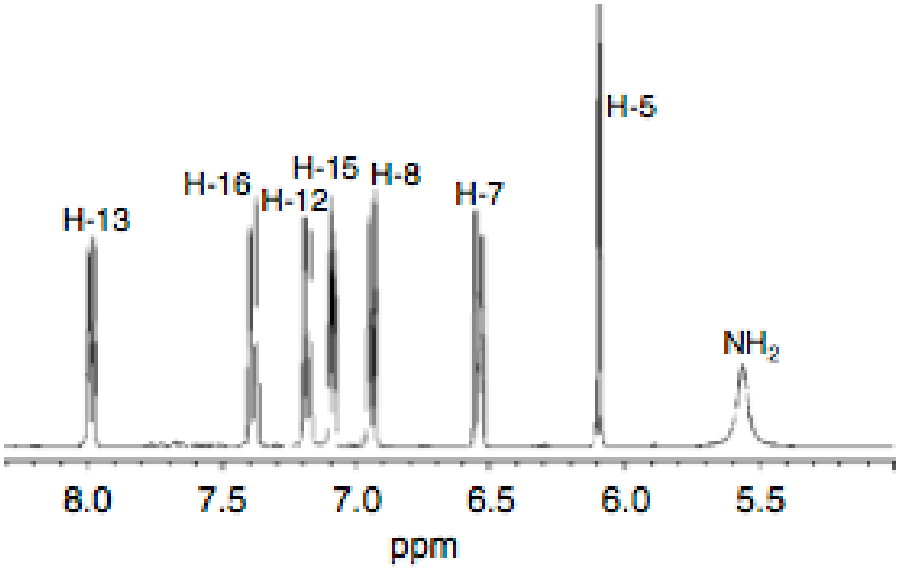

Spectrum 4.1: (revisited) Expansion of the 400 MHz ^{1}H NMR Spectrum of OFP-NH_2 with Assigned Protons (Spectrum 4.1 reproduced from reference 35 with permission from the authors)

With the coordination of the CLSR, the ^{1}H spectrum would be expected to resolve into two sets of peaks, each resulting from one of the two newly formed diastereomers. The NH_2 peak was expected to be the most affected peak on the spectrum, as the lone pair on the nitrogen would be coordinating directly with the metal ion of the CLSR. The site of coordination being on the peak at 5.5 ppm should reveal a splitting of this singlet into two separate singlets. The CLSR metal should dictate the chemical shift of these peaks.

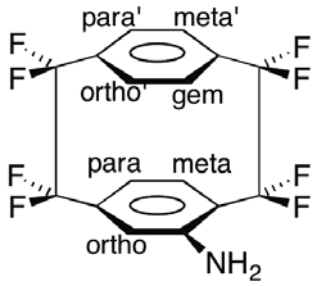

Figure 4.6: Proton Positions for OFP-NH_2

With the *ortho* hydrogen (H-5) being adjacent to the amino substituent, it was predicted that the singlet produced from this atom would appear to split and become an apparent doublet, that would in fact be two singlets, again, each arising from one of the two enantiomers. With through space interactions, it was predicted that the *gem* hydrogen (H-13) should also undergo a change in chemical shift. As the *gem* is shown in the ^{1}H spectrum as a doublet, two doublets should appear when the CLSR is implemented. Indeed, all of the peaks should show separation and chemical shift change but these experiments will indicate where the separation takes place.

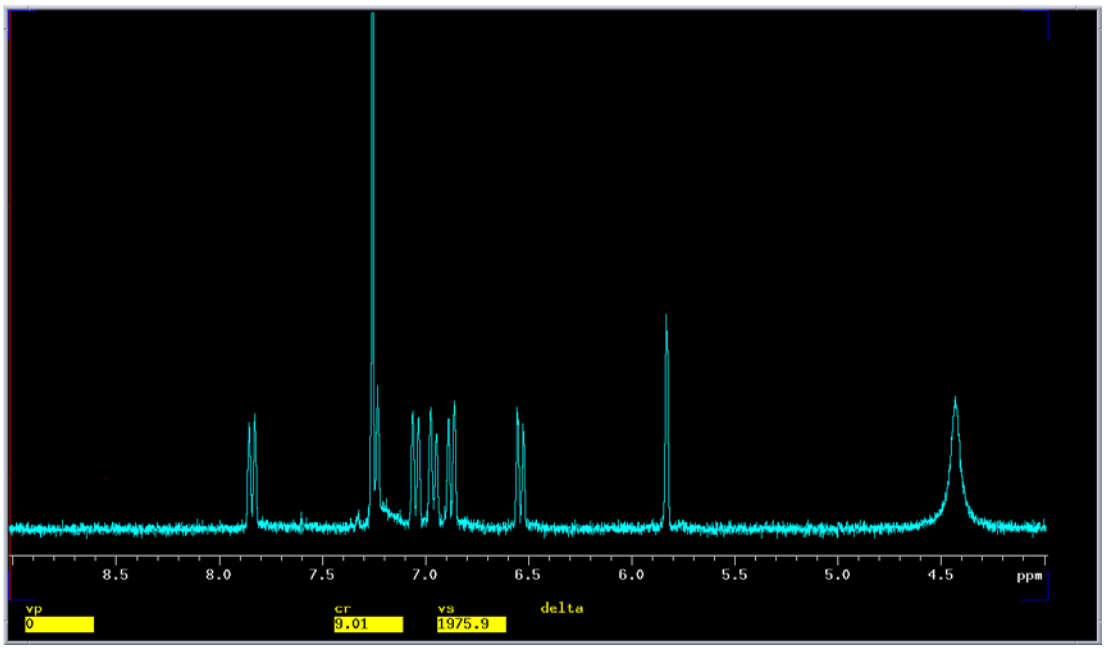

Spectrum 4.2: ^{1}H NMR OFP-NH_2

^{1}H spectra with Ytterbium (Yb) HFC

For ^{1}H spectra, Yb-HFC served as a CLSR, as predicted, by bonding with the lone pair on the nitrogen of the amino group to form diastereomers. This CLSR did exactly what was predicted of it by giving some anticipated separation of the peaks, but some unanticipated results were also seen. The *ortho* peak seen at approximately 5.8 ppm should have shown some resolution into two distinct singlets.

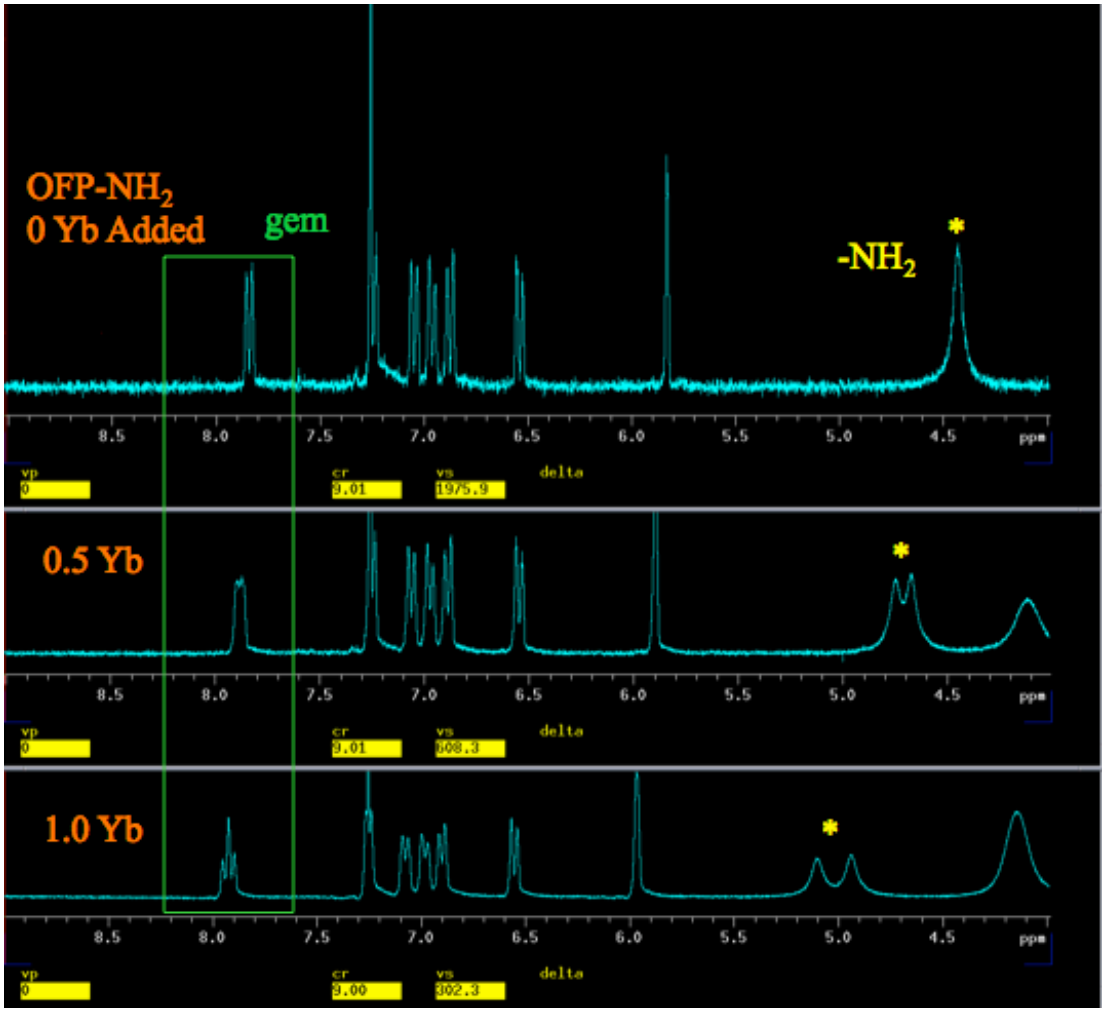

Spectrum 4.3: ^{1}H NMR of OFP-NH_2 with 0-1.0 equivalents of Yb-HFC

With as little as half of an equivalent added to the sample, the beginning of diastereomeric separation began. The singlet from the amino group began to split into two singlets, each one arising from each of the newly formed diastereomers. This almost immediate result was expected and predictably appeared as, once again, the CLSR has coordinated to the amino substituents giving rise to these peaks.

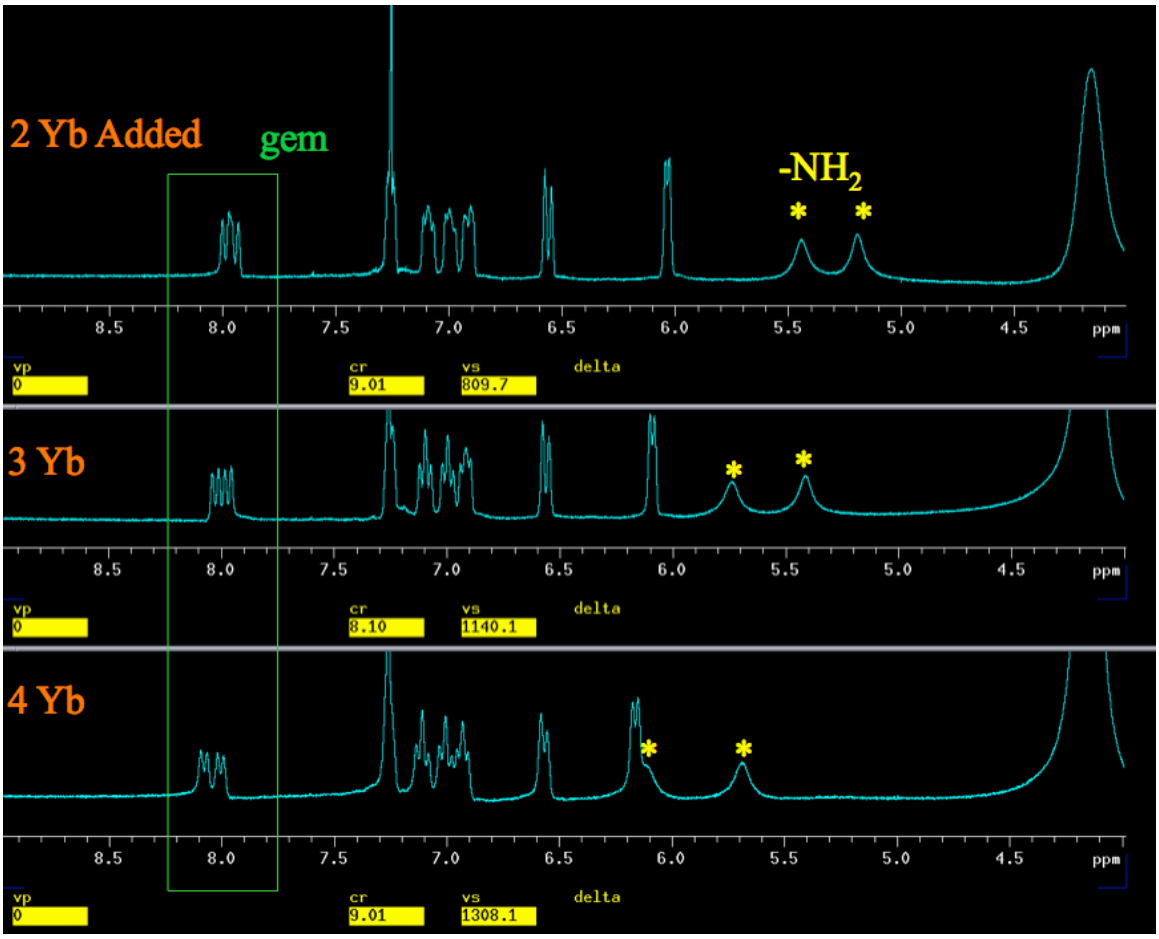

Spectrum 4.4: ^{1}H NMR OFP-NH_2 with 2-4 equivalents of Yb-HFC

In addition to the amino group peak separation, the gem peaks showed excellent resolution with the Yb-HFC CLSR. With the initial addition of half an equivalent, the doublet peaks at approximately 7.8 ppm began to appear to shift downfield. The addition of a one total equivalent showed the original doublet becoming what appeared to be triplet. That triplet was in fact the beginning of the resolution of the two doublets that would be formed and can be seen as early as the addition of three equivalents were added. Also at this point, the amino peaks have been clearly separated and can be seen to be moving further and further downfield with each addition. With the addition of four

equivalents, the two doublets arising from the *gem* protons are fully resolved. The amino singlets have shifted so far downfield that they are now interfering with the *ortho* hydrogen peak. These two peaks had fully resolved and demonstrated exactly what was predicted of them. The *ortho* peak had been expected to also display similar results and this singlet shifted downfield as each increasing equivalents was added to the tube and began to broaden with as little as 1.0 equivalents added. Increasing increments of the Yb HFC continued to shift the peak downfield and after 4.0 equivalents were added, the singlet split into a "doublet' or more correctly, two singlets, each from one of the diastereomers.

The excellent results from the Yb-HFC were encouraging and other CLSRs were investigated. The results from the Eu-HFC are discussed next.

^{1}H spectra with Eu-HFC

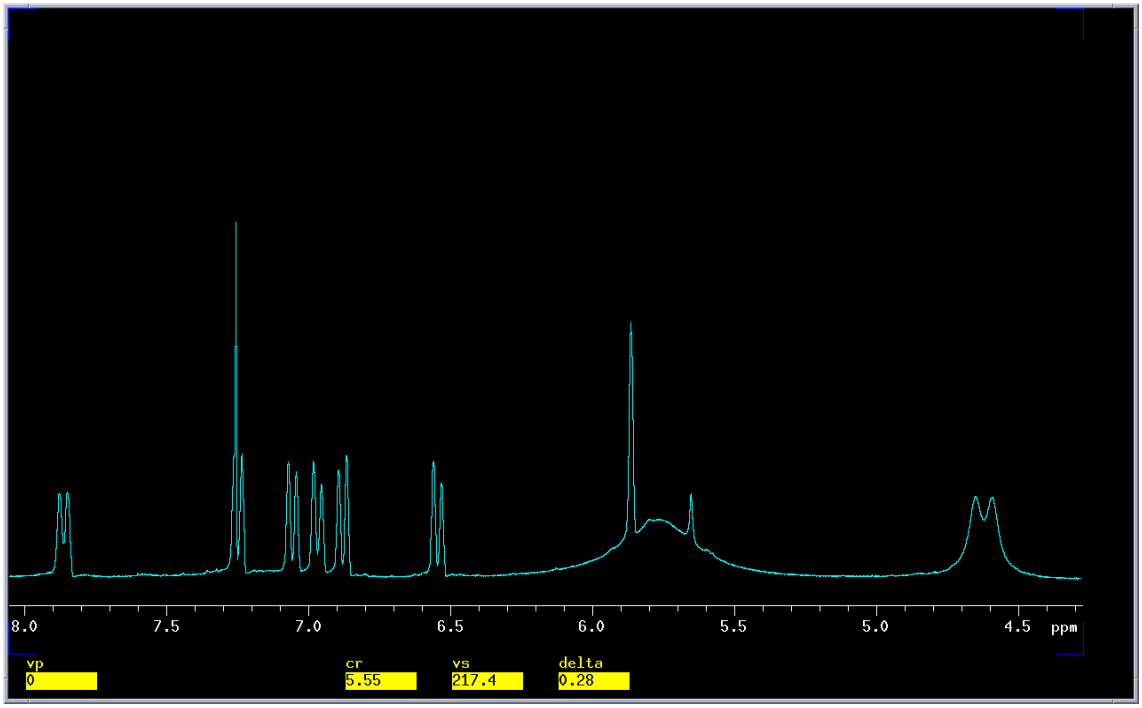

Spectrum 4.6: ^{1}H NMR with 0.5 equivalents of Eu-HFC

With just one half of an equivalent of the Eu-CLSR, the singlet at 4.4 ppm begins to resolve in what appears to be a doublet. That "doublet" is in actuality a singlet from the amino substituent of each of the diastereomers. The peak at approximately 6.1 ppm is non-existent in the original ^{1}H spectrum and grows with each increased equivalent so it was deduced that it could only arise from the CLSR itself. These effects are clearly indicated in the 0.5 and 2.0 equivalents spectra.

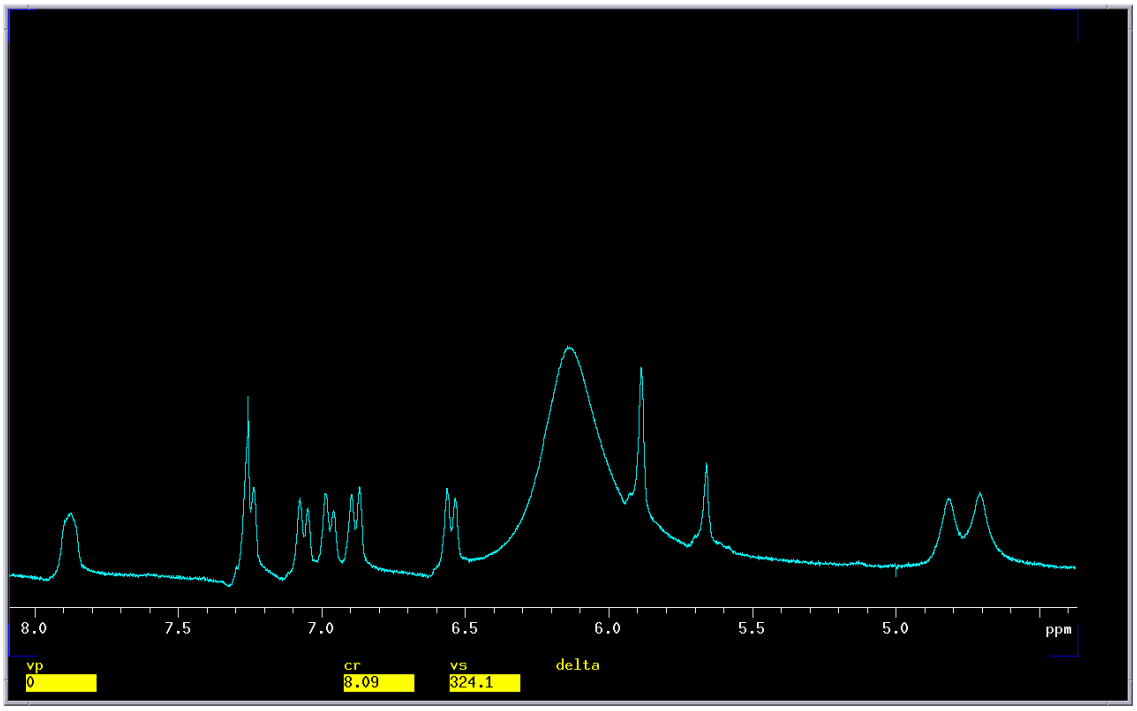

Spectrum 4.7: ^{1}H NMR with 2.0 equivalents of Eu-HFC

With just two equivalents, there was a clear separation of the two singlet peaks at 4.7 ppm. The gem shift peaks at around 7.9 ppm began to show signs of resolution into two doublets as the peak has become broader and has shifted downfield. More equivalents may have given the doublet separation that was anticipated. The baseline distortion of these peaks would not allow for accurate integration so that true quantification of these peaks could be obtained. In conjunction with the increased enormity of the peak at 6.1 ppm revelation that only further baseline distortion would come from the addition of more equivalents.

^{19}F OFP-NH$_2$ Analysis

It was expected that the ^{19}F spectra would be equally as effected as the ^{1}H spectra were while using the same CLSR. Analyzing the effect of each CLSR with the ^{19}F spectra should further prove the enantiomeric differentiation. The ^{19}F assignments from Chapter 3 are revisited.

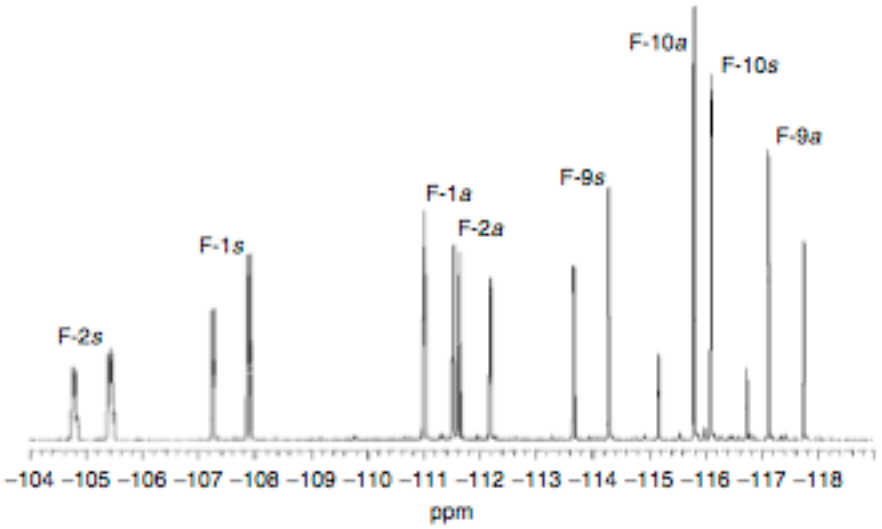

Spectrum 4.8: Expansion of the 400 MHz ^{19}F spectrum of OFP-NH$_2$ with assigned Fluorines (reproduced from reference 35 with permission from the authors) revisited

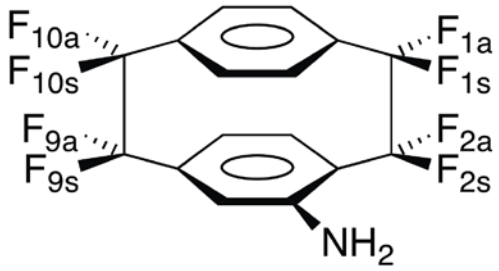

Figure 4.7: Fluorine Positions for OFP-NH$_2$

It would be predicted that the F-2a and F-2s peaks would show the biggest chemical shift change when coordination with the CLSR took place. This is because the ligand would

be predictably close in bonds and through space to the F-2 atoms. Using the same methodology, the F-9a and the F-9s Fluorines should also show some resolution of peaks as they are proximal to the site of coordination. Also the F-1a and F-1s atoms could show a chemical shift change as well as coordination takes place on the same bridge side of the molecule. The only place that would not entirely be expected to have a significant shift change would be the F-10 atoms as they are the furthest away from the ligand both through bonds and through space.

For comparative purposes, the Expanded ^{19}F spectrum of OFP-NH_2 is shown here.

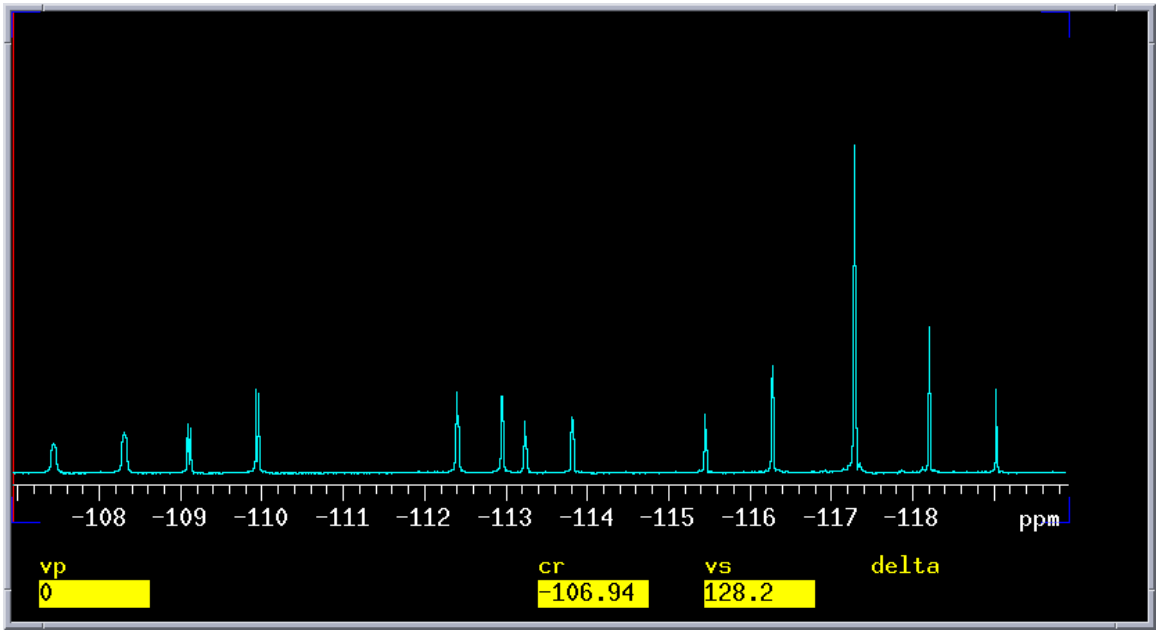

Spectrum 4.9: ^{19}F NMR OFP-NH_2

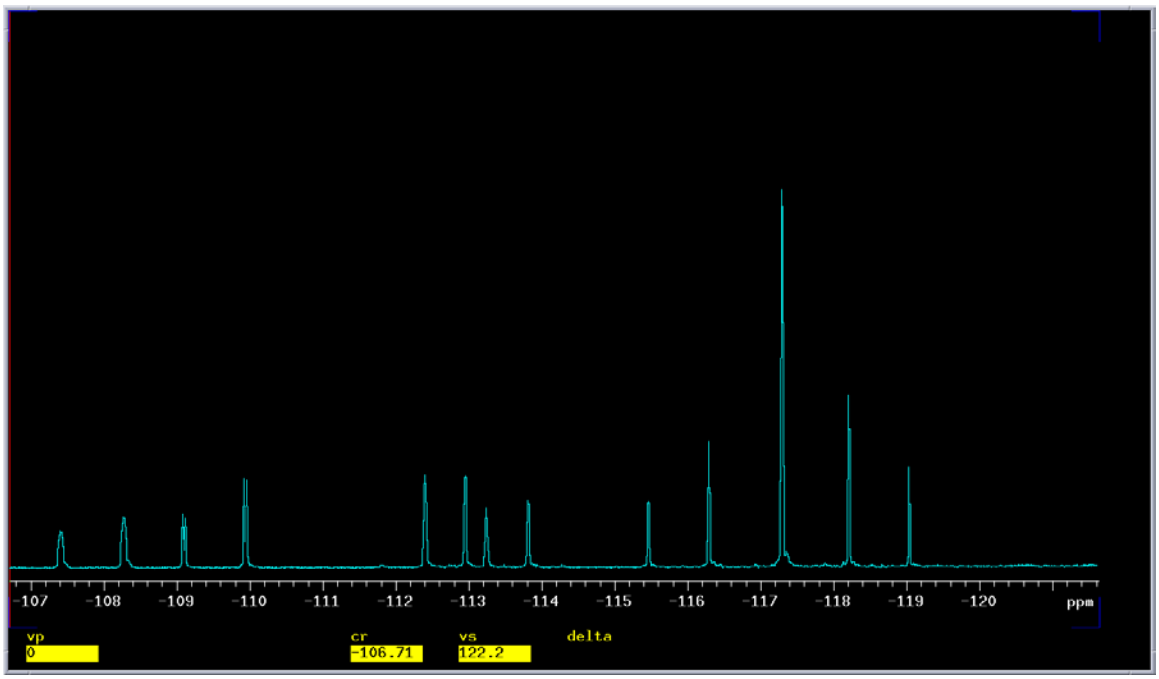

Spectrum 4.10: ^{19}F NMR OFP-NH$_2$ with 0.5 equivalents of Eu-HFC

The F-1s and the F-2s doublets show the largest variation with this CLSR. With the addition of one equivalent of the CLSR the doublets are beginning to show resolution as the peaks begin to appear to broaden and overlap. This is the beginning transition that leads to the enantiomeric peak separation.

Spectrum 4.11: ^{19}F NMR OFP-NH_2 with 1.0 & 3.0 equivalents of Eu-HFC

With each addition of the CLSR, the peaks in the range of -110 to-107 ppm (F-1s and F-2s) were still the most responsive to this effect. The doublets began to separate and become a pair of doublets. Each individual doublet arose from each of the diastereomers. These doublets were stemming from the same atoms but now had different chemical shifts.

With the addition of three equivalents, the F-1s and F-2s were resolving into what would appear to be a quartet. An additional Eu-HFC equivalent showed that the quartet was in

fact resolving into two doublets that stemmed from the two different diastereomers. This was the best result that had been seen at this point and the effect of the Yb-CLSR on the ^{19}F spectra was the next step of this research.

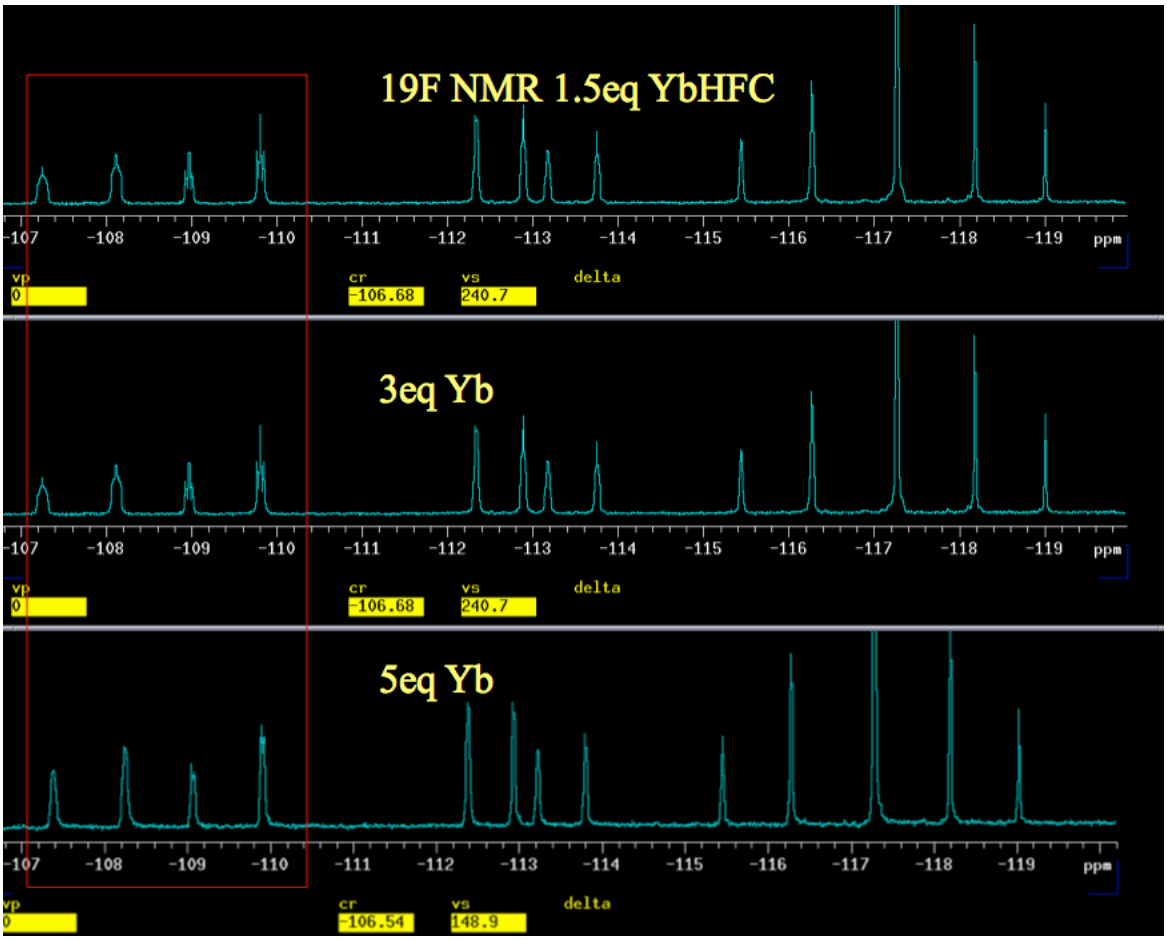

Spectrum 4.12: ^{19}F NMR OFP-NH_2 with 1.5-5.0 equivalents of Yb-HFC

The F-1s and F-2s region of these spectra seen between -110 and -107 ppm did begin to reveal a possibility of good separation. Upon the addition of multiple equivalents, the peaks did not further resolve and these peaks were minimally affected.

Praseodymium (Pr)-HFC

Proton NMR analysis with the Pr-HFC CLSR at first appeared to be giving the same type of resolution of the Amino substituent peak as the Eu-HFC had given. The *gem* position peaks also appeared to mimicking the Eu-HFC as well. With several equivalents of the Pr-HFC, the amino peak began to split was compromised by a hump of a peak at approximately 4.5 ppm. This CLSR would interfere with the shifts of the analyzed peaks for this system. The higher the concentration of shift reagent, the more distorted the spectra became. Analysis of the ^{19}F spectra also proved to no avail as very little to no resolution was seen and baseline distortion began from -111 to -108 ppm. Further Pr-HFC exploration was suspended. The spectra for these experiments can be found in the Appendix.

Chiral Solvating Agents

Chiral Solvating Agents are similar to CLSRs as they will interact with the substrate and form diastereomers. Unlike the CLSR's co-ordination, these interactions are usually hydrogen bonding and polarity based. 2,2,2-trifluoro-1-(9-anthryl)ethanol (Pirkle's alcohol) is a widely used CSA in part because it's very effective ability to bond with Lewis bases such as amino groups.

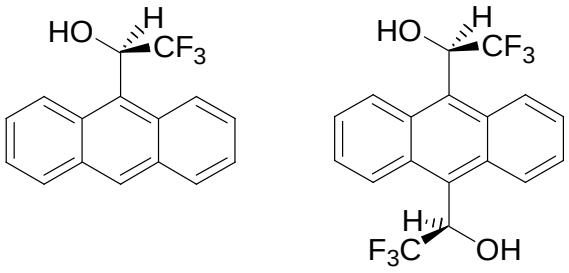

Pirkle's alcohol **Pirkles Difuctional Analogue**

Figure 4.8: Pirkle's Alcohol and Pirkle's Difunctional Analogue

Trials run with Pirkle's alcohol showed degeneration of the spectra giving very complex coupling and therefore very complicated peak revelation. It is for this reason that further investigation was suspended. The spectra derived from analysis with Pirkle's alcohol can be found in the Appendix.

No Chiral Derivatizing Agents were employed in this research, as they form covalent bonds with the substrate and this type of bonding would have been difficult to remove from the compounds studied.

Conclusion

The Yb-HFC worked very well in discriminating between the enantiomers in the ^{1}H NMR of OFP-NH_2. Baseline separation was achieved for both the amino and the gem position hydrogens to give true integration and quantification of results. Eu-HFC worked best for the ^{19}F NMR of OFP-NH_2 although the full resolution of peaks was not achieved for the ^{19}F spectra.

Chapter 5: Chirality and *ortho'*-di NH_2

Enantiomeric Differentiation of *ortho'*-di NH_2

With the application of the chiral lanthanide shift reagent on the di-substituted pseudo ortho-di-NH_2 molecule, it was expected that the effect of the shift reagent would be increased, as there could now be two possible sites of coordination. If results were seen when one amino group was coordinated to the lanthanide ion, then it was predicted that two amino groups could give even better results. Although it is possible to have two points of coordination, one at each of the nitrogen's lone pairs, it is most often seen that only one coordination per molecule takes place due to the kinetically unstable conformation of two sites of coordination per molecule.[27] Having two possible sites of coordination in each molecule would statistically increase the likelihood of molecules coordinating so an increased effect would be presumed.

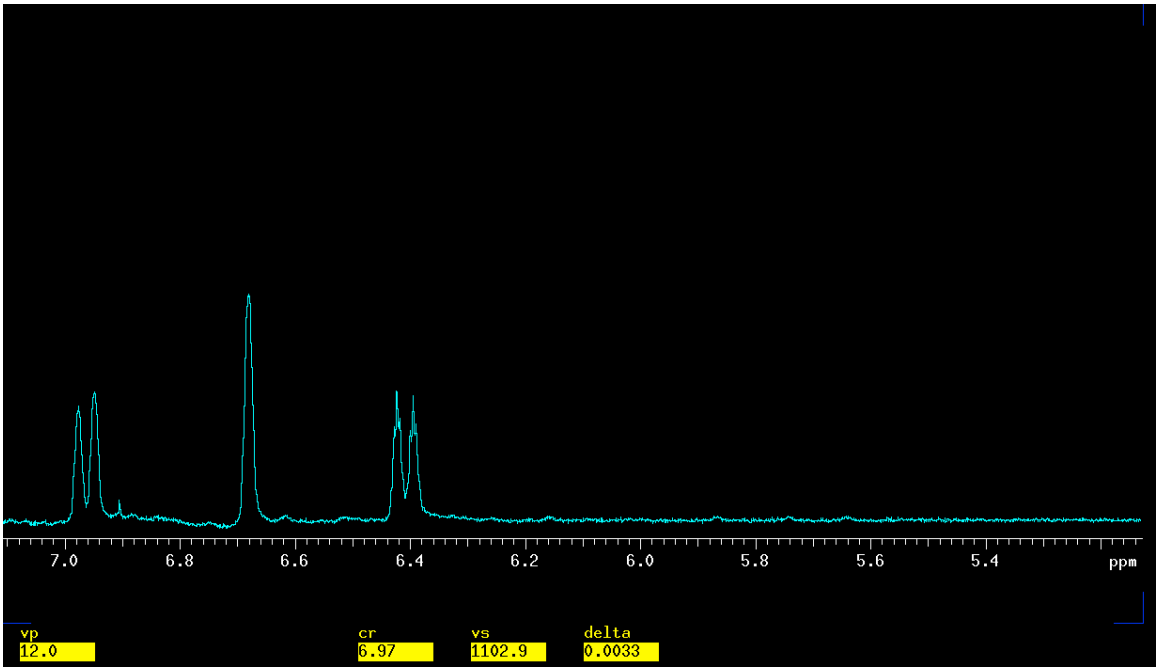

Spectrum 5.1: ^{1}H NMR of ortho' OFP-diNH_2

The ^{1}H NMR of ortho' OFP-diNH_2 in Spectrum 5.1 shows the two doublets and the singlet that have already been assigned by Roche and Marchione as follows: the *para* Hydrogen (H-7) appears as a doublet at 6.38 ppm, the *ortho* Hydrogen (H-5) is a singlet at approximately 6.68 ppm and the *meta* Hydrogen (H-8) appears as a doublet at approximately 6.98 ppm.[32]

The proton NMR showed the best results with the mono substituted OFP-NH_2 when coordinated to the Yb^{+3} HFC CLSR. For this reason, the Yb^{+3} CLSR was utilized to test the effects on the disubstituted analog.

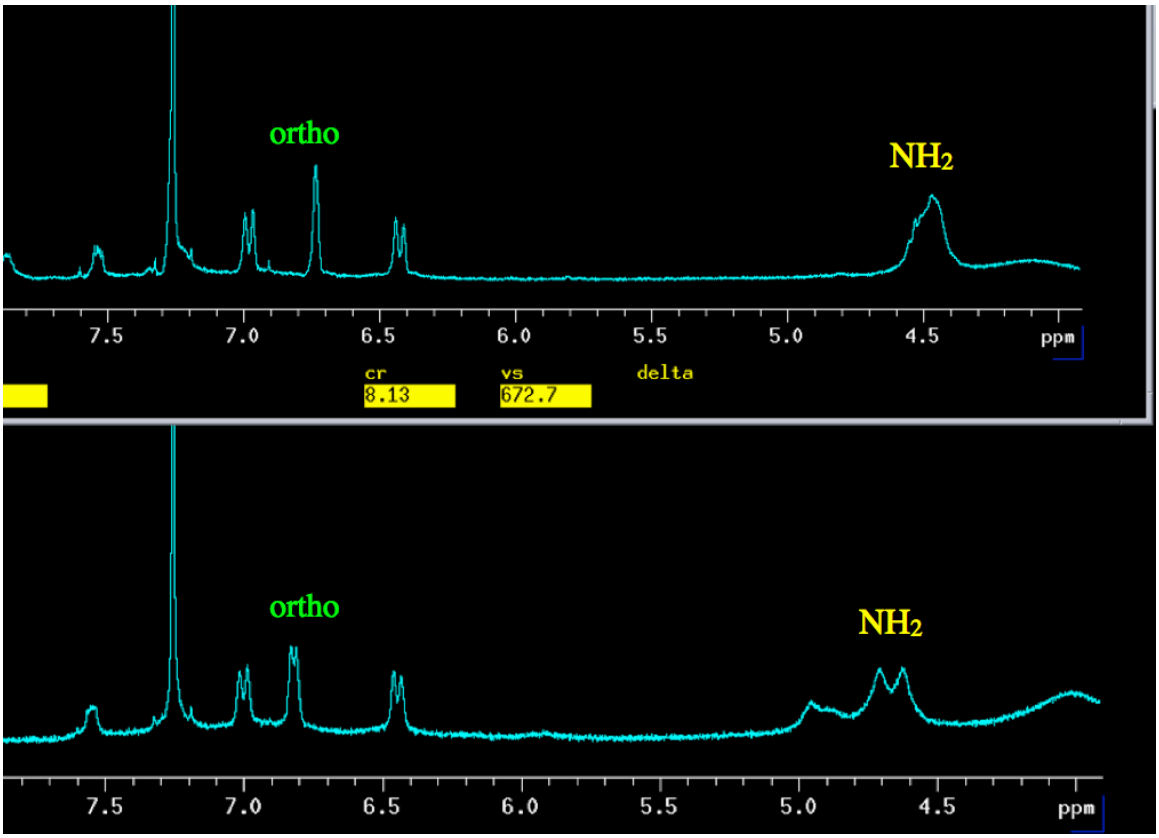

Spectrum 5.2: ^{1}H NMR of OFP-di amino with 0.5 and then 0.75 eqs. of Yb-CLSR

With the first addition of 0.5 equivalents, the amino peak began to broaden and the *ortho* showed a slight broadening as well. The employment of 0.75 equivalents began to show

peak resolution of both the amino and *ortho* peaks. As these peaks shift downfield, the base of the amino peak is the most affected as far as line broadening. The *ortho* peak is also resolved into two singlets and the effect was most prevalent with the addition of one equivalent of the Yb-HFC CLSR.

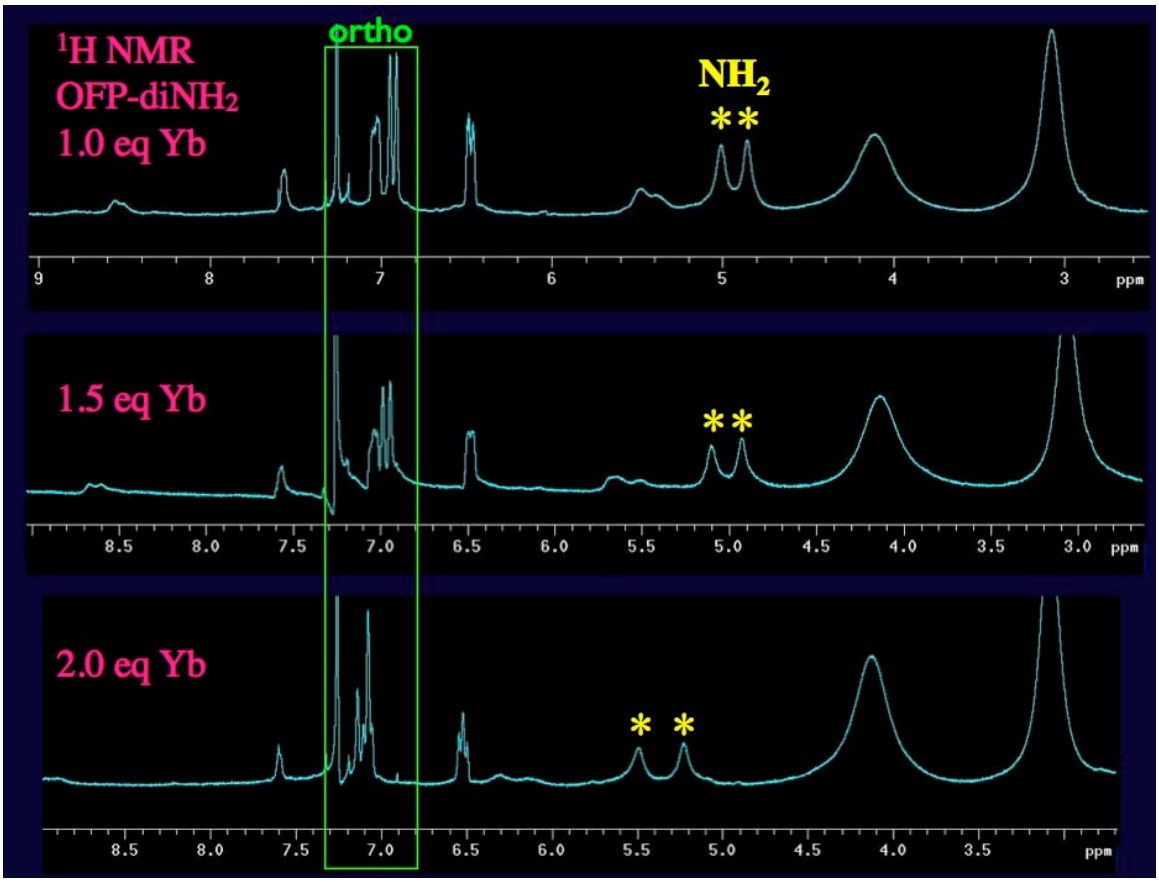

Spectrum 5.3: ^{1}H NMR of di-NH$_2$ OFP with Yb-CLSR

With each increase of the Yb^{+3} CLSR, the amino peak continued to separate. 1.0 equivalent shows the amino peak resolving but not quite as completely as it was anticipated to do. The *ortho* peak, however, has achieved near baseline separation at this point. With the additional half equivalent, a total of 1.5 eq., the amino peak becomes even more resolved and the *ortho* peak, which had baseline separation before, now is

shifted downfield and overlapped with other peaks on the spectrum. With only 2.0 equivalents of the chiral reagent, the amino peaks have achieved baseline separation and the *ortho* peak has merged with other peaks and is barely detectable at this point. Each of these new amino singlets was derived from the one original singlet after coordination. Each singlet arises from each of the enantiomers just as it did with the mono substituted OFP-NH_2.

The most fascinating aspect of this experiment was seen with the *ortho* peak as it showed no splitting with the mono substituted OFP-NH_2 but did resolve with the di substituted molecule. As more of the CLSR is added, the *ortho* peak, at approximately 7.9 ppm, begins to split. The original singlet is seen in the spectrum with 0.5 equivalents of shift reagent at approximately 6.7 ppm. With just 0.75 equivalents, the peak already begins to shift downfield and resolve not into a doublet, but into two singlets at close but different chemical shifts.

The reason for the splitting of the *ortho* peak in the di-substituted moiety does not stem from the proton being solely in the *ortho* position. In the di substituted derivative, the *ortho* site to one of the amino groups is also the *gem* site to the other amino group!

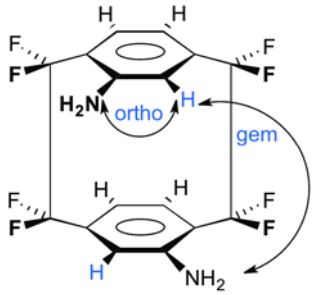

Figure 5.1: Di substituted Showing *ortho* as *gem*

As the proton is simultaneously *ortho* to one amino substituent *and gem* to the other substituent, the *gem* shift effect is being demonstrated at that position. The *gem* effect is prevalent as it is a result of the electronic interactions of the molecule. Not only are there two aromatic rings that are attached in a rigid position, which has profound effects on the ^{1}H NMR before any substitution takes place, but with the addition of an amino group, which is an excellent lone pair donator, the lone pair of electrons also interact with the electronics of the rings. This *gem* shift is seen in the mono substituted OFP-$NH_{2,}$ which has one of these lone pairs available for donation, and once there is disubstitution of the amino groups, two lone pairs of electrons are available to interact with the ring. This electronic interaction allows for the *gem* position proton to be affected and detected differently by NMR. These interactions are the reason for the splitting of the ortho peak in the di amino derivative.

^{19}F NMR of *ortho'*-di NH_2

Although the enantiomeric discrimination of the monosubstituted derivative was not effective with the ^{19}F NMR spectra, it was expected that the *ortho*'-di NH_2 could potentially show better results. Experiments were run with the Yb-HFC CLSR which showed very little effect on the disubstituted analog. The ^{19}F NMR of these trials can be found in the Appendix.

Analysis of Achiral Shift Reagents

To indisputably establish the effectiveness of the CLSR in these NMR spectra, it was an integral part of this research to prove that it was indeed the different enantiomers of OFP-NH_2 that caused the resolution of the peaks and not another reason. One such cause could stem from the coordination of any Lanthanide Shift Reagent to the lone pair on the nitrogen. The possibility that any coordination could enable the two hydrogens on the amino group to somehow behave differently from one another could allow each of these hydrogens to be detected by NMR to be different entities.

Without any complexation of the amino peak, the hydrogens on the amino group are chemically equivalent. This gives a single signal as a broad singlet whose broadness is due to the rotation and exchange of the hydrogens on the amino group with the hydrogens from the solvent. Upon complexation of the nitrogen with the LSR or bonding with another chiral reagent, the hydrogens become chemically different to each other and could potentially give separate NMR peaks.

There are three possible reasons for the splitting of the amino peak in the ^{1}H NMR spectra. When the achiral LSR is added, the differences in equilibrium and rotation along with the varying rate of exchange on the "NMR time scale" could give two sharp singlets, two broad singlets, or one very broad singlet. The NMR time scale is the averaging of two peaks and is the reciprocal of the difference in the frequency of the peaks. This gives the time that the frequencies would have to remain distinct in order to be distinguishable by NMR. This is dependent upon the fixed rigidity of the complex, which can be in equilibrium with slow rotation or fast equilibrium with rapid rotation or minimal

interaction. The effects of these two achiral shift reagents were explored to determine which effect they would have on the amino peak.

The first of these reagents was Resolve-Al™ Yb, Tris(2,2,6,6-tetramethyl-3,5 heptanedionato)ytterbium, $Yb(tmhd)_3$. The achiral structure of Resolve-Al™ Yb is shown in Figure 5.2.

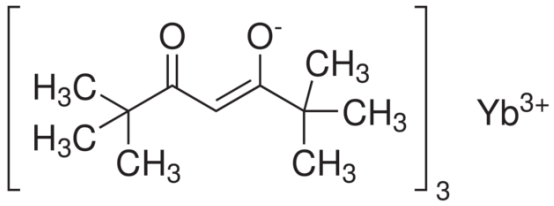

Figure 5.2: Achiral reagent Tris(2,2,6,6-tetramethyl-3,5-heptanedionato)ytterbium $Yb(tmhd)_3$

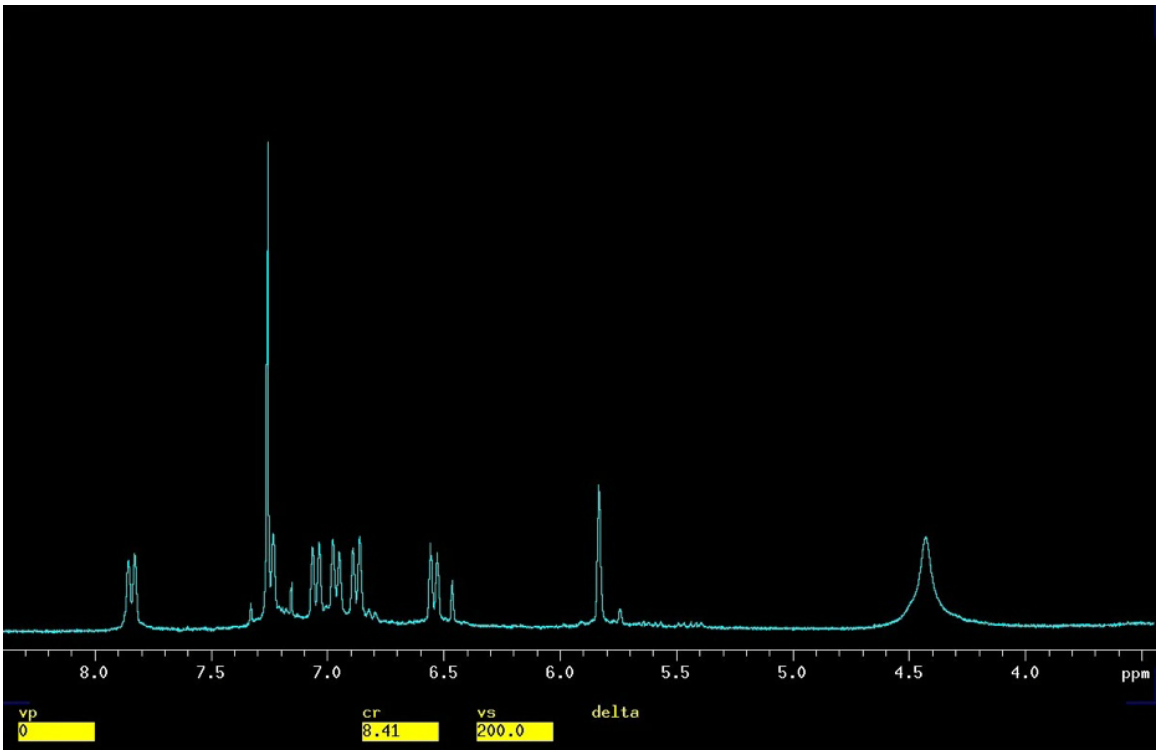

Spectrum 5.4: ^{1}H NMR of OFP-NH_2 (revisited)

The ^{1}H OFP-NH_2 spectrum is reintroduced here for comparison. Previous analysis has shown a separation and chemical shift change of the amino peak with as little as 0.5 equivalents of the Yb-CLSR. Therefore it was presumed if the amino peak was going to split with the achiral shift reagent that it would be rapidly evident.

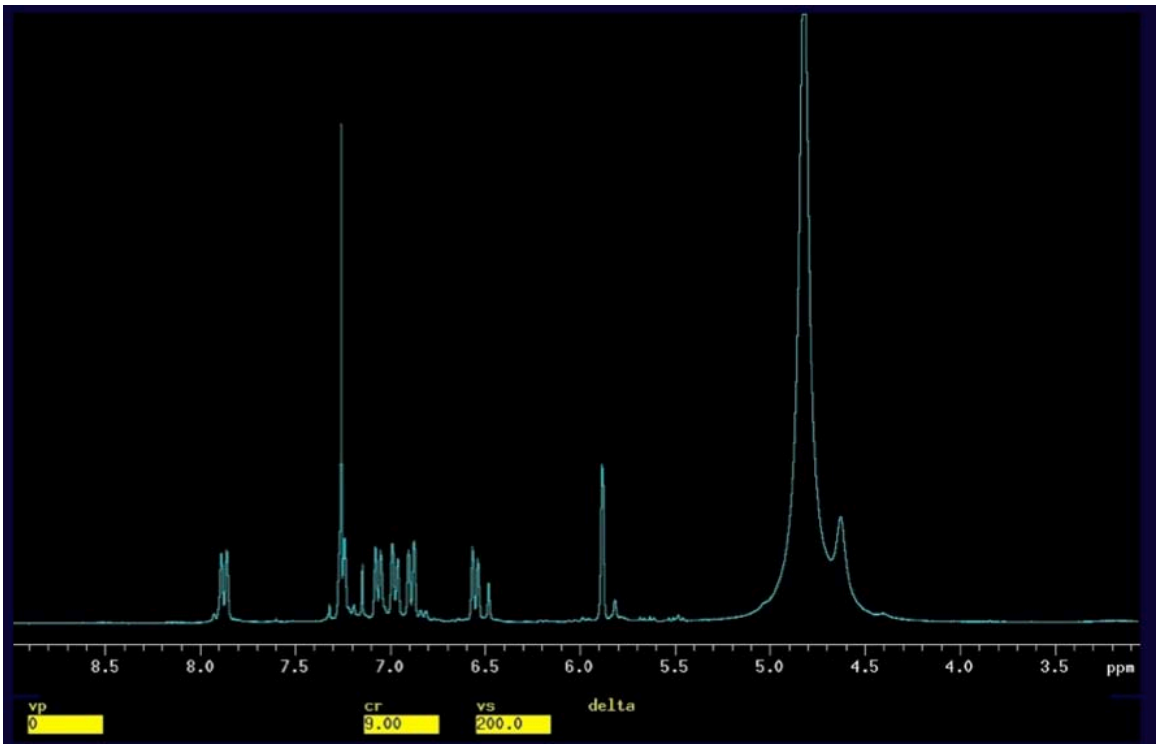

Spectrum 5.5: ^{1}H NMR OFP-NH_2 0.5 eq Yb(tmhd)$_3$ Achiral LSR

Using the Yb-LSR and paying close attention to the amino peak at approximately 4.4 ppm, the effects of the LSR was analyzed. The very large and broad peak that spans from 4.5-5.2 ppm was not seen in the original ^{1}H spectrum of OFP-NH_2 and also was not seen in any of the spectra that used any CLSR. The only cause of this peak could be from the LSR itself. This was an unfortunate property of this particular shift reagent peak as it happened to fall almost exactly on the peak of interest. Additional equivalents were added in hopes that the large and broad peak would shift further downfield than the amino peak to enable analysis of the amino peak.

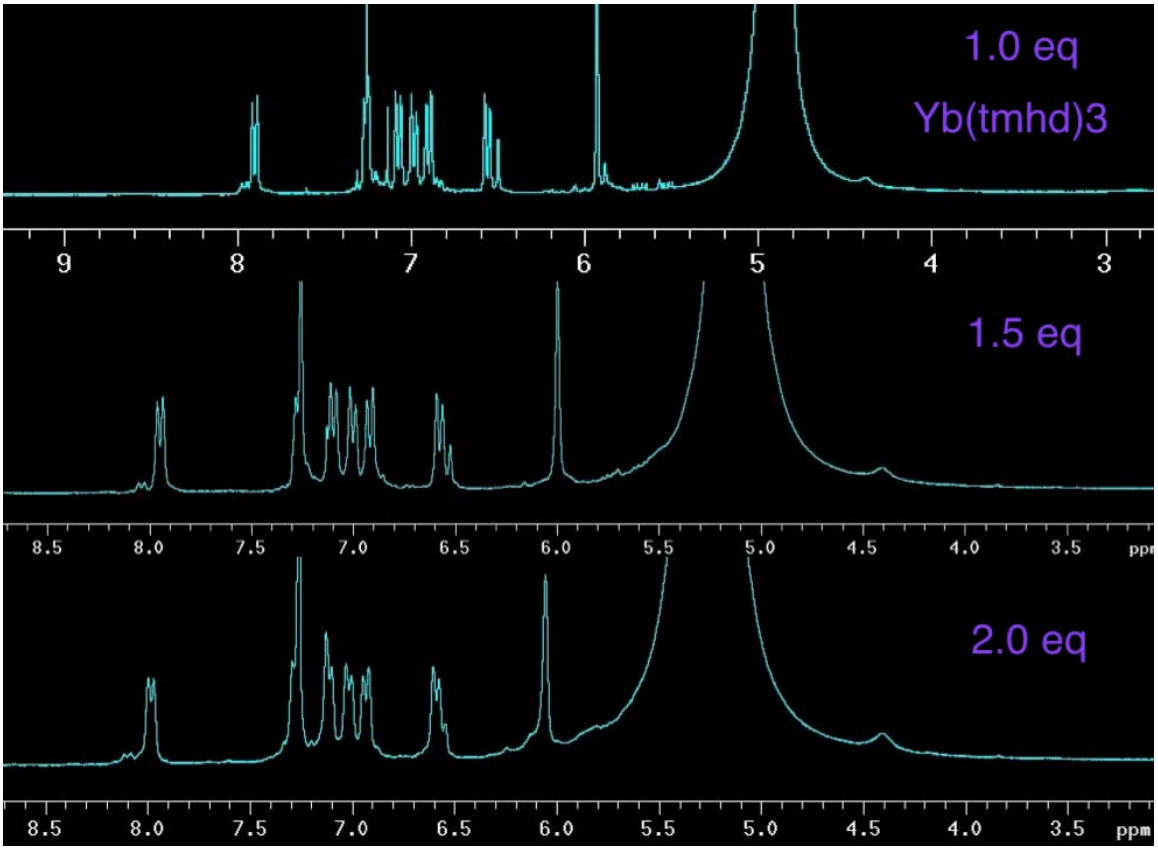

Spectrum 5.6: ^{1}H NMR of OFP-NH2 1.0-2.0 Equivalents of Yb(tmhd)$_3$ Achiral LSR

With each addition of the Yb(tmhd)$_3$ the LSR peak becomes more and more enormous and shifts slightly downfield. The amino peak is barely detectable with 2.0 equivalents so further experimentation with this LSR was ceased**.**

Resolve-Al^{TM} YbFOD, tris(6,6,7,7,8,8,8-heptafluoro-2,2-dimethyl-3,5-octanedionato)ytterbium, YbFOD was used as the second achiral shift reagent to prove that the differentiation was not the cause of these two amino group protons. The peaks from this shift reagent would not interfere with the peaks of interest. The structure of Resolve-Al^{TM} YbFOD is shown in Fig. 5.3.

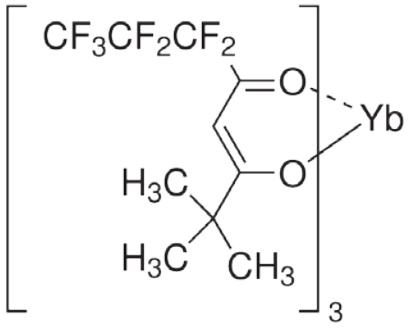

Figure 5.3: Structure of Resolve-Al™ YbFOD

Achiral shift reagent, Resolve-Al™ YbFOD was utilized with same method as the previous LSR. Expectations of almost immediate results were anticipated if this LSR were going to have an effect on this ^{1}H NMR spectrum.

With the addition of one equivalent of the LSR very little change in chemical shift was apparent. The amino peak has shown no indication of resolving and, fortunately, no large shift from this LSR is visible in this spectrum Additional equivalents were added to try ensure that a larger concentration of the LSR would not effect this amino peak.

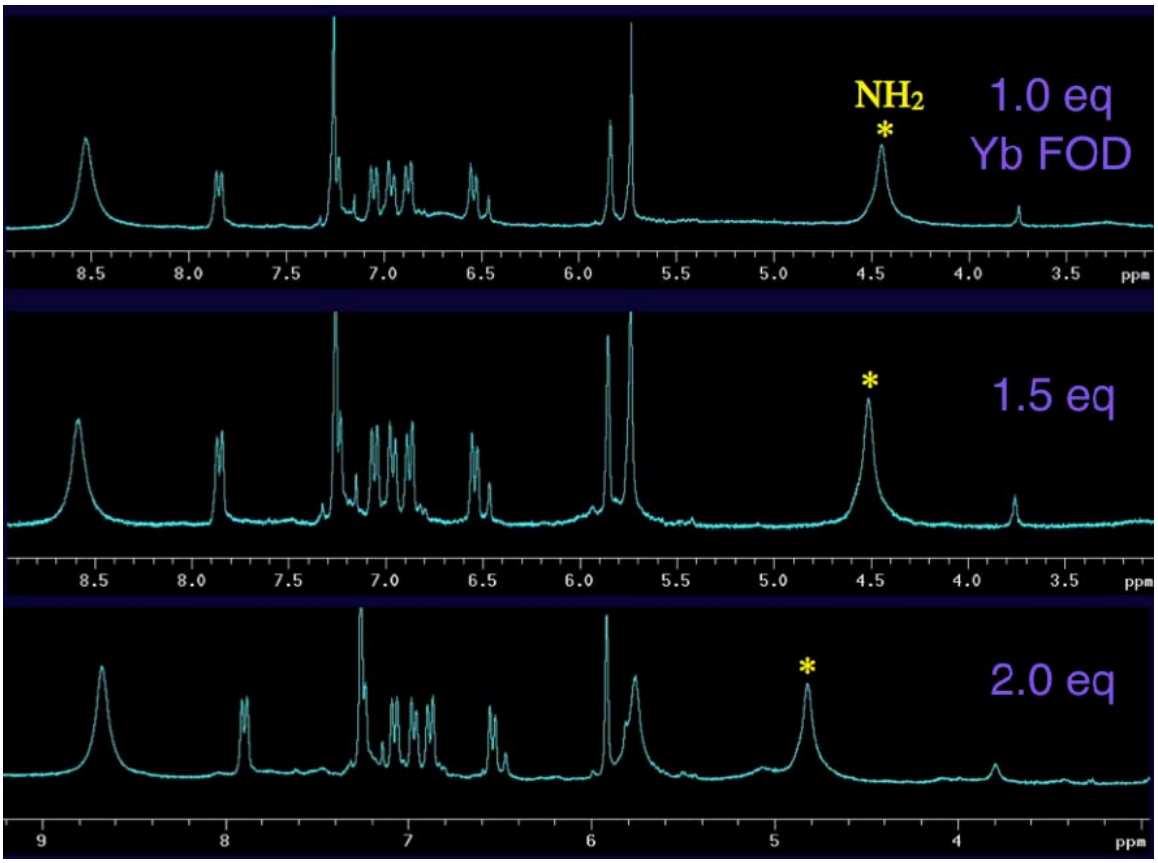

Spectrum 5.8: ^{1}H NMR of OFP-NH_2 with 1.0-2.0 Equivalents of Achiral LSR, YbFOD

In these spectra, it is evident that the amino peak is shifting downfield with as little as one equivalent; the peak is seen at approximately 4.45 ppm. With the additional half equivalents added, the chemical shift change continues as it appears at 4.50 ppm. The amino peak continues to shift with the two equivalents but no separation is perceptible at all.

This indicates that it is not the two hydrogens that are behaving differently to one another. This proves that the two diastereomers that are formed by coordination are giving rise to the two singlets that each stem from the amino group on each of the enantiomers.

Conclusion

As predicted, the Yb-HFC worked very well in discriminating between the enantiomers in the ^{1}H NMR of *ortho'* OFP-diNH_2 just as it did with the monosubstituted derivative**.** Conclusive evidence of the discrimination of these newly formed diastereomers was confimed by the use of an achiral Lanthanide Shift Reagent, Yb-FOD. The achiral LSR showed no separation of any of the peaks on the ^{1}H NMR spectrum of OFP-NH_2.

Chapter 6: Conclusion and Future Work

Conclusion

For the very first time, a full multinuclear unambiguous assignment of ^{1}H, ^{13}C, and ^{19}F spectra for a monosubstituted OFP derivative, OFP-NH_2 has been described. This significant accomplishment was realized with the utilization of several NMR experimental techniques. NMR (1D) was used in conjunction with 2D, COSY and HETCOR NMR, to definitively establish these assignments. The assignments were confirmed using a 400 MHz NMR machine and nOe experiments, NOESY and HOESY, further corroborated these results. This research led to the publication in the Journal of Magnetic Resonance in Chemistry in 2005.[35]

These assignments allowed for the chiral discrimination of enantiomers of OFP-NH_2. Shift reagents, which included Chiral Lanthanide Shift Reagents and Chiral Solvating Agents, were used to determine the effectiveness of differentiating between the enantiomers. The CLSRs proved to be best method for this investigation, but the CLSR that worked best for the ^{1}H NMR spectra did not work best for the ^{19}F NMR spectra. Yb-HFC showed the best resolution of peaks for the proton spectra while Eu-HFC worked best for the fluorine spectra.

The method utilized for enantiomeric discrimination of a monosubstituted derivative also was successful for a disubstituted derivative, *ortho*' OFP-diNH_2.

Future Work

These unambiguous assignments led to the enantiomeric differentiation of both a mono- and di- substituted OFP derivative. The disubstituted analog studied in this thesis was the *ortho*' isomer. Upon completion of this research and using the methods described in this thesis, it was possible to do the same unambiguous multinuclear assignments on both the *para*' and *meta*' isomers. This research was done and published in the MRC as this thesis was being written, during the Fall 2012.[46]

Other work completed and discussed in this thesis established a methodological use to distinguish each enantiomer in an NMR spectrum. This method is applicable to discriminate enantiomers of other compounds and can therefore be used to monitor chiral resolution of these compounds. In the future, this approach could be used to monitor the chiral resolution of both OFP-NH_2 and *ortho*'-diNH_2.

Once enantiopure forms of OFP-NH_2 and *ortho*'-diNH_2 become available, those enantiopure versions, R and S from OFP-NH_2 and R,R and S,S, from the di-substituted compound, could themselves be used as chiral shift reagents. There is potential for the pharmaceutical industry to utilize any of these new chiral shift reagents to produce enantiomerically pure forms of medications, which could reduce or eliminate unwanted or harmful side effects from both common and novel medications.

The analysis that was described and applied to discriminate the *ortho*' diNH_2 could be applied to both the *meta*' and *para*'diNH_2 isomers. The chiral discrimination method used in this thesis was then utilized by a former researcher from the Roche Group, Kasey

Cox. Kasey was able to complete the chiral discrimination of both of these disubstituted isomers with CLSRs. The results of the chiral discrimination of OFP-NH_2 and *ortho*' OFP-diNH_2 discussed in this thesis along with the chiral results work completed by Kasey will be written and submitted for publication sometime this year (2013).

Appendix

NMR Spectra that did not show significant results

Analysis of the spectra shown in this appendix was an integral part of finding the methods that did work and were reported in the body of this thesis.

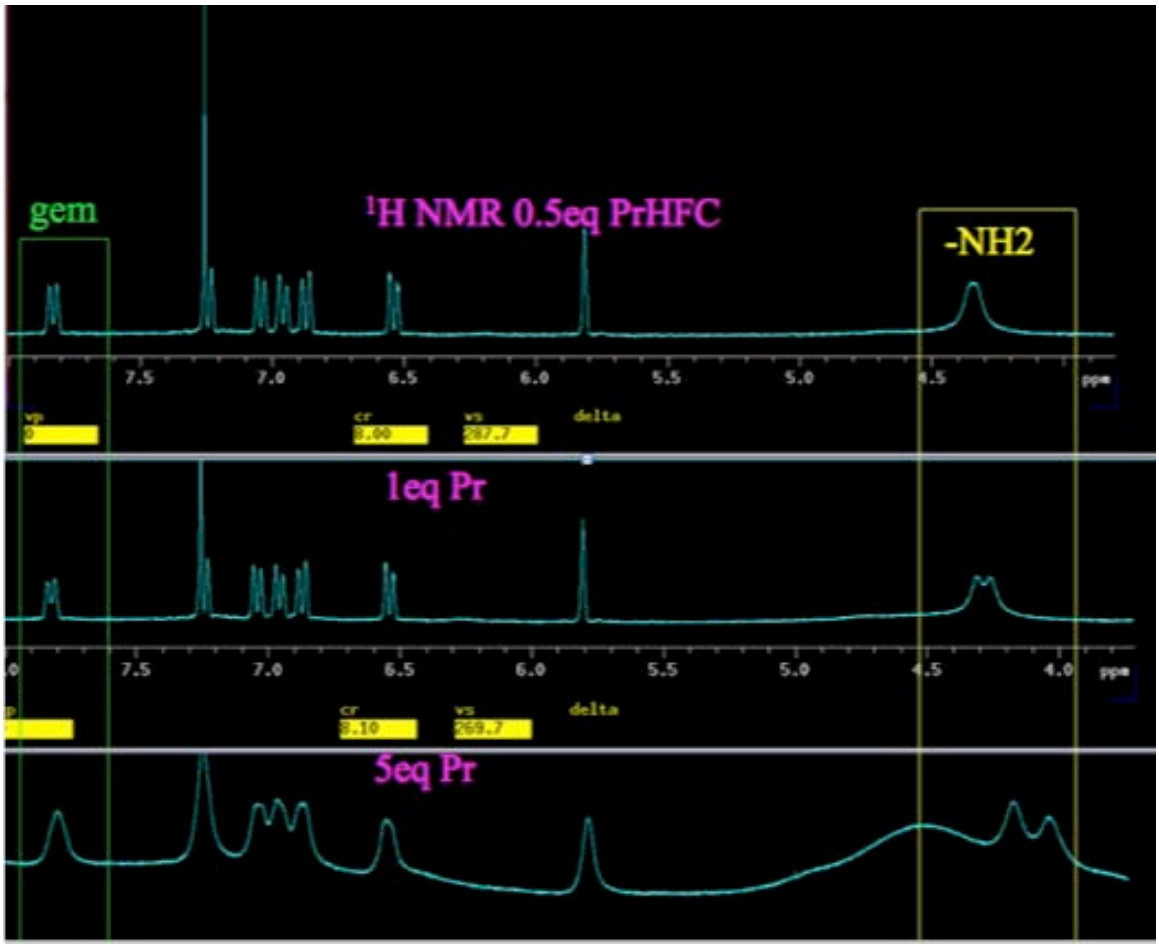

Spectrum A.1: ^{1}H NMR OFP-NH_2 with 0.5-5 Equivalents of Pr-HFC

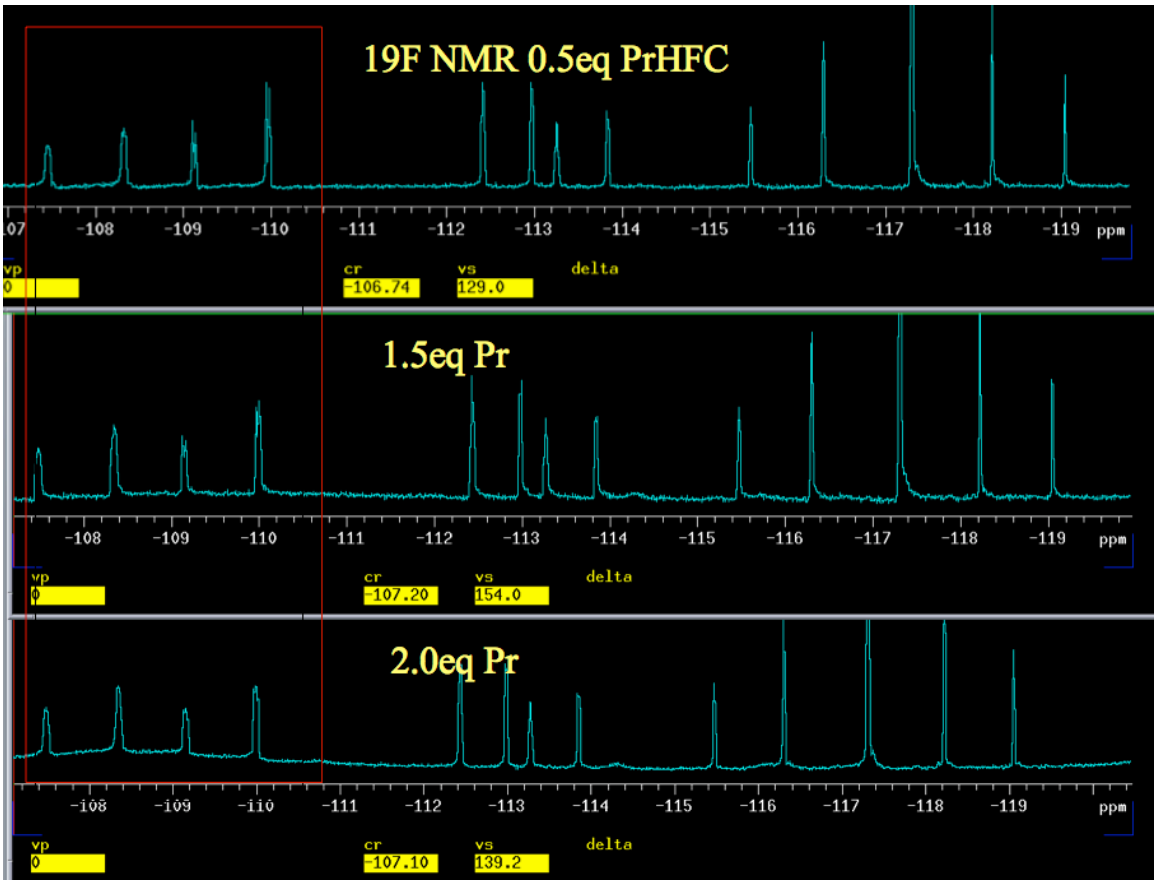

Spectrum A.2: ^{19}F NMR OFP-NH_2 with 0.5-2.0 Equivalents of Pr-HFC

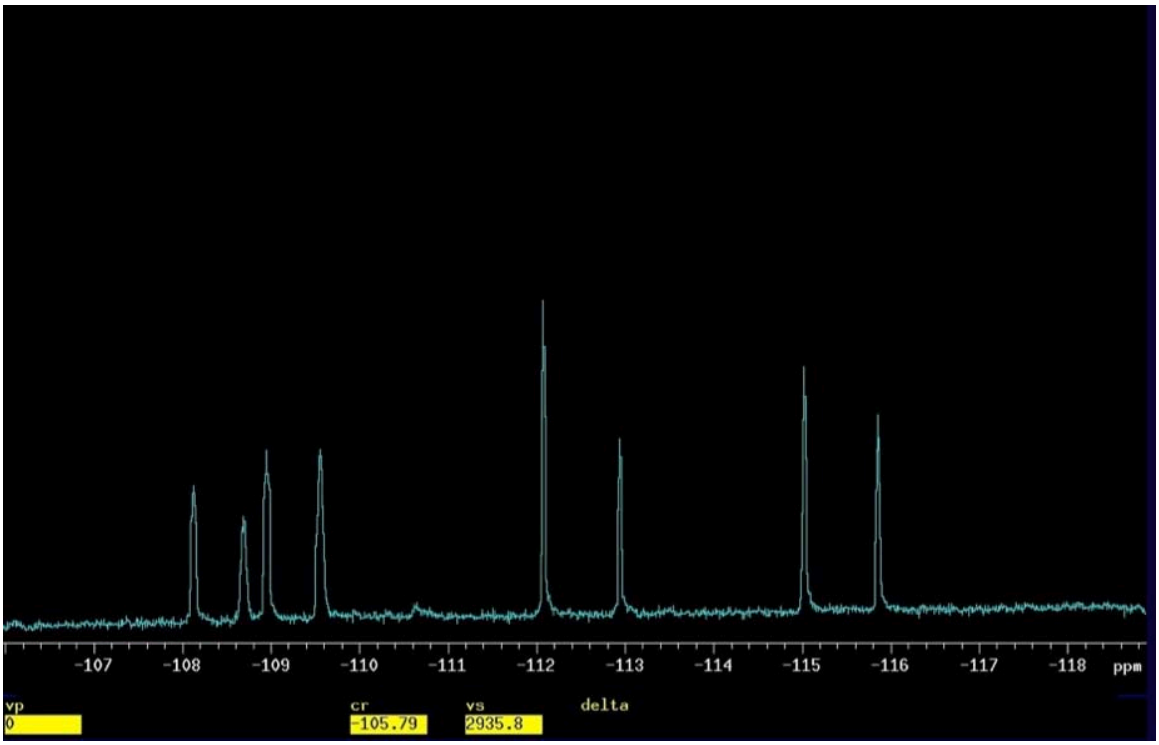

Spectrum A.3: ^{19}F NMR OFP-diNH_2 0.5 Equivalents of Yb-HFC

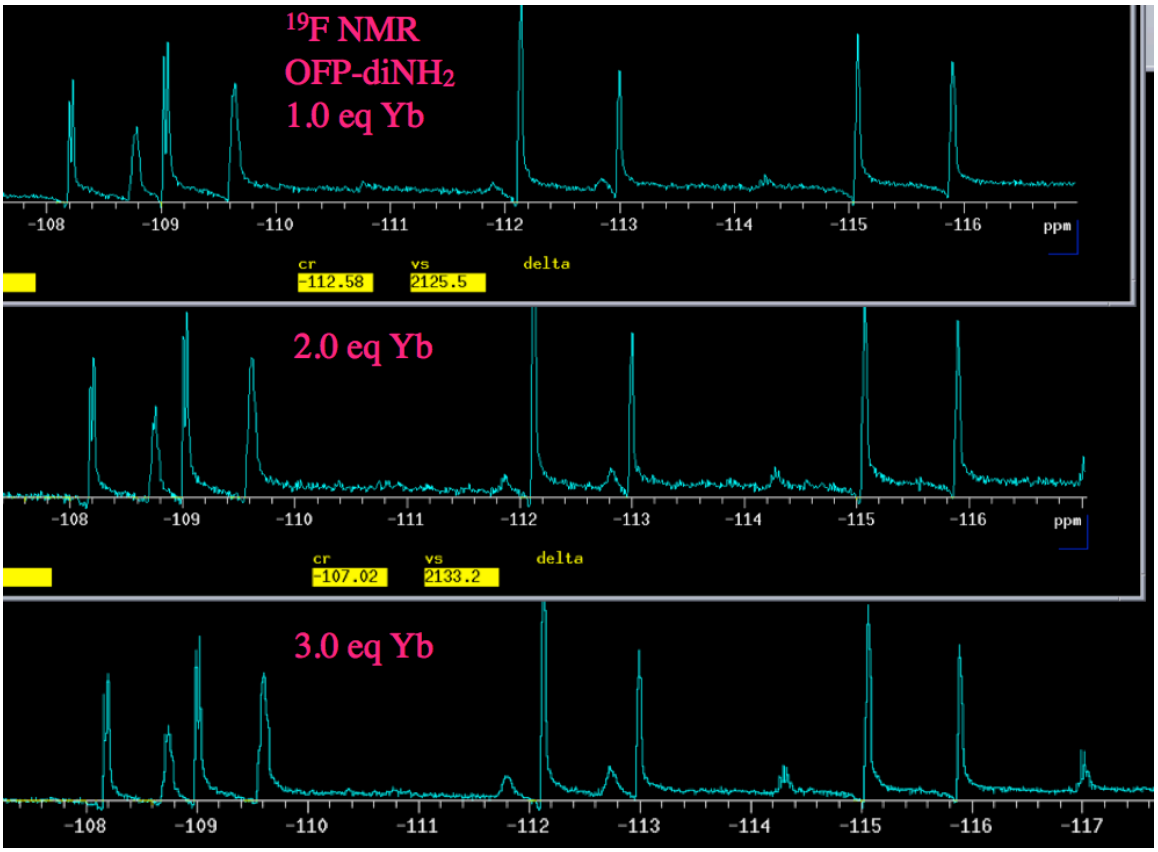

Spectrum A.4: ^{19}F NMR OFP-diNH$_2$ 1.0-3.0 Equivalents Yb-HFC

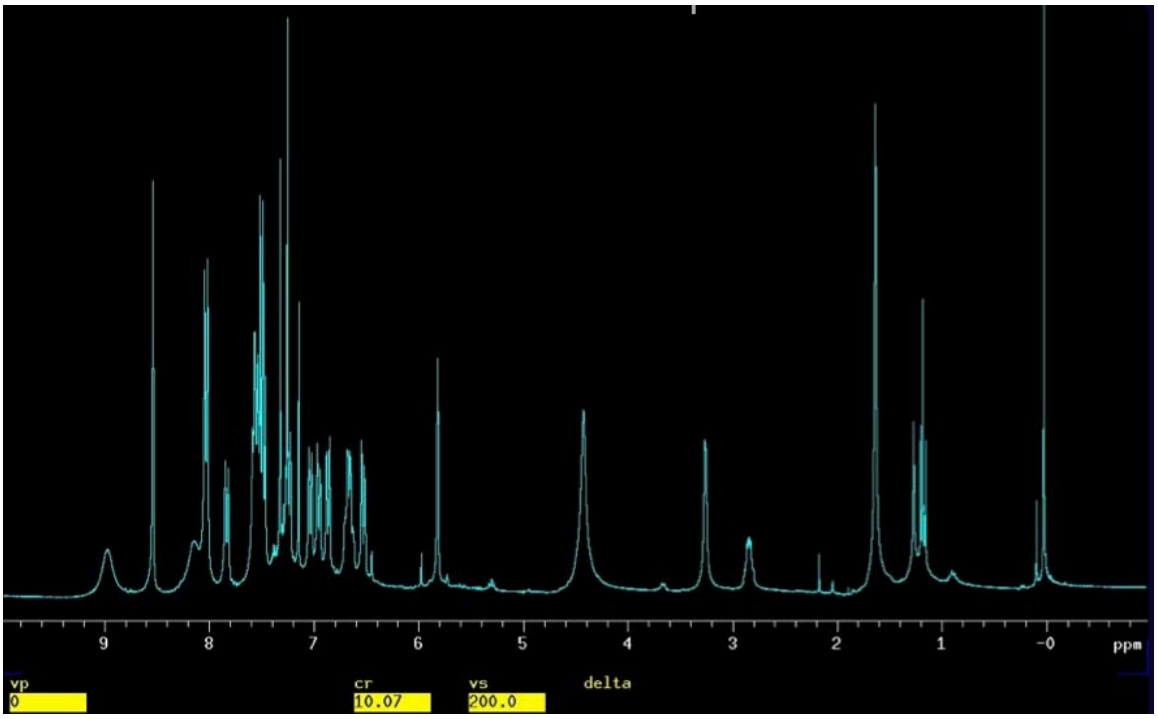

Spectrum A.5: ^{1}H NMR OFP-NH_2 0.5 Equivalents Pirkle's Alcohol

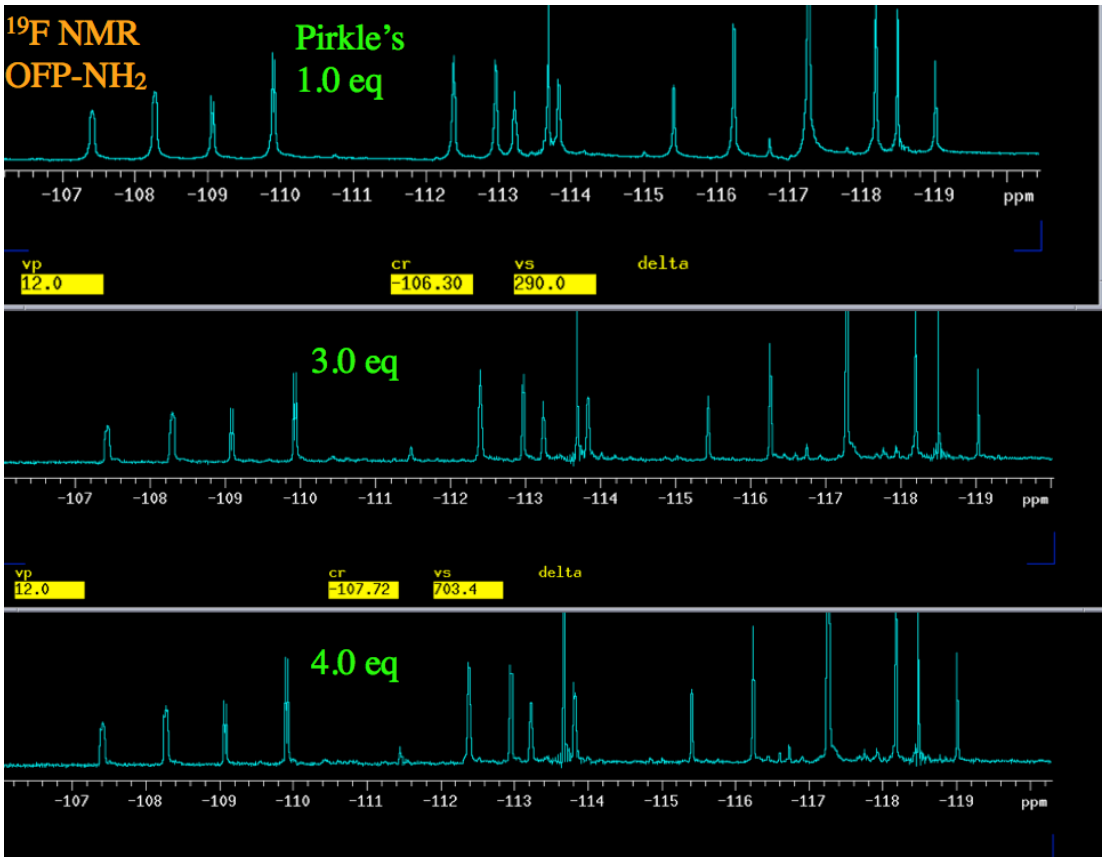

Spectrum A.6: ^{19}F NMR OFP-NH_2 1.0-4.0 Equivalents Pirkle's Alcohol

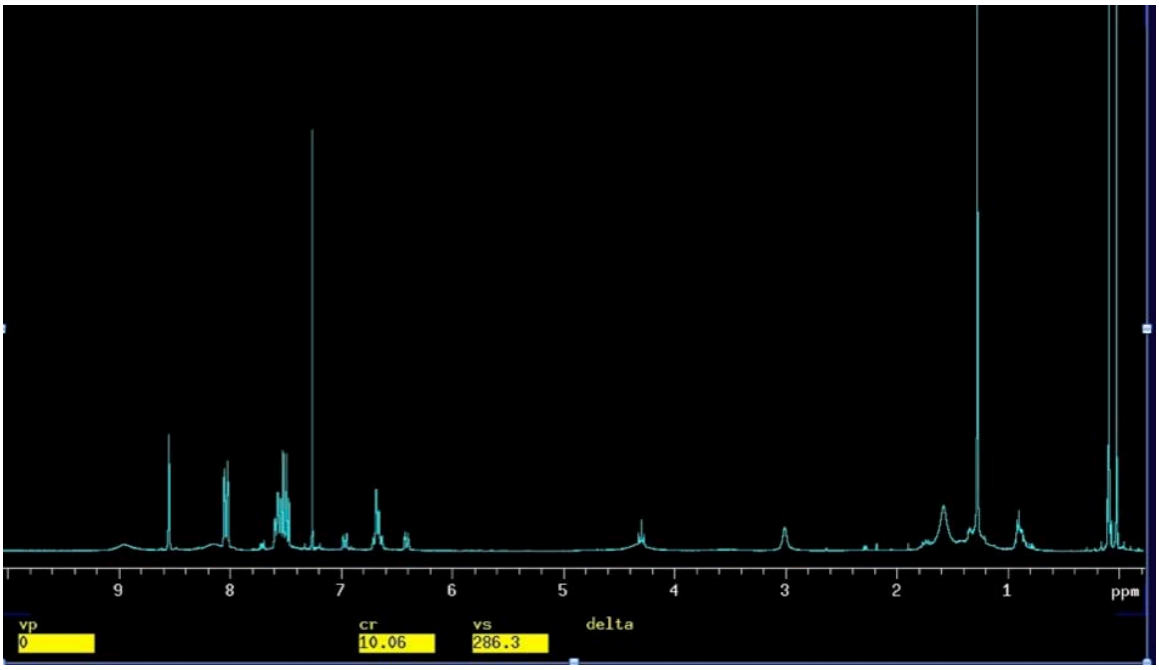

Spectrum A.7: ^{1}H NMR OFP-diNH_2 0.75 Equivalents Pirkle's

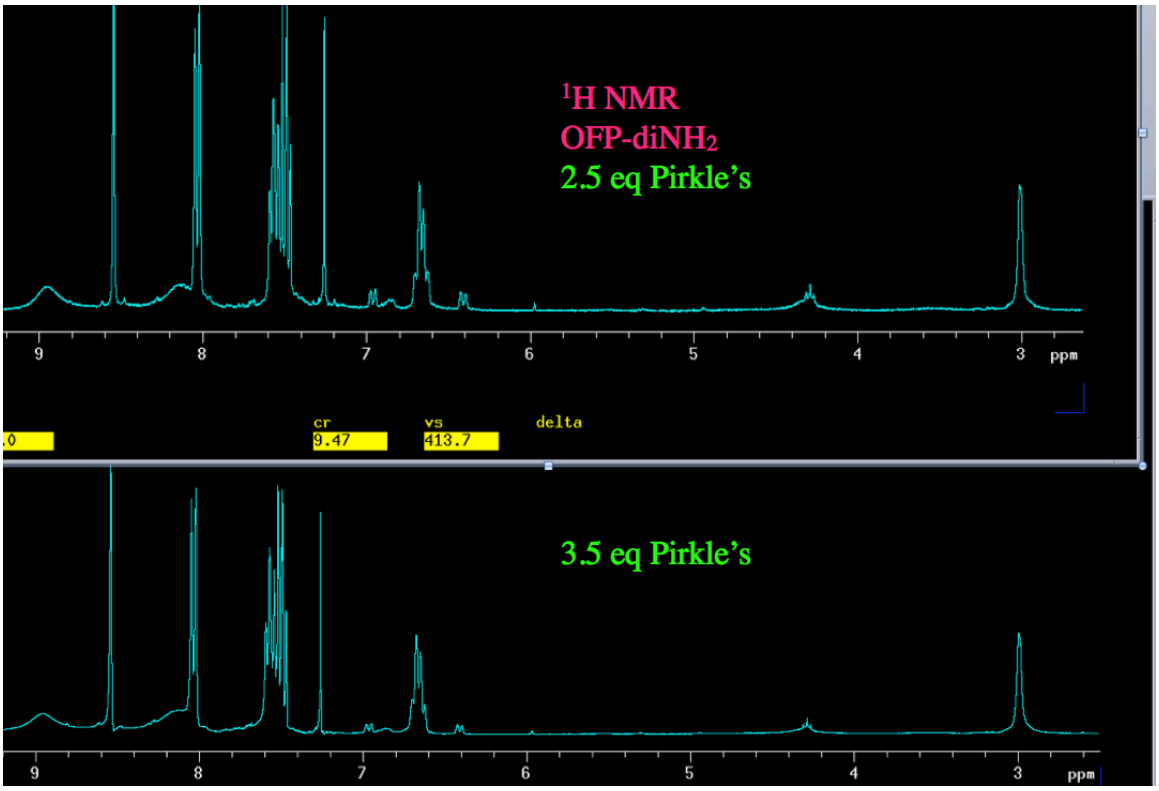

Spectrum A.8: ^{1}H NMR of *ortho'*diNH$_2$ With 2.5 and 3.5 Equivalents Pirkles Alcohol

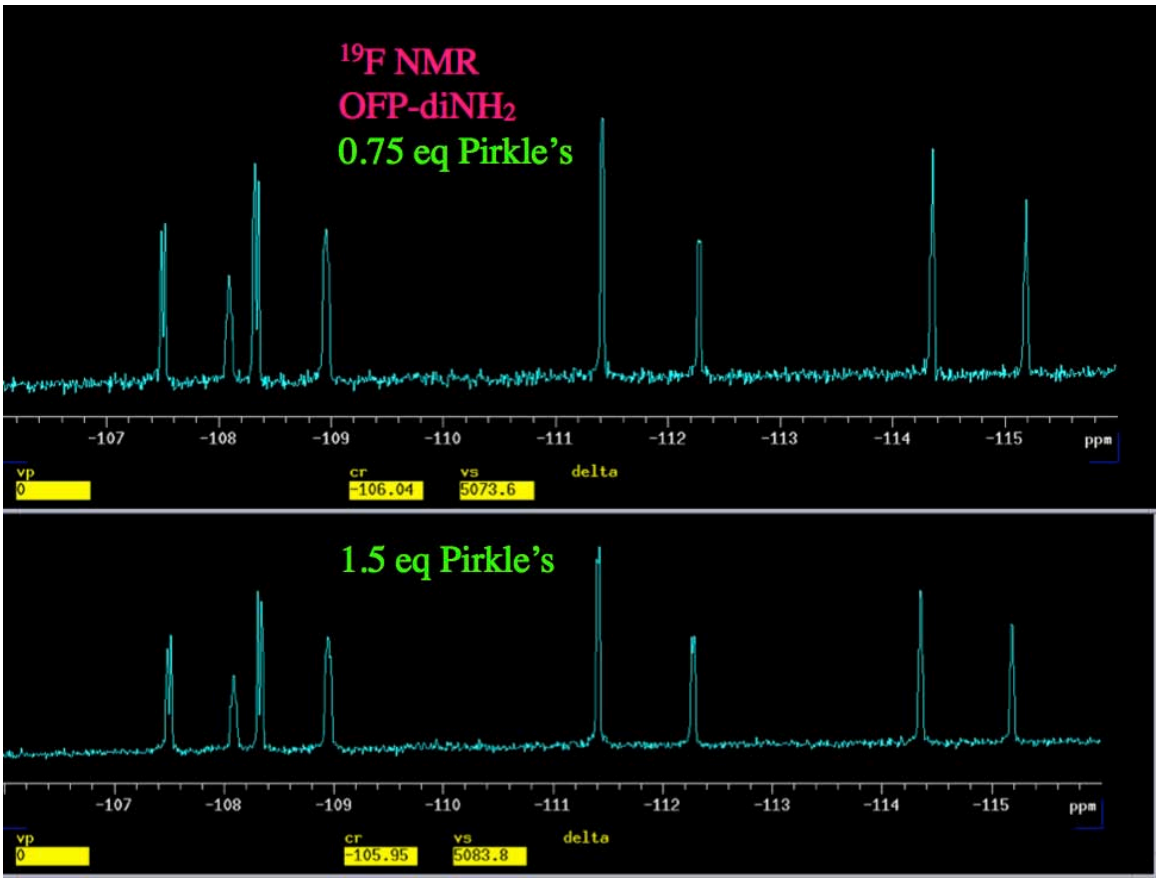

Spectrum A.9: ^{19}F NMR of *ortho*' diNH$_2$ with 0.75 and 1.5 Equivalents of Pirkles Alcohol

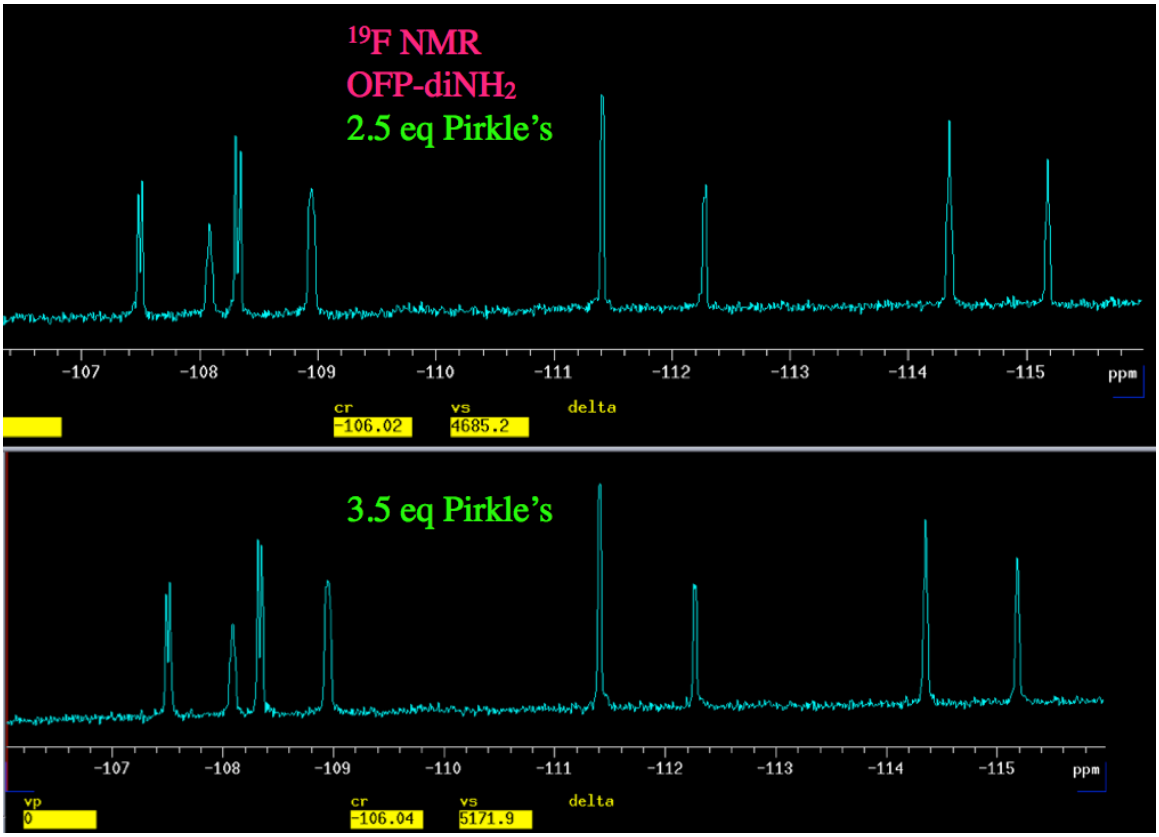

Spectrum A.10: ^{19}F NMR of *ortho'*diNH$_2$ With 2.5 and 3.5 Equivalents Pirkles Alcohol

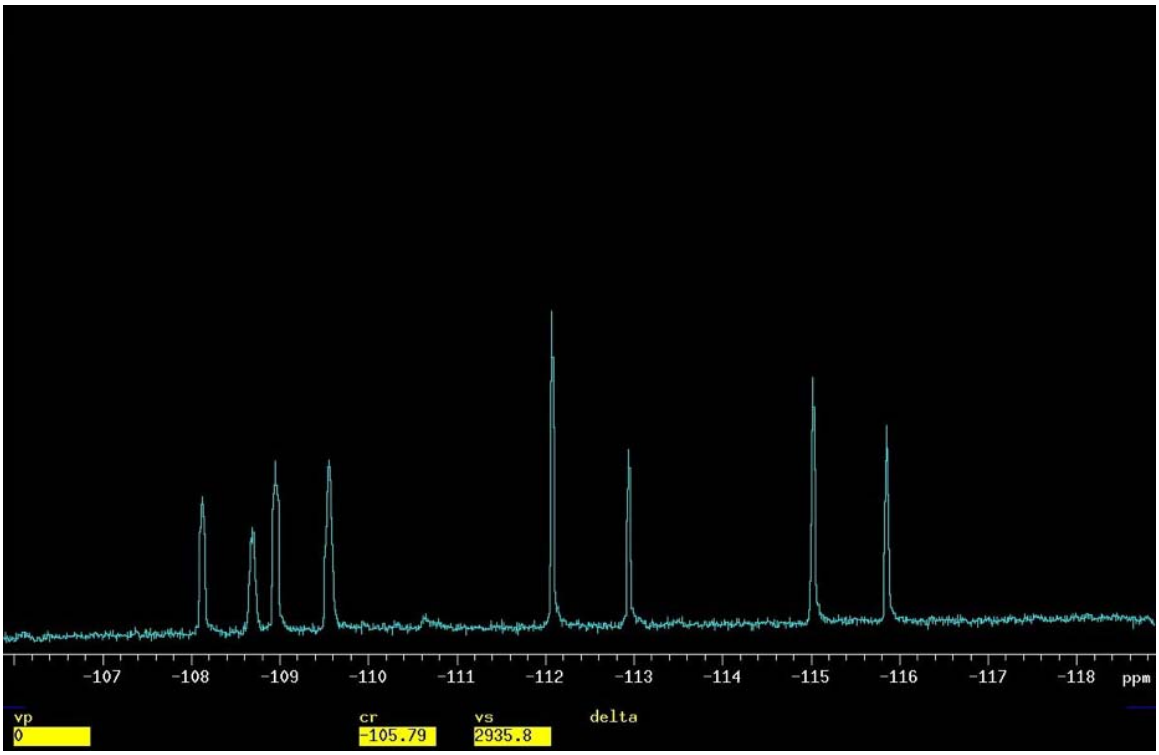

Spectrum A.11: ^{19}F NMR OFP-diNH_2 0.5 Equivalents Yb-HFC

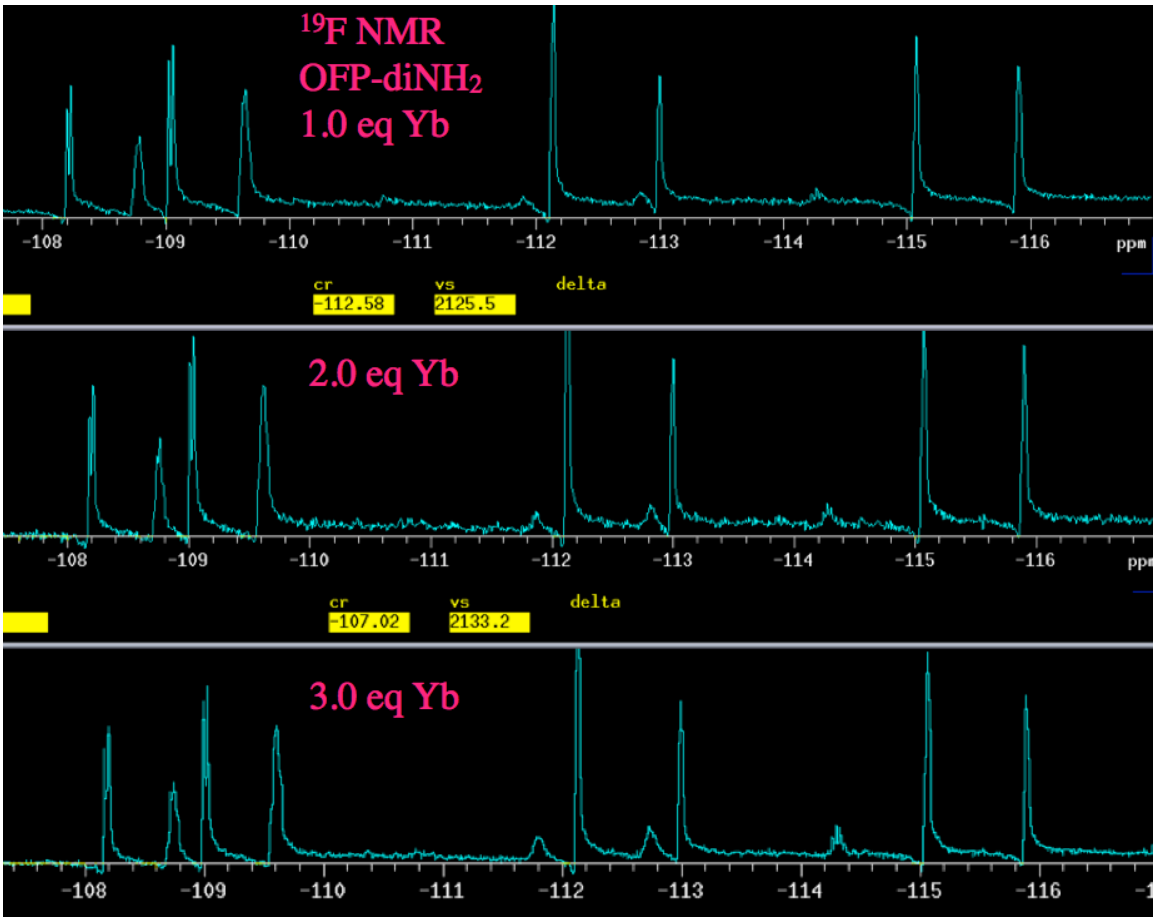

Spectrum A.12: ^{19}F NMR OFP-diNH$_2$ 1.0-3.0 Equivalents Eu-HFC

Endnotes

1) M. M Pellegrin, *Rect. Trav. Chim.*, Pays-Bas, **1899**, 18, 457.
2) B. H. Smith, *Bridged Aromatic Compounds*, Academic Press, New York, **1964**.
3) L. Rossa, F. Vögtle, V. Boekelheide, I. Tabushi, K. Yamamura, *Top. Curr. Chem.*, **1983**, 113, 1–185.
4) F. Vögtle, *Top. Curr. Chem.*, **1983**, 115, 1–163.
5) F. Diederich, *Cyclophanes*, Royal Society of Chemistry, London, **1991**.
6) F. Vögtle, *Cyclophane Chemistry*, Wiley, New York, **1993**.
7) E. Weber, *Top. Curr. Chem.*, **1994**, 172, 1–210.
8) V. V. Kane, W. H. de Wolf, F. Bickelhaupt, *Tetrahedron*, **1994**, 50, 4575–4622.
9) G. J. Bodwell, *Angew. Chem. Int. Ed. Engl.*, **1996**, 35, 2085–2088.
10) A. de Meijere, B. König, *Synlett*, **1997**, 11, 1221–1232.
11) G. J. Bodwell, in *Organic Synthesis Highlights IV* (Ed: H. G. Schmalz), Wiley-VCH, New York, **2000**, pp. 289–300.
12) H. Hopf, *Classics in Hydrocarbon Chemistry*, Wiley-VCH, Weinheim**, 2000**.
13) R. Gleiter, H. Hopf, *Modern Cyclophane Chemistry*, Wiley-VCH, Weinheim, **2004**.
14) D. J. Cram, H. Steinberg, *J. Am. Chem. Soc.*, **1951**, 73, 5691- 5704.
15) W. M. Schubert, W. A. Sweeney, H. K. Latourette, *J. Am. Chem. Soc.*, **1954**, 76, 5462-5466.
16) D. J. Cram, J. M. Cram, *Acc. Chem. Res.*, **1971**, 4, 201-213.
17) C. J. Brown, A. C. Farthing, *Nature*, **1949**, 164, 915-916.
18) J. F. Leibman, A. Greenberg, *Chem. Rev.*, **1976**, 76, 311–365.
19) S. W. Chow, L. A. Pilato, W.L. Wheelwright, *J. Org. Chem.*, **1970**, 35, 21-22.
20) W. R. Dolbier Jr., J. X. Duan, A. J. Roche, *Org. Lett.*, **2000**, 2, 1867-1869.
21) A. J. Roche, W. R. Dolbier Jr., *J. Org. Chem.*, **1999**, 64, 9137-9143.
22) A. J. Roche, B. Canturk, *J. Fluorine Chem.*, **2005, 1**26, 483-490.
23) W. R. Dolbier Jr., *Guide to Fluorine NMR for Organic Chemists*, John Wiley & Sons, Hoboken, **2009**.
24) A. J. Roche, W. R. Dolbier, Jr., *J. Org. Chem.*, **2000**, 65, 5282-5290.
25) W. R. Dolbier Jr., W. F. Beach, *J. Fluorine Chem.*, **2003**, 1, 97-104.
26) E. Eliel, S. H. Eilen, M. P. Doyle, *Basic Organic Stereochemistry*, Wiley, New York, **1994**.
27) H. Duddeck, E. D. Gomez, *Chirality*, **2009**, 21, 51-68.
28) R. S. Cahn, C. K. Ingold, V. Prelog, *Angew. Chem. Int. Ed Engl.*, **1966**, 5, 385-415.
29) R. S. Cahn, C. K. Ingold, V. Prelog, *Experimenta*, **1959**, 12, 81-124.
30) A. D. McNaught, A. R. Wilkinson, *The Compendium of Chemical Terminology*, John Wiley & Sons, Hoboken, **1997**.
31) A. E. Lovely, T. J. Wenzel, *Chirality*, **2008**, 20, 370-378.
32) A. J. Roche, A. A. Marchione, *Magn. Reson. Chem.*, **2009**, 47, 428-436.
33) L. Ernst, K. Ibrom, *Modern Cyclophane Chemistry*, Wiley-Weinheim, Hoboken, **2004**, 381.

34) N. E. Jacobson, *NMR Spectroscopy Explained*, John Wiley & Sons, Hoboken, **2007**, 64-69.
35) A. J. Roche, A. A. Marchione, S. A. Rabinowitz, *Magn. Reson. Chem.*, **2005**, 43, 1016-1022.
36) J. Battiste, R. A. Newmark, *Prog. Nucl. Magn. Reson. Spectrosc.*, **2006**, 48, 1-23.
37) R. H. Contreras, J. E. Peralta, *Prog. Nucl. Magn. Reson. Spectrosc.*, **2000**, 37, 321-425.
38) D. A. Lanfranchi, M.Blanc, M. Velluntini, P. Bradesi, J. Casanova, F. Tomi, *Magn. Reson. Chem.*, **2008**, 46, 1188-1194.
39) T. J. Wenzel, J. D. Wilcox, *Chirality*, **2003**, 15, 256-270.
40) D. A. Lanfranchi, M.Blanc, M. Velluntini, P. Bradesi, J. Casanova, F. Tomi, *Spectroscopy Letters*, **2010**, 43, 36-43.
41) M. Raban, K. Mislow, *Tetrahedron Lett.*, **1965**, 4249-4353.
42) J. Knobloch, J. D. Shaughnessy Jr., U. Rüther, *FASEB*, **2007**, 21, 1410–21.
43) M. D. McCreary, D.W. Lewis, D. L. Wernick, G.M. Whitesides, *J. Am. Chem. Soc.*, **1974**, 96, 1038-1054.
44) T. J. Wenzel, *Discrimination of Chiral Compounds Using NMR Spectroscopy*, Wiley, Hoboken, **2007**.
45) G. M. Whitesides, D.W. Lewis, *J. Am. Chem. Soc.*, **1970**, 92, 6979-6980.
46) A. J. Roche, A. A. Marchione, *Magn. Reson. Chem.*, **2012**, 50, 809-812.

Bibliography

Battiste, J. Newmark, R. A., *Prog. Nucl. Magn. Reson. Spectrosc.*, **2006**, 48, 1-23.

Bodwell, G. J., *Angew. Chem. Int. Ed. Engl.*, **1996**, 35, 2085–2088.

Bodwell, G. J., in *Organic Synthesis Highlights IV* (Ed: H. G. Schmalz), Wiley-VCH, New York, **2000**, pp. 289–300.

Brown, C. J., Farthing, A. C., *Nature*, **1949**, 164, 915-916.

Cahn, R. S., Ingold, C. K., Prelog, V., *Angew. Chem. Int. Ed Engl.*, **1966**, 5, 385-415.

Cahn, R. S., Ingold, C. K., Prelog, V., *Experimenta*, **1959**, 12, 81-124.

Chow, S. W., Pilato, L. A., Wheelwright, W.L., *J. Org. Chem.*, **1970**, 35, 21-22.

Contreras, R. H., Peralta, J. E., *Prog. Nucl. Magn. Reson. Spectrosc.*, **2000**, 37, 321-425.

Cram, D. J., Cram, J. M., *Acc. Chem. Res.*, **1971**, 4, 201-213.

Cram, D. J., Steinberg, H., *J. Am. Chem. Soc.*, **1951**, 73, 5691- 5704.

de Meijere, A., König, B., *Synlett*, **1997**, 11, 1221–1232.

Diederich, F., *Cyclophanes*, Royal Society of Chemistry, London, **1991**.

Dolbier Jr., W. R., *Guide to Fluorine NMR for Organic Chemists*, John Wiley & Sons, Hoboken, **2009**.

Dolbier Jr., W. R., Beach, W. F., *J. Fluorine Chem.*, **2003**, 1, 97-104.

Dolbier Jr.,W. R., Duan, J. X., Roche, A. J., *Org. Lett.*, **2000**, 2, 1867-1869.

Duddeck, H., Gomez, E. D., *Chirality*, **2009**, 21, 51-68.

Eliel, E., Eilen, S. H., Doyle, M. P., *Basic Organic Stereochemistry*, Wiley, New York, **1994**.

Ernst, L., Ibrom, K. *Modern Cyclophane Chemistry*, Wiley-Weinheim, Hoboken, **2004**, 381.

Gleiter, R., Hopf, H., *Modern Cyclophane Chemistry*, Wiley-VCH, Weinheim, **2004**.

Hopf, H., *Classics in Hydrocarbon Chemistry*, Wiley-VCH, Weinheim**, 2000**.

Jacobson, N. E., *NMR Spectroscopy Explained*, John Wiley & Sons, Hoboken, **2007**, 64-69.

Kane, V. V., de Wolf, W. H., Bickelhaupt, F., *Tetrahedron*, **1994**, 50, 4575–4622.

Knobloch, J., Shaughnessy Jr., J. D., Rüther, U., *FASEB*, **2007**, 21, 1410–21.

Lanfranchi, D. A., Blanc, M., Velluntini, M., Bradesi, P., Casanova, J., Tomi, F. *Magn*. *Reson*. *Chem*., **2008**, 46, 1188-1194.

Lanfranchi, D. A., Blanc, M., Velluntini, M., Bradesi, P., Casanova, J., Tomi, F. *Spectroscopy Letters*, **2010**, 43, 36-43.

Leibman, J. F., Greenberg, A., *Chem*. *Rev*., **1976**, 76, 311–365.

Lovely, A. E., Wenzel, T. J., *Chirality*, **2008**, 20, 370-378.

McCreary, M. D., Lewis, D.W., Wernick, D. L., Whitesides, G.M., *J*. *Am*. *Chem*. *Soc*., **1974**, 96, 1038-1054.

McNaught, A. D., Wilkinson, A. R., *The Compendium of Chemical Terminology*, John Wiley & Sons, Hoboken, **1997**.

Pellegrin, M. M., *Rect*. *Trav*. *Chim*., Pays-Bas, **1899**, 18, 457.

Roche, A. J., Canturk, B., *J. Fluorine Chem.*, **2005, 1**26, 483-490.

Roche, A. J., Dolbier Jr., W. R., *J*. *Org*. *Chem*., **1999**, 64, 9137-9143.

Roche, A. J., Dolbier Jr., W. R., *J*. *Org*. *Chem*., **2000**, 65, 5282-5290.

Roche, A. J., Marchione, A. A., *Magn*. *Reson*. *Chem*., **2009**, 47, 428-436.

Roche, A. J., Marchione, A. A., *Magn*. *Reson*. *Chem*., **2012**, 50, 809-812.

Roche, A. J., Marchione, A. A., Rabinowitz, S. A., *Magn*. *Reson*. *Chem*., **2005**, 43, 1016-1022.

Rossa, L., Vögtle, F., Boekelheide, V., Tabushi, I.,Yamamura, K., *Top. Curr*. *Chem*., **1983**, 113, 1–185.

Raban, M., Mislow, K., *Tetrahedron Lett*., **1965**, 4249-4353.

Schubert, W. M., Sweeney, W. A., Latourette, H. K., *J. Am. Chem. Soc*., **1954**, 76, 5462-5466.

Smith, B. H., *Bridged Aromatic Compounds*, Academic Press, New York, **1964**.

Vögtle, F., *Top. Curr. Chem*., **1983**, 115, 1–163.

Vögtle, F., *Cyclophane Chemistry*, Wiley, New York, **1993**.

Weber, E., *Top. Curr. Chem*., **1994**, 172, 1–210.

Wenzel, T. J., *Discrimination of Chiral Compounds Using NMR Spectroscopy*, Wiley, Hoboken, **2007**.

Wenzel, T. J., Wilcox, J. D., *Chirality*, **2003**, 15, 256-270.

Whitesides, G. M., Lewis, D.W., *J. Am. Chem. Soc*., **1970**, 92, 6979-6980.